Application of electrodialysis in integrated microbial fermentation and enzymatic biotransformation processes

A thesis submitted to the University College London
for the degree of
ENGINEERING DOCTORATE

by

Michael Wong
BEng

September 2010

Advanced Centre of Biochemical Engineering
Department of Biochemical Engineering
University College London
Torrington Place
London
WC1E 7JE

Table of Contents

Abstract

Electrodialysis (ED) is an established technology used to transport small ions from one solution to another through an ion exchange (IE) membrane under the influence of an applied electric potential difference. This project aimed to develop a novel integrated bioreactor-ED system and to explore its application to a variety of bioprocesses including microbial fermentation and enzymatic bioconversion.

A custom ED module was first designed and constructed that enabled the flexible configuration of different IE membranes. In order to establish the performance of the ED module for extraction of charged organic molecules the mass transfer rate of acetate, lactate and malate were first quantified as a function of key operating parameters such as membrane area and current applied. For extraction of acetate mass transfer rates of up to 2.5 $g.L^{-1}.h^{-1}$ could be achieved.

The primary application considered for ED was to overcome inhibition by metabolic acetate by-product formation in fed-batch *Escherichia coli* (*E.coli)* fermentation. Conventionally, a controlled substrate feeding strategy would be employed to repress acetate formation but at the expense of bioreactor productivity. With the application of the integrated bioreactor-ED system it was shown that acetate was removed instantly as it was formed during fermentation. For the heterologous expression of the model protein GFP this resulted in enhancement of protein production by up-to four fold. The level of enhancement depended upon the rate of acetate removal, residence time of feed in the ED module and reducing ammonium toxicity. Additionally a novel ED configuration incorporating a bipolar membrane was used to facilitate bipolar

electrodialysis (BPED). In addition to normal ED function the BPED module generate hydroxide ions *in situ* to facilitate pH control without the requirement for extraneous acid/base addition. BPED was shown to achieve the same enhanced levels of GFP production but with a 50% reduction in base addition.

The wider application of both ED and BPED technology to enzymatic bioconversions was also investigated for the lipase catalysed hydrolysis of ethyl acetate and fumaric acid. ED and BPED were used in both phases of the bioprocess, which included the initial pH adjustment and *in situ* removal of inhibitory molecule. In this case result showed a two-folded increase in product yield and base addition was reduced by 60% when ED was applied.

Overall this work has shown the wide range of potential applications and benefits of a novel integrated bioreactor-ED technology. It illustrates some of the critical design aspects for larger scale application and also considers the regulatory and commercial potential of the technology.

Thesis declaration

I, Michael Wong, hereby declare that this thesis is my own work and effort and that it has not been submitted anywhere for any award. Where other sources of information have been used, they have been acknowledged.

Signature: …….

Date: …….

Acknowledgements

I would like to thank my supervisors Professor Gary J Lye and Professor John M Woodley for this assistance, direction and support both at undergraduate level and throughout the course of my EngD research.

Also, I acknowledge the financial support of the UK Engineering and Physical Sciences Research Council (EPSRC).

Nomenclature

Abbreviations

A	Anode
AEM	Anion exchange membrane
BPED	Bipolar electrodialysis
BPM	Bipolar membrane
C	Cathode
CEM	Cation exchange membrane
DCW	dry cell weight
d_i	diameter of impeller
DOT	Dissolved oxygen tension
d_t	diameter of fermenter
E.coli	Escherichia coli
ED	Electrodialysis
EDF	Electrodialysis fermentation
F	Feed
GFP	Green Fluorescent Protein
LB	Luria bertani
OD	Optical density
R	Recovery
rpm	Revolutions per minute
v/v	Volume per volume
v/w	Volume per weight
vvm	Volume per volume per minute
U	activity

Chemicals and elements

$(NH_4)_2HPO_4$	Ammonium phosphate
Cl^-	Chloride ion
$CoCl_2.6H_2O$	Cobalt (II) chloride

$CuCl_2.2H_2O$	Copper (II) chloride
EDTA	ethylene-diaminetetra acetic acid
Fe	Iron
H^+	Proton or hydrogen ion
H_2	Hydrogen gas
H_2	Hydrogen gas
H_2O	Water
H_3BO_3	Boric acid
KH_2PO_4	Potassium phosphate
$MgSO_4.7H_2O$	Magnesium sulphate
$MnCl_2.4H_2O$	Manganese chloride
Na^+	Sodium ion
$Na_2MoO_4.2H_2O$	Sodium Molybdate Dihydrate
PO_4^{2-}	Phosphate ion
SO_4^{2-}	Sulphate ion
$Zn(CH_3COO)_2.2H_2O$	Zinc Acetate Dihydrate

Units

A	Amp
cm	centimetre
g	gram
h	hour
L	Litre
m	metre
M	molar
min	minute
mL	millilitre
^oC	Degree Celsius
s	second
V	Volt
µ	micro-
W	Watt
kW	Kilowatt

List of figures

List of tables

Chapter 1

General introduction

1.1 Electrodialysis

1.1.1 Definitions and parameters

Electrodialysis (ED) involves the transport of salt ions from one solution through ion exchange membranes to another solution under the influence of an applied electric potential difference (Banasiak *et al.,* 2007)).

Electrokinetics describes the movement of molecules or particles due to the presence of an electric field, which is generated by the passing of current between the two electrodes (Lee and Moon. 2005). The main types of current that have been employed for commercial or experimental applications of ED are alternating current (AC) and direct current (DC). In AC, the electric charge periodically reverses direction, whereas in DC, the flow of electrons occurs only in one direction (Ruiz *et al.,* 2006). Therefore, the application of a low level DC field is most suitable for the purpose of electrodialysis and it is in used to all the studies presented in this thesis.

Figure 1.1 shows the main effects of applying low-level DC on the movement of ions and molecules while the terminology of this field is further defined below:

- Electromigration (EM) involves the migration of ions towards an electrode of

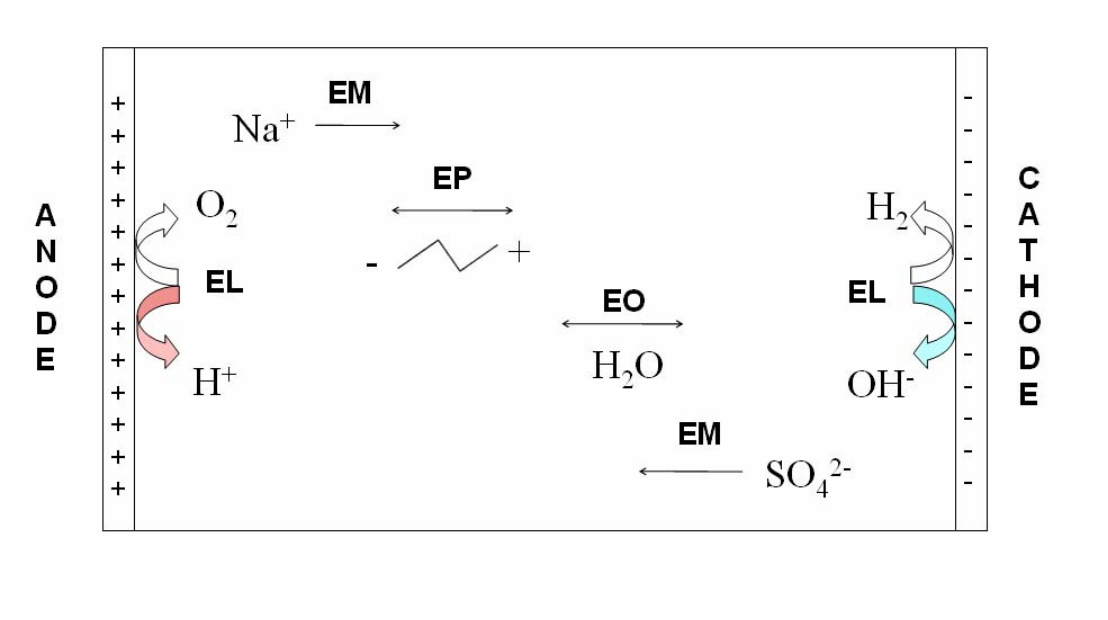

Figure 1.1. The effect of an electric field on the movement of ions and molecules. An electric field causes four main phenomena specifically includes electromigration (EM), electrophoresis (EP), electrolysis (EL) and electroosmosis (EO).

opposite charge (Leah *et al.,* 2000).

- Electrophoresis (EP) involves the migration of charged particles towards the electrodes as a consequence of their orientation within the electric field. These particles can be proteins or nucleic acids and their mobility is affected by both the porosity of the medium and the conductivity of the solution in which they are dissolved (Smara *et al.,* 2007).
- Electrolysis (EL) is the splitting of water molecules near the electrode surfaces, generating hydroxyl ions and hydrogen ions. This is one of the major factors of free ion generation of within an electric field, which causes the evolution of hydrogen gas and hydroxyl ions at the cathode, and oxygen and hydrogen ions at the anode (Hu *et al.,* 1999).
- Electroosmosis (EO) is the movement of water molecules plus particles due to the interaction with a charged surface. The characterisation of particle and ion movement is complicated because of the many parameters involved. These include acidity, water content, voltage applied and temperature (Wang *et al.,* 2006).

1.1.2 Ion exchange membranes

1.1.2.1 Cation and anion exchange membranes

Changes in the concentration of an electrolyte can be achieved by electrodialysis if ion exchange membranes are used (Xu, 2005). Two main types of membranes exist for this application: anionic and cationic. Anion exchange membranes (AEM) allow only anions to migrate when a DC electric field is applied while cation exchange membranes allow only cation to pass across the membrane (Koter, 2008). Anion exchange membranes contain fixed cationic groups within the pores of the membranes. The

exclusion of cation by the anionic exchange membranes is due to the repulsion of cations in solution by the fixed cations bound to the membrane. In contrast cation exchange membranes (CEM) contain fixed anionic groups and operate similarly to AEM in that anions in solution are repelled by fixed anions bound to the resin (Bazinet and Araya-Farias, 2005).

The use of ion exchange membranes and an applied potential for concentrating and electrolyte solution is termed electrodialysis (Meng *et al.,* 2008). Cations are attracted to the cathode (negatively charged electrode) and anions to the anode (positively charged electrode). Figure 1.2 shows how that if a cationic membrane is interposed between the two electrodes, only cations can pass across the membrane and conversely only anions can pass through anion exchange membranes. Extending this principle, if an electrodialysis cell comprising of alternate anion and cation exchange membrane is used, it is possible to create compartments where molecules are separated according to their charges.

The application of membrane separation techniques has the potential to solve many of the problems associated with downstream processing of biological processes (Xu. 2005). This can lead to increases in bioreactor productivity (Yi *et al.,* 2008), lower energy consumption for downstream processing, overcoming feed-back inhibition (Min-tian *et al.*,2005) and enhanced product recovery (Lee *et al.,* 1998). However, there are disadvantages in the use of membranes such as difficulty of sterilisation (Xu, 2005), biofouling of the membranes (Xu and Huang. 2008), slow transfer through the membranes and discrepancy between the optimal conditions for the membranes and for the bioprocess (Meng *et al.,* 2005; Pourcelly. 2002). Overall, considering the potential advantages ion exchange membranes may have in enhancing bioreactor productivity or simplifying downstream processing, it is still considered beneficial to consider new

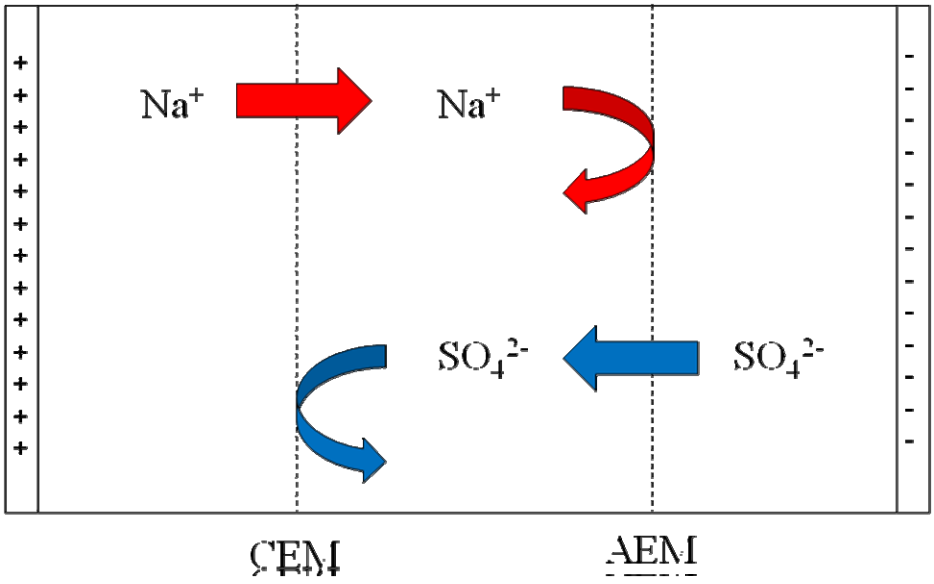

Figure 1.2. The functioning of anion exchange membrane (AEM) and cation exchange membrane (CEM) in the formation of sodium sulphate. Cation exchange membrane only allows the passage of cations whilst preventing the passage of anions. Conversely, anion exchange membrane is permeable to anions but impermeable to cations.

applications of membrane technology despite its drawbacks.

1.1.2.2 Bipolar membrane

Bipolar membrane (BPM) is the combination of anion and cation exchange characteristics within a single membrane (Huang *et al.,* 2007). It provides a unique feature by the dissociation of water into hydroxyl and hydrogen ions without any accompanying electrochemical reaction taking place (Mier *et al.,* 2008). The side of the membrane facing the anode has anion exchange properties and that facing the cathode has cation exchange membrane properties as shown in Figure 1.3. Due to their unique characteristics, bipolar membranes have been used for acidifying specific compartments of chemical reactors (Xu. 2002). Metal-nanotubule membranes with electrochemically switchable ion-transport selectivity have also reported (Raissouni *et al.,* 2007)

1.1.2.3 Solute mass transfer rate across ion exchange membrane

A general mathematical model of ion transfer rate is given by equation 1.1 (Sadrzadeh *et al.,* 2006). It shows the transfer rate is directly proportional to current applied and the area of ion exchange membrane.

$$- d(CV)/dt = \eta NI/zF = \eta NAi/zF \qquad \text{eq 1.1}$$

Where C - Concentration of ions in the feeding compartment (F)

V - Volume of the feed solution (L)

η - Current efficiency

N - Number of cell pairs

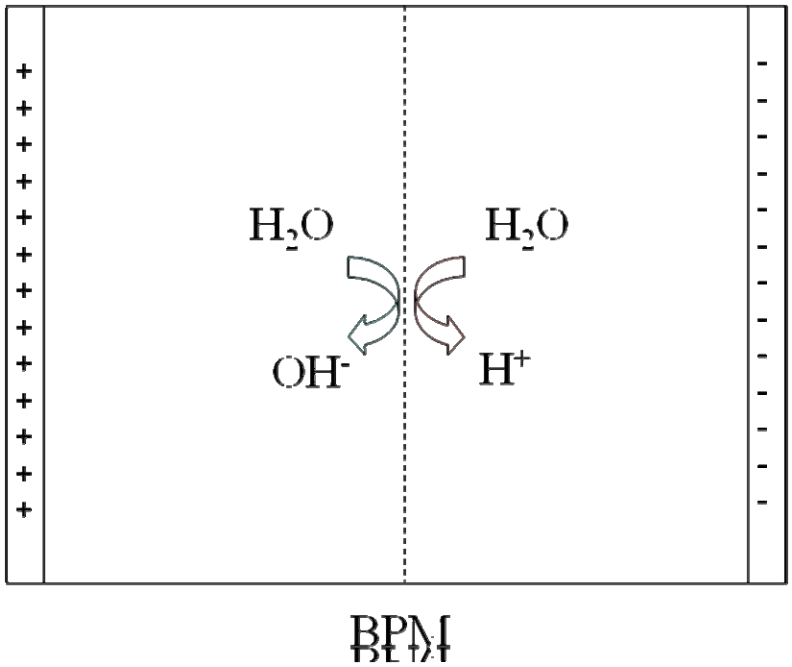

Figure 1.3. The functioning of a bipolar membrane. The bipolar membrane (BPM) splits water molecules and produce hydroxyl ions on the side of the membrane facing the anode and protons on the side of the membrane facing the cathode.

I - Current (A)

z - Charge of the ion

F - Faraday constant ($C.equivalent^{-1}$)

A - Area of electrode (cm^2)

i - Current density ($A.cm^{-2}$)

1.1.3 Applications of electrodialysis

ED has been used since 1890 for the demineralisation of sugar syrup (Oanizza and Cerisola. 2005). Since then it has been widely applied in a number of different fields such as water treatment (Sadrzadeh *et al.,* 2007), clean-up of contaminated soil and the concentration of bacterial solutions (Jackman *et al.,* 1999). However, this study will mainly focus on the utilisation of ED in fermentations and bioconversion processes relevant to the modern (bio-) pharmaceutical industry sectors.

Electrodialysis potentially provides great advantages for industrial bioproduction of valuable compounds because it could enhance downstream processing and releases the biocatalyst from end-product (or by-product) inhibition (Habova *et al.,* 2004). This is especially important in the case of fermentation systems, where feedback inhibition often limits product yield (Lee *et al.,* 1998). Lactic acid fermentation is a typical example of where overcoming end-product inhibition is critical for the productivity of continuous fermentation (Hirata *et al.,* 2005). In electrodialysis fermentation of *Lactobacillus*, lactate was removed and accumulated in a separate reactor (Choi *et al.,* 2002). Gao *et al* (2004) demonstrated the reduction of lactate inhibition, resulting in a two times increase in lactic acid production.

Electrodialysis for ions separation within bioprocesses is another important application for bioproduction such as acid removal from organic solutions (Wang *et al.,* 2006),

desalting of amino acids, demineralisation of cheese whey (Shen *et al*., 2006) and nitrate removal in drinking water (Mondor *et al.*, 2006). To date bioprocesses using free enzyme systems have benefited from ED techniques for the electrochemical regeneration of co-factors (Vuorilehto *et al.,* 2004). Built-in electrodialysis systems have also been used for the separation of phenylacetic acid, 6-aminopenicillanic acid and Penicillin G under constant voltage but only at small scale (Xu and Huang, 2008).

1.2 *E.coli* fermentations

1.2.1 Fermentations

1.2.1.1 *E.coli*

Escherichia coli (E.coli) is one of the most important organism of choice for the synthesis of a wide variety of recombinant proteins for therapeutic (Sandoval-Basurto *et al.,* 2004), diagnostic and industrial applications (Varma *et al.,* 1993). *E.coli* generates acetic acid as an undesirable metabolic by-product during fermentation that has several negative effects on cell growth and protein production (Han *et al.,* 1992).

1.2.1.2 Batch and fed-batch fermentation

Batch fermentation is a standard method used in the industrial production of microorganisms, where the sterile growth medium is inoculated with microorganisms and no additional medium is added. Fed-batch fermentation is one of the high cell density techniques developed to improve fermentation productivity and provide benefits such as enhanced downstream processing and lower production costs (Lee, 1996). The mostly employed technique is the application of a controlled feeding

strategy to standard batch fermentation (Akesson *et al.,* 2000). Fed-batch fermentation is defined as a process in which one or more nutrients are fed to the fermenter during cultivation and the products remain in the bioreactor until the end of the process. The advantage of fed-batch over batch fermentation is evident when changing the concentration of a nutrient increases the productivity yield of the desired metabolite (Henes and Sonnleitner. 2007). Shiloch and Fass (2005) compared batch and fed-batch cultivation for *E.coli* fermentation and noted a five folded increase in the cell dry-cell-weight (DCW) by the introduction of feeding.

1.2.2 Acetic acid as a fermentation by-product

1.2.2.1 Formation

Figure 1.4 shows the key steps involved in glycolysis, the TCA cycle and the two pathways for the formation of acetate. The direct route is through pyruvate to acetate by pyruvate oxidase (Ko *et al.,* 1993). However, the primary passage to acetate is the three-step pathway from pyruvate, acetyl-CoA, acetyl phosphate to acetate (Kim and Cha. 2003). This is caused by the high flux of acetyl-CoA, preventing it from entering the TCA cycle. At this point, further increase in glucose uptake results in overflow metabolism of acetyl-CoA to acetate (Xu *et al*., 1999). The reasons/mechanisms responsible for by-product acetic acid formation during *E.coli* fermentation have been reported by many researchers (Han *et al.,* 1992; Kleman *et al.,* 1994; Xu *et al.,* 2002). These include the specific oxygen uptake rate reached its maximum value near the threshold dilution rate (Akesson *et al.,* 1999), the accumulation of $NADH_2$ switches carbon flow toward acetic acid (van de Walle and Shiloach, 1998) and the limited

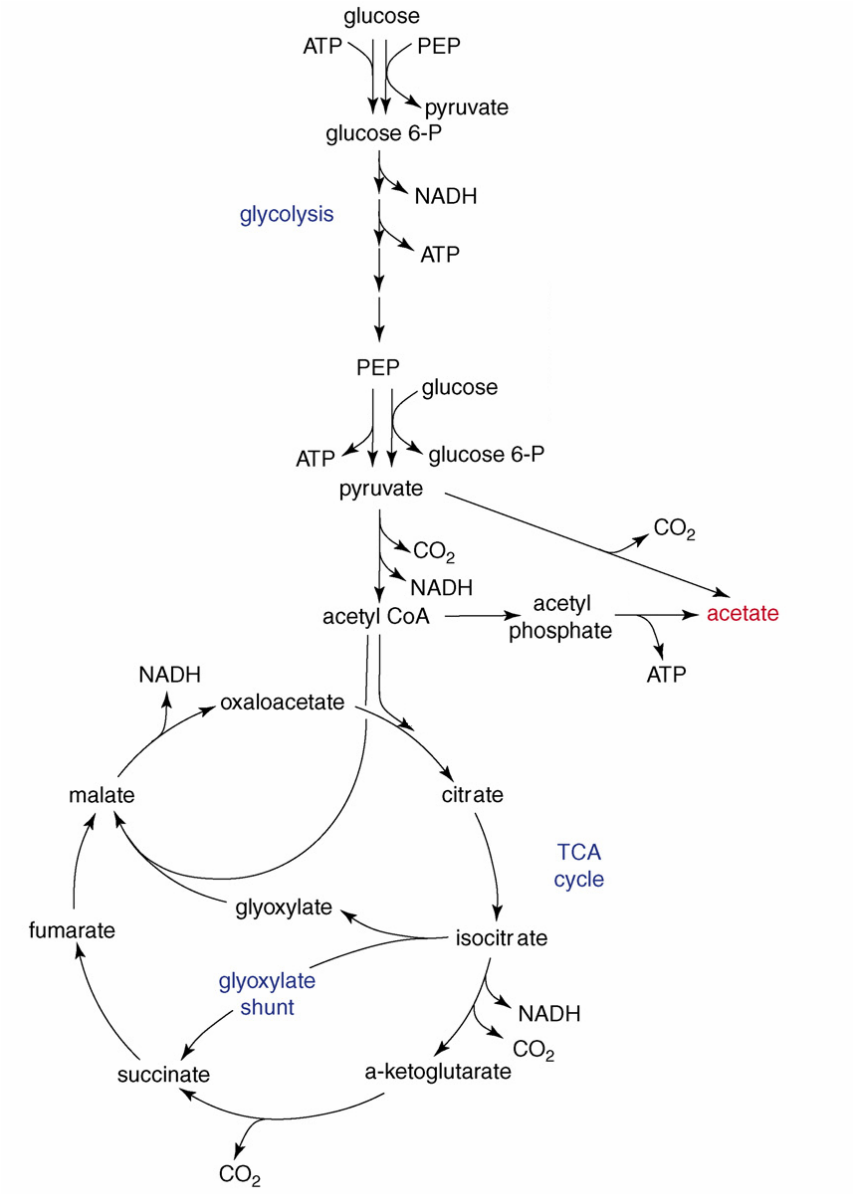

Figure 1.4. Key biochemical pathways in *E.coli* involved in the aerobic consumption of glucose and the synthesis of acetate, carbon dioxide and biomass. *E.coli* consumes glucose and simultaneously generates pyruvate from PEP. Acetate is formed from pyruvate by pyruvate oxidase and acetate kinase, due to the limited capacity of TCA cycle. Figure reproduced from Eiteman and Altman(2006).

capacity of the tricarboxylic acid (TCA) cycle (Eiteman and Altman, 2006).

The concentrations of acetate produced have been reported to vary between 1 and 30 $g.L^{-1}$ of culture, depending on the strain and growth medium composition (Kleman *et al.,* 1991; Luli and Strohl, 1990). For example, during batch fermentation, *E.coli* JM109 accumulated 5 $g.L^{-1}$ of acetate, whereas *E.coli* BL21 only produced 2 $g.L^{-1}$ (Luli and Strohl, 1990).

1.2.2.2 Inhibition

Growth inhibiting concentrations of acetate vary for different strains but generally range from 5 to 10 $g.L^{-1}$ (Kleman *et a.,l* 1994; Luli and Strohl, 1990). The detrimental effect of acetate is increased by the associated accumulation of salts as a result of the acid and base addition used for fermenter pH control (Turner *et al.,* 1994). Therefore, an increase of acetate may also lead to an increase in the concentration of ammonia in the medium as ammonia is often used in pH control. Thompson *et al.,* (1985) reported concentrations of ammonia above 2.89 $g.L^{-1}$ causes a reduction in the cell growth of *E.coli*.

Acetate inhibits growth to a greater extent for recombinant cells than for competent cells (Koh *et al.,* 1992) and recombinant protein production can be significantly reduced by acetate accumulation (Lee, 1996, Han *et al.,* 1992, Choi *et al.,* 2006). Various strategies have been developed to limit acetate accumulation or reduce its negative effects to increase the productivity of recombinant proteins processes (Eiteman and Altman, 2006). In this study, electrodialysis will be used to try and overcome this challenges associated with acetate inhibition.

1.3 Bioconversion

1.3.1 Lipase and ethyl acetate

Lipase enzymes exist widely throughout nature in microbial, plant and animal systems (Reis *et al.,* 2008). Lipases now represent a powerful tool for catalysing stereoselective hydrolysis, esterification and transesterisification reactions widely used in industry (Hwang and Park. 1997). The majority of lipases are expressed extracellularly and are of molecular weights between 20 and 60 kDa (Stuer *et al.,* 1986). They have diverse functions in the degradation of food and fat and are shown to synthesise aliphatic, aromatic (Krisha *et al.,* 1999) and other esters in non-aqueous and biphasic systems (Krisha *et al.,* 2000). The employment of lipases to catalyse esterification and transesterisification reactions in organic solvents has shown increased enzyme activity and possessed region-specificity and stereo-selectivity (Hari Krishna and Karanth. 2002). Most importantly, lipases do not require cofactors for activity. In this work, the hydrolysis of ethyl acetate, shown in scheme 1.1, will be studied. This is one of the solvent systems catalysed by lipase in which ethanol and acetate are formed.

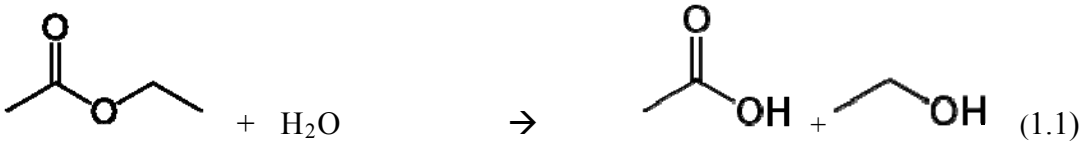

(1.1)

Ethyl acetate (Lipase) Acetate Ethanol

1.3.2 Fumarase and malic acid

L-malic acid is one of the most popular organic acids for food, pharmaceutics and cosmetic products (Presecki *et al*., 2007). It can be produced by fermentation or

enzymatic conversion from fumaric acid. Scheme (1.2) shows fumaric acid is transformed into malic acid by the addition of a water molecule to the double bond.

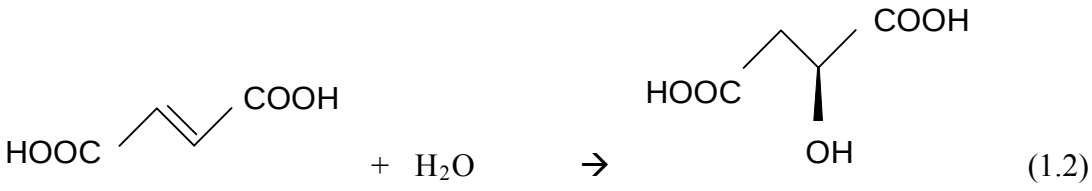

(1.2)

Fumaric acid (Fumarase) L-malic acid

The process is a typical equilibrium reaction and catalysed by fumarase enzyme (Belafi-Bako *et al.,* 2004). Fumarase is a homologous enzyme and stereospecific, acting only on the trans-isomer. In the current industrial enzymatic process fumaric acid is converted to L-malic acid by immobilised cells of *Leuconostoc* and *Brevibacterium* species containing fumarase. The yield of process reaches 70% of theoretical and the unconsumed fumarate is recycled (Belafi-Bako *et al.,* 2004)..

1.4 Aims and objectives

The aim of this project is to explore the potential application of ED as an *in-situ* technique for removal of inhibitory products or by-products from biological processes. As described in Section 1.1.3, electrodialysis potentially has wide application for removal of small charged molecules in fermentation and bioconversion to overcome problems with product or by-product inhibition. The project deliverable would be a generic technology for enhancing bioconversion productivity and recombinant protein production capable of being reproduced at pilot scale. The main objectives of the investigation are summarised below:

- The initial work is to focus on the design and construction of a laboratory scale electrodialysis system. The detailed design is described in Section 2.1.1, while Section 2.2.1 describes some of the key operational parameters for ED application. Once manufactured, the rate of ion removal as a function of current and voltage applied, flow rates and membrane area per unit volume is demonstrated. Common organic acids such as lactic acid and acetic acid are studied as model solutes for their removal from aqueous solutions under the influence of an applied electric field using ion exchange membranes. This provides the benchmark solute mass transfer rates and also establishes reproducible operation of the ED system. The results of these mass transfer studies are presented and discussed in Chapter 3.

- Once the system is characterised, its application to *in situ* removal of toxic by-products in *E.coli* fermentation is first demonstrated. The model system chosen is *E.coli* TG1 pGLO in which the accumulation of inhibitory acetate has detrimental effects on cell growth and the synthesis of recombinant protein. Therefore, the productivity is expected to enhance with the application of ED which is studied as a function of acetate removal. The results of this work are presented and discussed in Chapter 4.

- The time of induction is a critical factor which influences the synthesis of recombinant protein in *E.coli* fermentation. In Chapter 4, induction of protein synthesis took place at late exponential phase. Similar experiments are carried out here except that the fermentations are induced at early exponential phase. This will enable comparison to be made between the two approaches and help

define optimum conditions for ED process design. The results of this work are presented and discussed in Chapter 5.

- Having established ED as an *in situ* acetate removal technique, a novel configuration of ED is next investigated. This involves the use of an alternative bipolar membrane module and a PID controller as described in Section 2.2.4. The use of bipolar electrodialysis (BPED) has the potential to minimise the addition of ammonium hydroxide for pH control in *E.coli* fermentation, where an excess of ammonia can be toxic to the cells. The results of this work where ED is used for simultaneous acetate removal and pH control are presented and discussed in Chapter 6.

- The versatility of the ED system is next examined by demonstrating the applications of ED to enzymatic bioconversion processes. The hydrolysis of ethyl acetate and bioconversion of fumaric acid are investigated in which ED is used for *in situ* product removal, pH control and initial pH adjustment. The results of this work are presented and discussed in Chapter 7.

- As an EngD requirement, it is important to measure the performance of this technology and assess its applicability to industry. The bioprocess validation and management aspect of this work are presented and discussed in Chapter 8.

- Finally, Chapter 9 provides an overall summary of the project findings and suggestion for future work.

Chapter 2

Materials and Methods

2.1 Materials

2.1.1 Electrodialysis module

The electrodialysis module was kindly provided by EKB technology Ltd (Oxford, UK). The main components include ion exchange membranes and electrodes at each end of the module. As shown in Figure 2.1 this module consists of four equal volume compartments labelled anode compartment (A), recovery compartment (R), feed compartment (F) and cathode compartment (C). Compartment F contained the feed such as fermentation broth or organic acid where fermentation or bioconversion took place. Compartment R had the function of capturing the negatively charged reaction products and separate them from the rest of module. Compartment A and C were the two compartments in close contact with the anode and cathode, respectively. They had the function of keeping the near-electrode areas separate from compartment F and R. Compartment A, C and R contained the electrolyte, sodium sulphate purchased from Sigma-Aldrich Company Ltd (Dorset, UK). All compartments were 15 cm wide, 13.5 cm high and 1cm deep with a capacity of 500 mL. Each compartment is separated by an anion exchange membrane or a cation exchange membrane (Membrane International Inc, Glen Rock, USA) with an effective membrane area of 0.01 m^2 (10 cm

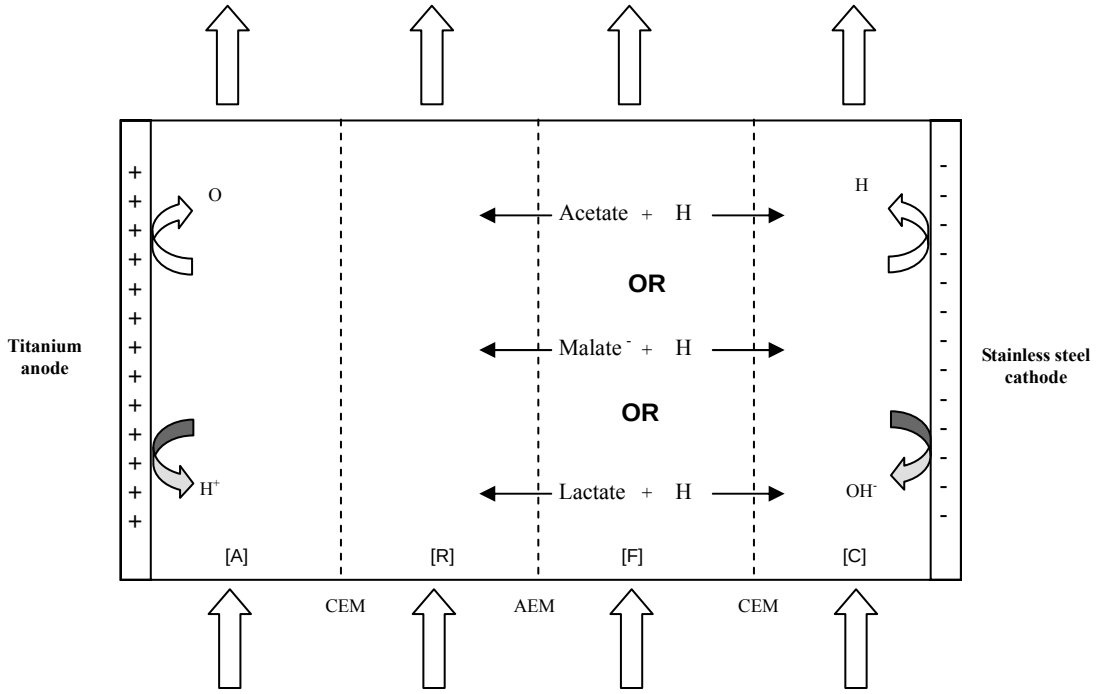

Figure 2.1a. Principle of electrodialysis module operation for acetic, malic or lactic acid removal: AEM, anion-exchange membrane; CEM, cation exchange membrane; A, anode compartment; R, recovery compartment; F, fermentation/feed compartment; C, cathode compartment.

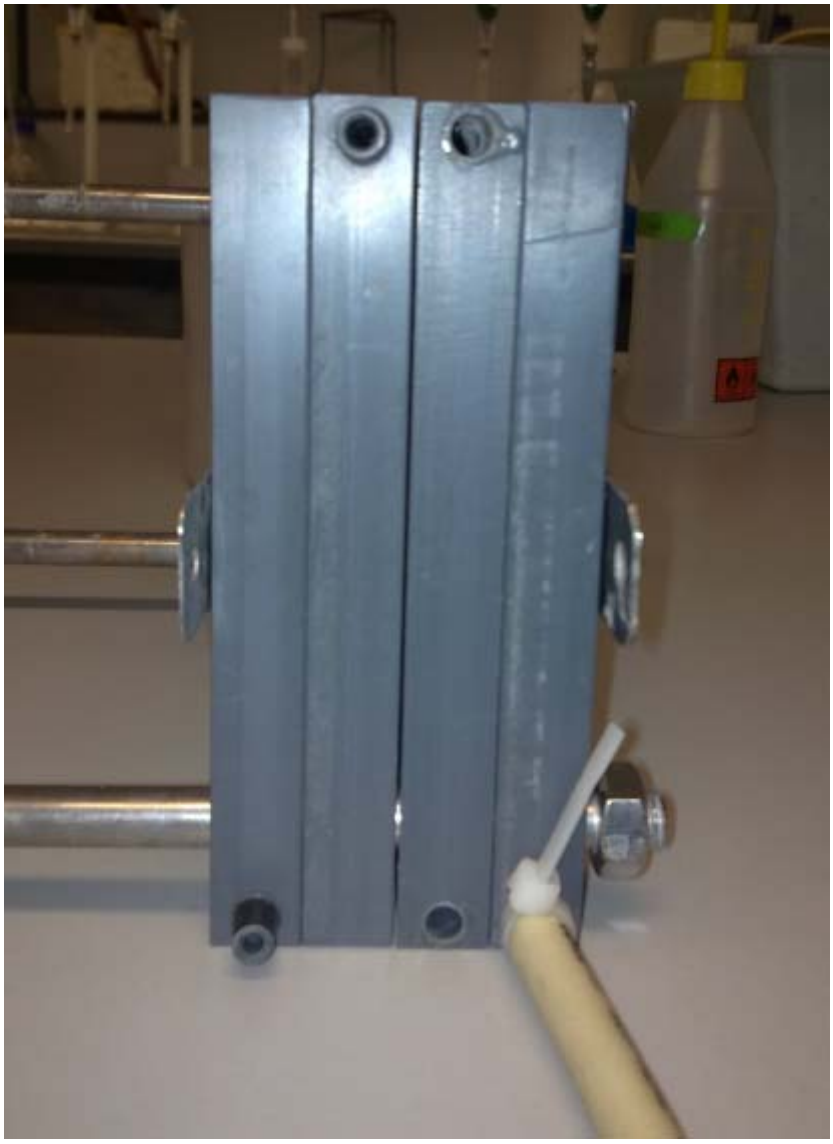

Figure 2.1b. Photograph of the electrodialysis module.

x 10 cm). The frame was made from poly vinyl chloride (PVC) and was held together after assembly by four stainless steel rods.

2.1.2 Plasmid

The plasmid vector pGLO (Bio-Rad Laboratories, Hertfordshire, UK) was chosen for this project, because it was commercially available and its protein can be easily assayed. It was used in Chapter 4, 5 and 6 for bacterial Green Fluorescent Protein (GFP) synthesis studies. It is a 5.4 kb plasmid that synthesises GFP in *E.coli* upon arabinose induction (Mosher, 2002). The promoter sequence controlling GFP synthesis regulates the transcription from the ara operon (P_{BAD}). Hence transcription only occurs when the activator protein AraC binds to a specific activator sequence (aral) just upstream of P_{BAD} in the presence of arabinose sugar. The *bla* gene coding for beta-lactamase confers ampicillin resistance.

2.1.3 Bacterial strains

Three Escherichia coli (*E.coli)* strains TG1, DH5α, HB101 were initially tested in shake flask cultures (see Section 2.2.2.3) before the best performing strain was taken further to fermentation scale. Strain selection was based on its cell growth rate and yield using different media, commercial availability and potential as an efficient host for GFP synthesis. The chosen *E.coli* strain in this study was *E. coli* Tg1 supE thi-1 Δ(lac-proAB) Δ(mcrB-hsdSM)5 (rK-mK-) [F' traD36, proAB, lacIq ΔM15] obtained from Bio-Rad Laboratories (Hertfordshire, UK).

2.1.4 Culture media

All media and stock solutions were prepared in reverse osmosis (RO) water. The complex LB medium consisted of 12 $g.L^{-1}$ of tryptone, 24 $g.L^{-1}$ of yeast extract and 10 $g.L^{-1}$ of NaCl. This medium was only used during initial strain selection studies (see Section 2.2.2.2). The dissolved LB solution was sterilised by autoclaving for 20 min at 121 ^{o}C.

The defined medium used for batch and fed-batch fermentation studies was prepared as described by Korz *et al* (1995). The composition of the initial batch medium and subsequent feed solution is given in Table 2.1. For preparation of a 4 L batch medium, $(NH_4)_2HPO_4$, KH_2PO_4, citric acid, EDTA and trace elements were first dissolved in 3.8 L distilled water in the fermenter and the solution was sterilised for 20 min at 121 ^{o}C. The feed solution of $MgSO_4$ and glucose were sterilised separately for 20 min at 121 ^{o}C in an atuoclave. After cooling, all solutions including the antifoam reagent, PPG, were combined and the pH was adjusted to 6.7 with 5 M aqueous NH_4OH prior to inoculation. 50 $mg.L^{-1}$ of ampicillin was also then added. All medium components were of the highest purity available were purchased from Sigma-Aldrich Company Ltd (Dorset, UK).

2.1.5 Organic acids and enzymes

Organic acids used in Chapter 3 (acetic acid, lactic acid and malic acid) and Chapter 7 (ethyl acetate and fumaric acid) were all purchased from Sigma-Aldrich Company Ltd. The enzymes, lipase and fumarase *from porcine heart*, used in Chapter 7 were also purchased commercially available at Sigma-Aldrich Company Ltd (Dorset, UK).

Table 2.1. Medium and feed composition used for batch and fed-batch fermentation of *E.coli* TG1 pGLO. Medium composition taken from Korz *et al* (1995)

Components	**Batch medium (L^{-1})**	**Unit (L^{-1})**	**Feeding solution (L^{-1})**	**Unit (L^{-1})**
Glucose	25.0	g	450.0	g
KH_2PO_4	13.3	g	-	g
$(NH_4)_2HPO_4$	4.0	g	-	g
$MgSO_4.7H_2O$	1.2	g	20.0	g
Citirc acid	1.7	g	-	g
EDTA	8.4	mg	13.0	mg
$CoCl_2.6H_2O$	2.5	mg	4.0	mg
$MnCl_2.4H_2O$	15.0	mg	23.5	mg
$CuCl_2.2H_2O$	1.5	mg	2.5	mg
H_3BO_3	3.0	mg	5.0	mg
$Na_2MoO_4.2H_2O$	2.5	mg	4.0	mg
$Zn(CH_3COO)_2.2H_2O$	13.0	mg	16.0	mg
Fe(III) citrate	100.0	mg	40.0	mg
Thiamine.HCl	4.5	mg	-	mg
Ampicillin	50.0	mg	25.0	mg
Antifoam PPG	0.1	mL	-	mL

2.2 Methods

2.2.1 Electrodialysis

During operations of ED (see Section 2.1.1), anions migrate through the anion exchange membrane but are unable to migrate through the cation exchange membrane. The feed is passed through compartment F during the electrodialysis phase, while 1 L of 2 M sodium sulphate is circulated in compartments A, R and C. All four channels are circulated at flow rates of 500 $mL.min^{-1}$ using a peristaltic pump (Watson-Marlow, Cornwall, UK). In this set-up, circulation through the electrodialysis cycle had a mean residence time of 20 s. When a constant current of 2 A is applied, an electric field is generated within the module. The negatively charged ions are attracted towards the anode compartment and penetrate the anion-exchange membrane. Consequently, anions (and other small charged molecules) are removed from the feed compartment and accumulates in the recovery compartment. When an anion is removed, it is replaced by the negatively charged sulphate ion of the electrolyte (sodium sulphate).

2.2.1.1 Mass transfer rate determination for organic acid removal

To investigate the design parameters of the electrodialysis module, mass transfer experiments were carried out using lactic, malic and acetic acid solutions as simple feed streams. 2 L of each organic acid solution was separately passed through the module as described in Section 2.2.1 at a range of initial feed concentrations (5, 10. 20 $g.L^{-1}$), flow rates (100, 300 and 500 $ml.min^{-1}$), ion exchange membrane per unit volume (50, 100, 200 $cm^2.L^{-1}$), voltages (10, 20 and 40 V), and electrolyte concentrations (0.1, 0.2, 0.4 M). Samples were taken from both compartments F and R at intervals of 30 min.

2.2.2 Batch and fed-batch fermentations

2.2.2.1 Transformation

100 μL of competent cells were transferred to a sterile microcentrifuge tubes and mixed with 5 μL (0.15 μg) of pGLO DNA. The mixture was cooled on ice for 30 min, and heat shocked at 42 ^{o}C for 45 sec. The heat-shocked cells were cooled on ice for 2 min, mixed with 0.9 mL of LB-medium, and incubated at 37 ^{o}C for 45 min with shaking. The transformants were then grown on LB agar plates at 37 ^{o}C overnight, containing 1 μg.mL^{-1} of the antibiotic ampicillin from Sigma-Aldrich Company Ltd (Dorset, UK). After transformation, stock cultures were maintained at -80 ^{o}C in 1.5 mL Eppendorf tubes containing 50% glycerol until use.

2.2.2.2 Pre-culture

To prepare the inoculum, 1 mL of *E.coli* Tg1 (pGLO) glycerol cell stock (Section 2.1.3) was transferred into 100 mL of the batch medium (Table 2.1) in a 1 L shake flask, and then incubated at 30 ^{o}C with shaking at 250 rpm on an orbital mixer for 12-14 h until the culture reached mid-exponential phase.

2.2.2.3 Shake flask fermentations

Small scale cultivations were performed in 1 L shake flasks, where 1 mL of glycerol stock (Section 2.1.3) was inoculated into 100 mL of the batch medium (Table 2.1). The flask was then incubated at 37 ^{o}C with shaking at 250 rpm on an orbital shaking platform for 10-12 h. In experiments to show the inhibitory effect of acetate accumulation (Section 4.2.1.2), 1, 3 and 5 g.L^{-1} of sodium acetate were added separately into three different shake flasks at the early exponential phase of growth.

2.2.2.4 Batch fermentations

Batch fermentations were carried out in a 7.5 L fermenter, as shown in Figure 2.2, (BioFlo 110, New Brunswick, Hertfordshire, UK) with a working volume of 4 L using a 5% v/v inoculation. The fermenter was fitted with a dual Rushton turbine impeller system (d_i/d_t = 0.25). Antifoam agent PPG was used for automatic foam control. Temperature (30 ± 0.1 ^oC) and pH (6.7 ± 0.1) in the fermenter were controlled automatically in all experiments via a cooling jacket and addition of 5 M ammonium hydroxide. The aeration rate was set at 1.5 vvm with a stirrer speed of 787 rpm. These conditions were kept constant in all experiments.

A number of on-line parameters were measured. pH was monitored using a combined pH gel electrode (Applikon Biotechnology Ltd., Gloucestershire, UK) and was calibrated before each culture using pH 4 and 7 solutions. Dissolved Oxygen Tension (DOT) was measured using an Applisens ADI dO_2 polargraphic probe (Applikon Biotechnology Ltd., Gloucestershire, UK). This was calibrated before each culture by nitrogen gas. The off-gas data for all fermentations was monitored by an online mass spectrometer (Prima 600, VG-gas Analysis, Winsford, Cheshire, UK) connected to the fermenter controls. Online data was logged by Propack data logging and acquisition software (Acquisition Systems, Guildford, Surrey), Bioview Software (Adaptive Biosystems, Watford, UK) or BioXpert data logging and acquisition software.

2.2.2.5 Fed-batch fermentations

The initial set-up and conditions used in fed-batch fermentations were the same as those for batch mode (Section 2.2.2.4). After almost complete consumption of the initial

glucose, as indicated by an on-line increase in DOT (see Figure 4.3b for an example), the fed-batch phase operation was started. Exponential feeding was carried out at a pre-determined rate corresponding to the maximum specific glucose uptake rate of the culture and hence the optimal growth rate (Xu *et al*., 1999).

2.2.2.6 Induction

When required GFP synthesis from the pGLO plasmid was induced by the aseptic addition of 0.25 % w/v L-arabinose. Induction took place at late exponential phase in Chapter 4 and early exponential phase in Chapter 5 and 6. The actual time of induction is indicated by an arrow on each figure describing fermentation kinetics.

2.2.3 Batch and fed-batch electrodialysis fermentations

The electrodialysis fermentation system built and used in this work is shown in Figure 2.3. Fermentations with the electrodialysis module were carried out with the 7.5 L fermenter (Figure 2.2) with an initial working volume of 4 L. Prior to operation, the electrodialysis module was chemically sterilised with 1 M sodium hydroxide. This resulted in a ratio of membrane area to initial fermentation volume of 2.5 m^2m^{-3}. Prior to actual EDF fermentations, two control experiments were carried out to investigate the impact of oxygen deficiency and the effect of the applied electric field towards the cells. The first was carried out under the same operating conditions and procedures for batch ED fermentations, except that no current was applied to the ED membrane stack. The second was carried out by replacing the anion exchange membrane between compartments R and F, with a cation exchange membrane. Hence when the current was applied to the system, all the ions were retained within compartment F.

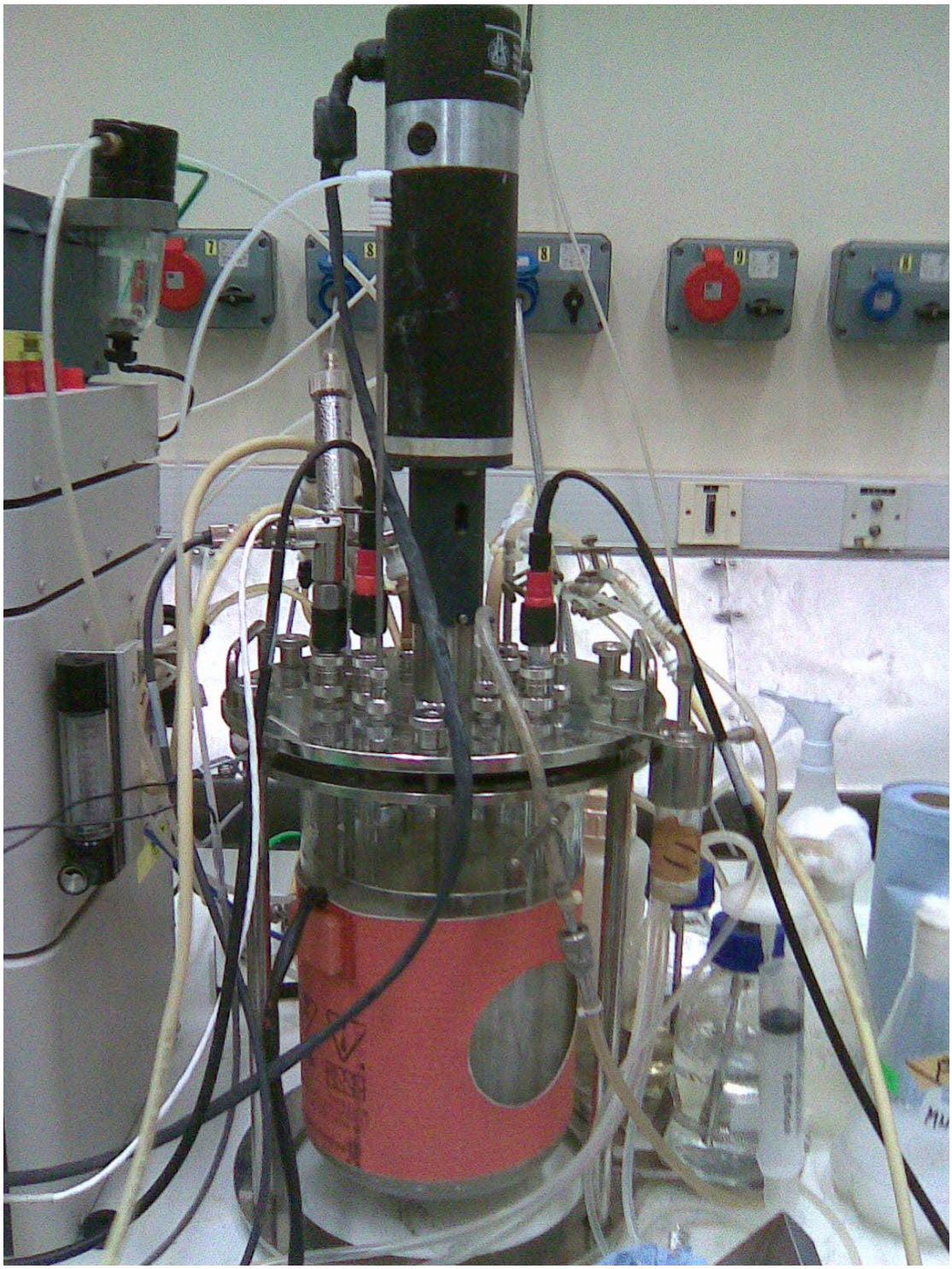

Figure 2.2. Photograph of the 7.5L New Brunswick Scientific BioFlo 110 modular benchtop fermenter.

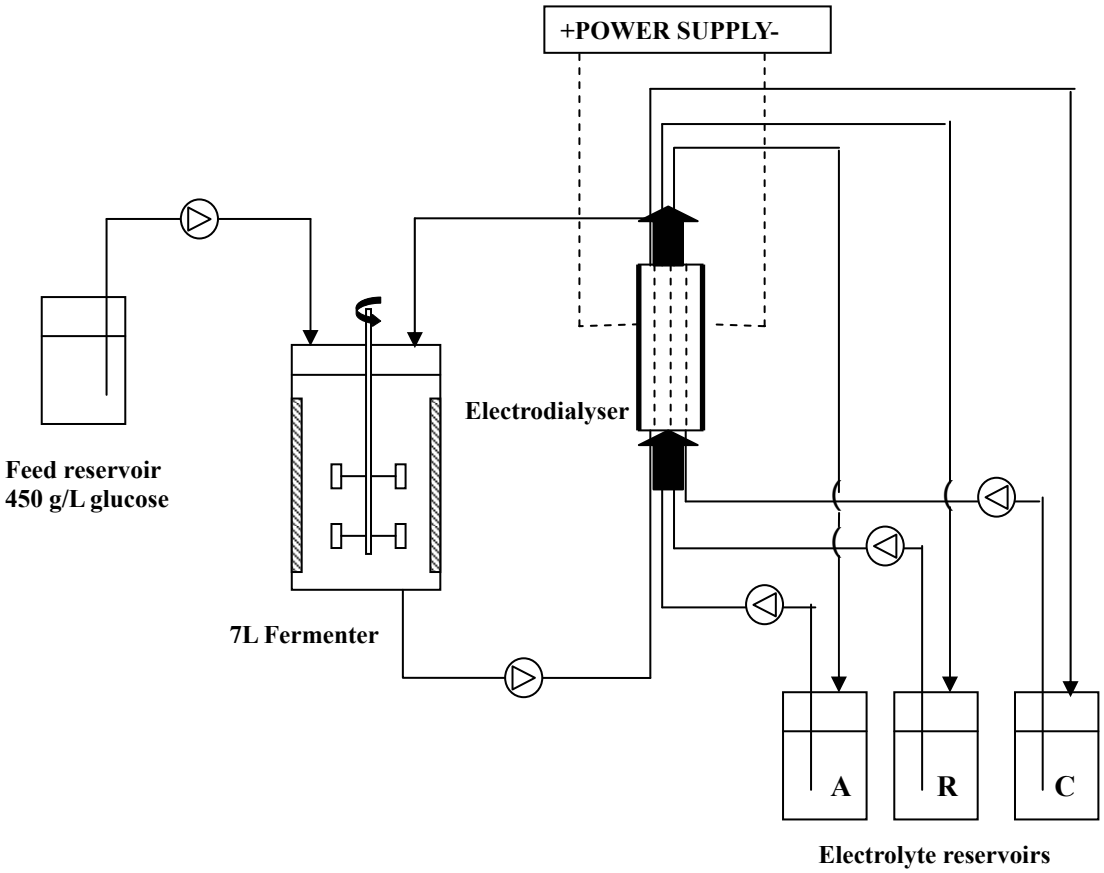

Figure 2.3(a). Experimental set-ups of the 7L batch/ fed-batch fermenter with detail of the electrodialysis module in a recycle loop and the associated electrolyte reservoirs.

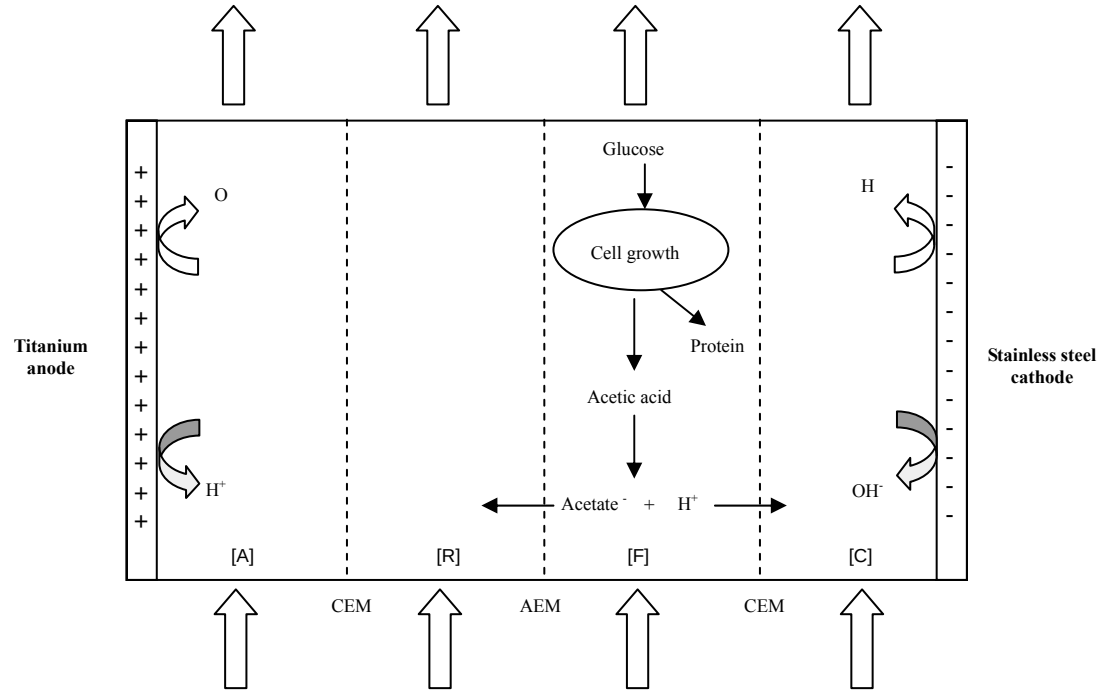

Figure 2.3(b). Principle of electrodialysis module set-up and operation for the *in situ* removal of acetic acid from *E.coli* fermentation broth.

Two controlled experiments were performed and the membrane configuration used is shown in Appendix B Figure B.2.

For both batch and fed-batch ED fermentations, a constant current of 2 A was applied to the electrodialysis module when acetic acid started to accumulate in the fermentation broth. This was indicated by the measured addition of ammonium hydroxide. The ED system was switched off when the fermentation reached the late exponential phase. At the end of each experiment, the electrolyte solution in reservoir R was sampled and analysed for the concentrations of acetate, glucose, biomass and GFP.

2.2.4 Bipolar electrodialysis module and fermentations

The standard operating procedures for bipolar electrodialysis (BPED) fermentation followed the methods described in Section 2.2.2 and 2.2.3. The only change made was replacing the electrodialysis module (Figure 2.1) with the BPED module (Figure 2.4a)

Figure 2.4(a) shows a schematic diagram and Figure 2.4(b) shows an actual photograph of the BPED system used for simultaneous acetate removal and fermenter pH control as described in Chapter 5. This BPED module consisted of six equal volume compartments fitted with two electrodes on each end, one-cation exchange, two-anion exchange and two-bipolar membranes (Neosepta, Tokuyama Corporation, Japan) having a total effective membrane area of 200 cm^2. Before operation, the module was chemically sterilised by 1 M sodium hydroxide. When BPED is applied, the fermentation broth is circulated through compartment F at a flow rate of 500 $mL.min^{-1}$, while 2 L of 2 M sodium sulphate flow through compartment A, R and C at the same rate. The automatic pH control was achieved using a proportional-integral-derivative

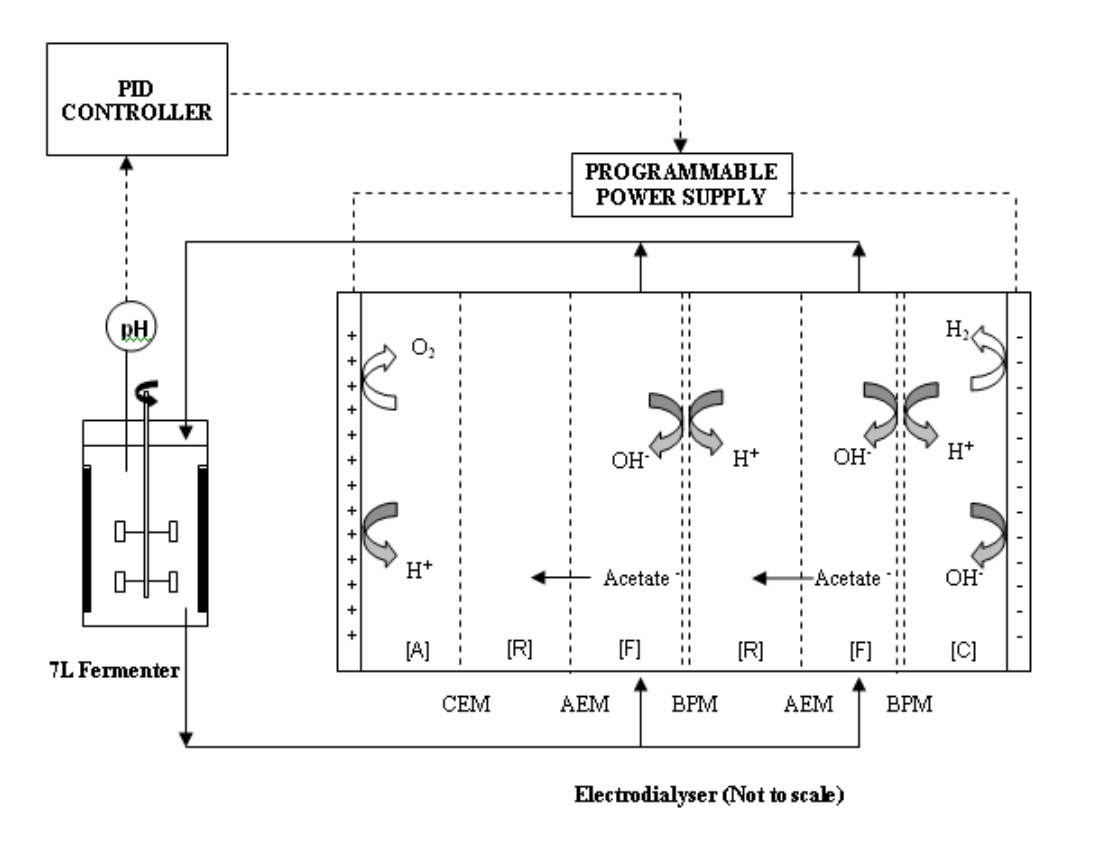

Figure 2.4(a) Principle of bipolar membrane electrodialysis module set-up and operation for the in situ removal of acetic acid from *E.coli* fermentation broth with simultaneous pH control: AEM, anion-exchange membrane; BPM, bipolar membrane; A, anode compartment; R, recovery compartment; F, fermentation compartment; C, cathode compartment.

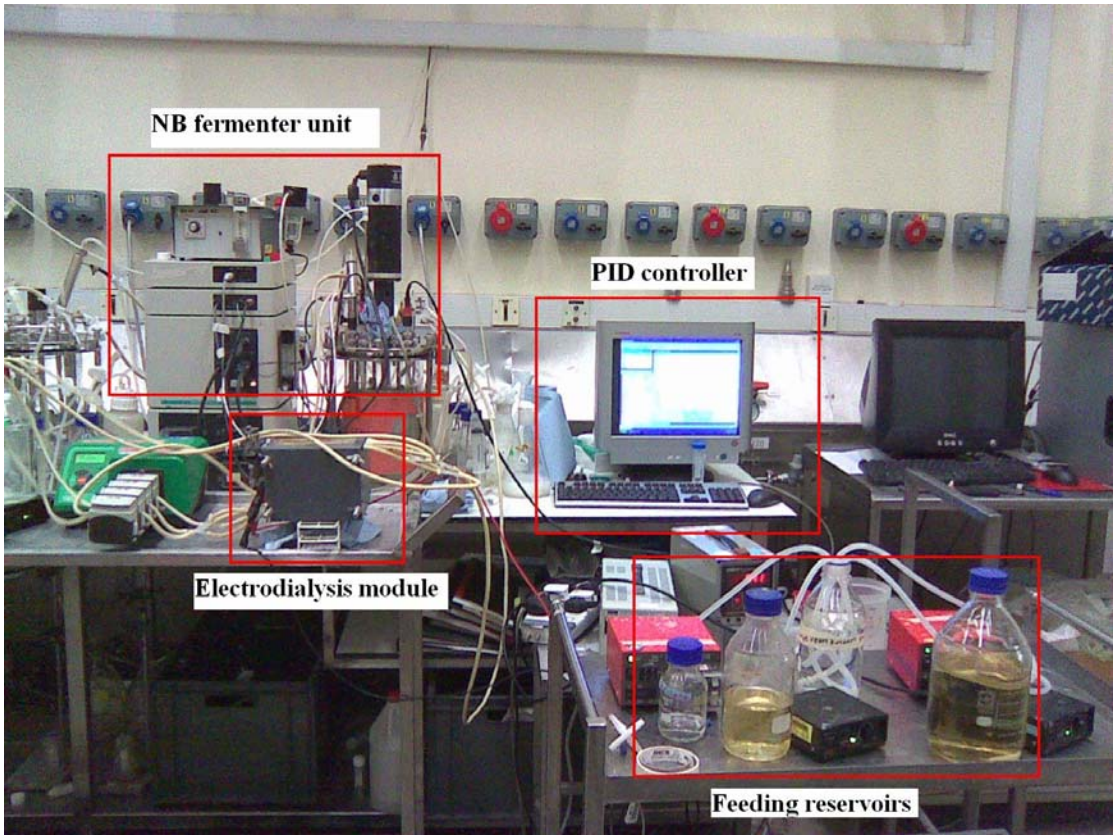

Figure 2.4(b) Photograph of the bipolar membrane electrodialysis fermentation system consisting of the NB (New Brunswick) fermenter unit, the bipolar electrodialysis module, the PC-based LabView PID controller and associated feeding reservoirs.

controller (Chen *et al*., 2005), linking measured pH and applied current via a LabView programme run on a PC. When the pH fell below the set point of 6.7, due to the production of acetic acid, the power output was increased accordingly, up to a maximum current of 5 A and a maximum voltage of 40 V. This results in the generation of hydroxide ions from the bipolar membrane in compartment F as well as removal of acetate ions from the fermentation broth in compartment F to compartment R via the anion exchange membrane. When the pH returned to pH 6.7, the current was switched off, so the pH remained constant and there would not be any removal of ions from compartment F.

The use of BPED allowed pH control without adding NH_4OH. However, another purpose of NH_4OH addition is to provide essential nitrogen source for cell growth, so it cannot be entirely eliminated. Therefore, the dynamic of PID controller was deliberately lowered by 20%, so the rate of hydroxyl ions produced was decreased. Consequently, NH_4OH was added from the standard pH controller attached to the fermenter to aid pH control and simultaneously supply nitrogen source to the cells.

2.2.5 Bioconversion *in situ* product removal

The potential of electrodialysis was further investigated by its application to *in situ* product removal and separation from enzyme catalysed bioconversions. The enzymatic hydrolysis of ethyl acetate and bioconversion of fumaric acid were studied. The bipolar electrodialysis bioreactor set-up was similar to the fermentation system described in Section 2.2.2.4 and the BPED system was used in Section 2.2.4.

2.2.5.1 Hydrolysis of ethyl acetate

3L of 20% v/v ethyl acetate was hydrolysed by adding 10 g of lipase and the mixture

was circulated through the bipolar electrodialysis module with a membrane configuration as shown in Figure 2.5(a). During hydrolysis, the inhibitory acetate was removed from compartment F to R and pH was maintained by the production of hydroxyl ions from the anodic side of the bipolar membrane. The operating conditions of the bioreactor were maintained automatically at 25 ^{o}C and pH 7 via a cooling jacket and addition of 1M ammonium hydroxide. The aeration rate was set at 1 vvm with stirrer speed of 400 rpm. When BPED was applied, the parameters of BPED system were as described in Section 2.2.4 with effective membrane are of 200 cm^2, recirculation flow rate of 500 $mL.min^{-1}$ and variable voltage applied according to pH. These conditions were kept constant in all ethyl acetate experiments

2.2.5.2 Bioconversion of fumaric acid

75 g of fumaric acid was dissolved in 3 L of 0.01 M sodium phosphate buffer with the addition of 2 M sodium hydroxide. Prior to the start of the bioconversion, the mixture was passed through the bipolar electrodialysis module as shown in Figure 2.5(b). The membrane configuration conserved all the ions within compartment F while the hydroxyl ions produced from the bipolar membrane adjusted the initial solution pH from 4 to 7.

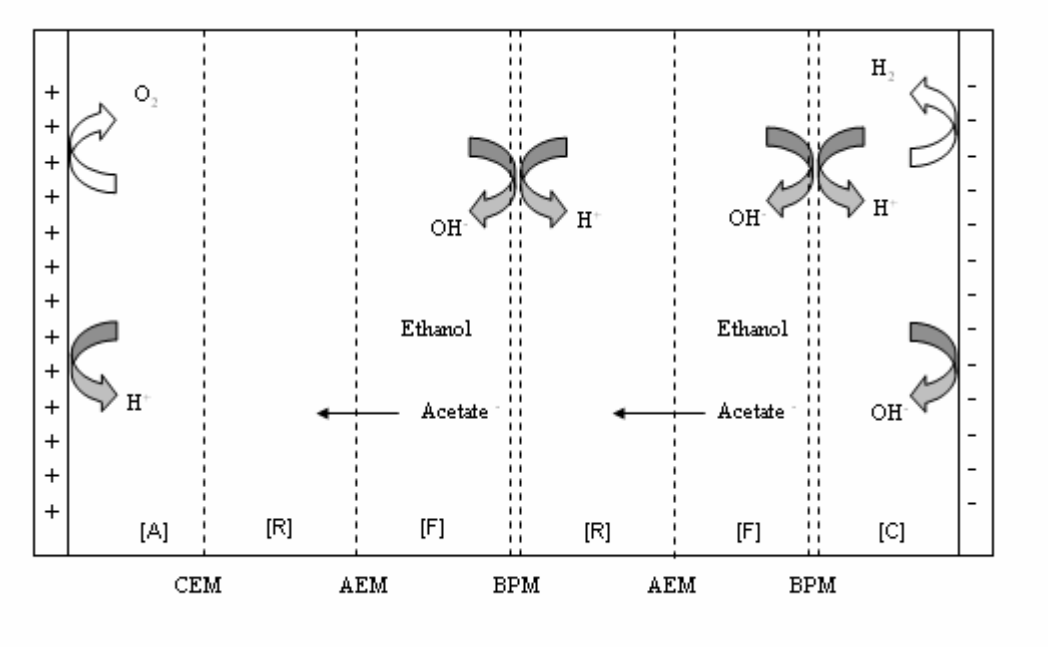

Figure 2.5(a) BPED module design and operation with membrane configuration of –C-A-B-A-B- for use with ethyl acetate. This serves to remove the negatively charged acetate ions from compartment F to R and provides pH control. (A: anion exchange membrane, B: bipolar membrane)

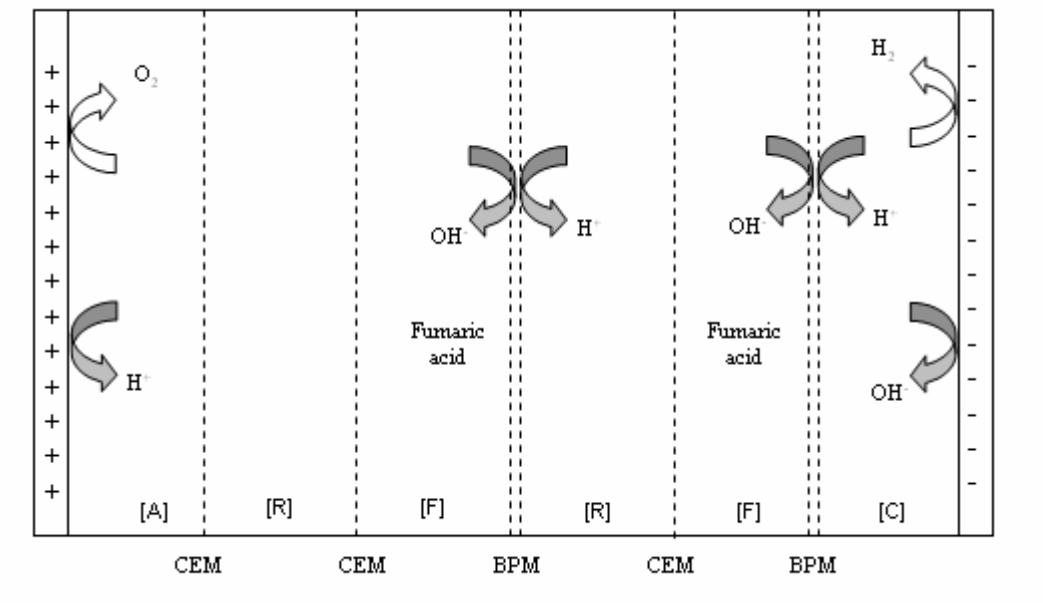

Figure 2.5(b) BPED module design and operation with a membrane configuration of –C-C-B-C-B-. This serves to provide hydrogen or hydroxyl ions without removal of other ions. (C: cation exchange membrane, B: bipolar membrane)

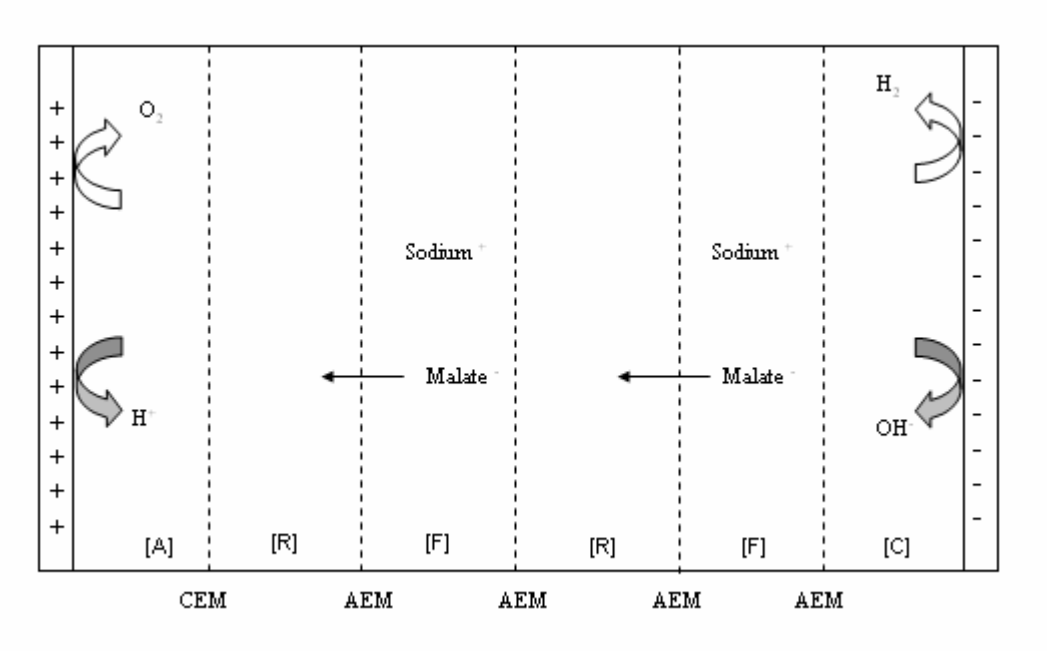

Figure 2.5(c) BPED module design and operation with membrane configuration of –C-A-A-A-A- for use with malate bioconversion. This serves to remove the negatively charged malate ions from compartment F to R. (A: anion exchange membrane, B: bipolar membrane)

10 mg of fumarase of activity 403 U.mg^{-1} protein was added to the bioreactor and fumaric acid was subsequently transformed to malic acid. However, the presence of sodium would cause the formation of sodium malate salt. Therefore, the solution was continuously circulated through the bipolar electrodialysis module again but with a different membrane configuration as shown in Figure 2.5(c). This converts sodium malate salt into free malic acid by the separation of sodium malate into the sodium cation and the malate anion, which then migrates through an anion exchange membrane from compartment F to R. The operating conditions of the bioreactor were maintained automatically at 25 ^{o}C and pH 7 via a cooling jacket and addition of 1M ammonium hydroxide. The aeration rate was set at 0.75 vvm with stirrer speed of 500 rpm. When BPED was applied, the parameters of BPED system were as described in Section 2.2.4 with effective membrane are of 200 cm^2, recirculation flow rate of 500 mL.min^{-1} and variable voltage applied according to pH. These conditions were kept constant in all ethyl acetate experiments.

2.2.6 Analytical methods

2.2.6.1 Biomass determination

The *E.coli* cell density was routinely determined by measuring the culture optical density (OD) at 600 nm using a spectrophotometer (Kontron Uvikon Spectrophotometer, Leeds, UK). Higher OD samples were diluted suitably with sterile media to have an absorbance in the range of 0.1-0.9. For the determination of dry cell weight, sample volumes of 10 mL were placed in 50 mL dried and pre-weighed Falcon tubes which were subsequently centrifuged for 20 min at 4,000 rpm and the cell pellets were dried at 100 ^{o}C in an oven until a constant weight was measured. The

calibration curve is shown in Figure 2.6.

2.2.6.2 GFP quantification

GFP is synthesized intracellularly, so it was necessary to first lyse cell samples, in order to measure the amount of GFP synthesised. 1 mL of culture sample was placed into a 1.5 mL Eppendorf tube and centrifuged at 13,000 rpm for 15 min. The supernatant was removed and the cell pellet was rinsed twice with phosphate buffered saline solution, before being mixed with 0.3 mL of Bugbuster^{TM} solution (Merck Chemicals Ltd, Nottingham, UK). The mixture was then incubated on a rotating mixer at 1,000 rpm (room temperature) until it was completely mixed. The cell debris was removed by centrifugation at 13,000 rpm for 15 minutes and the resultant supernatant used for GFP analysis. The concentration of GFP was quantified by the amount of fluorescence in each sample, using a calibration curve prepared with purified GFP. This was done using a Tecan Safire plate reader, at an excitation wavelength of 395 nm and an emission wavelength of 509 nm. Higher concentration GFP samples were diluted suitably with distilled water to have a relative fluorescence unit value beneath 1 x 10^5. The calibration curve is shown in Figure 2.7.

2.2.6.3 Glucose quantification

Glucose measurements were performed with a glucose analyser, BioProfile 400 (Nova biomedical Co., Waltham, USA). The machine was auto-calibrated each time before use and the measured glucose concentration is displayed. Culture samples were spun down and the supernatant was collected in a fresh tube and filtered using a 0.22μm syringe filter before being analysed by the glucose analyser. The calibration curve is shown in Figure 2.8.

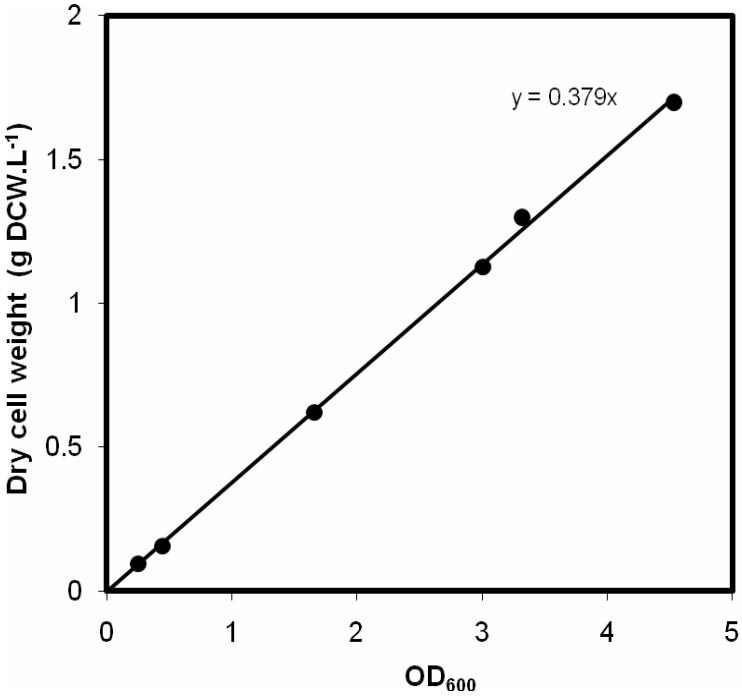

Figure 2.6 Correlation between dry cell weight (DCW) and optical density at 600 nm for *E.coli* TG1. Error quoted represent one standard deviation about the mean (n=3)

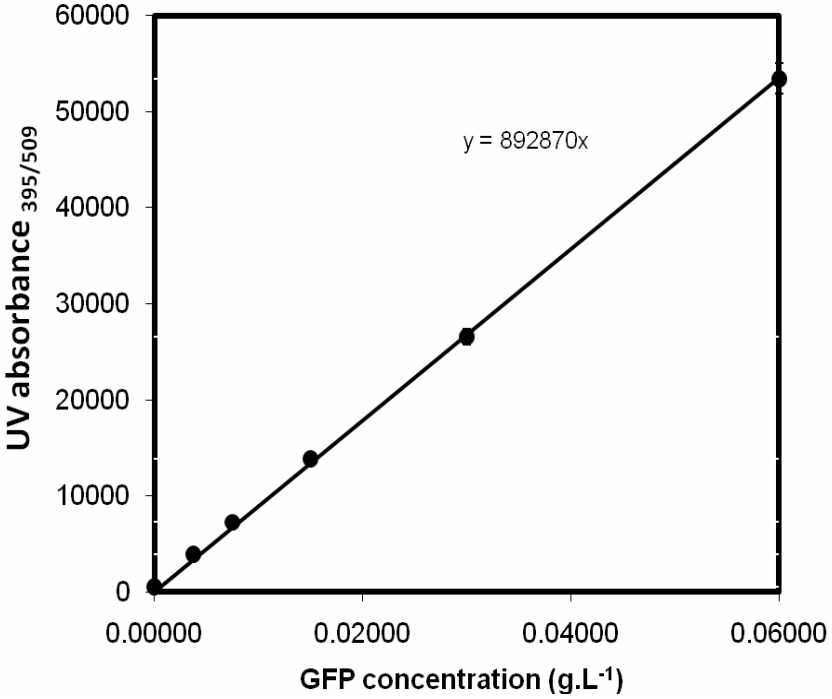

Figure 2.7 Quantification of GFP concentration with UV absorbance 395/509 nm. Error quoted represent one standard deviation about the mean (n=3)

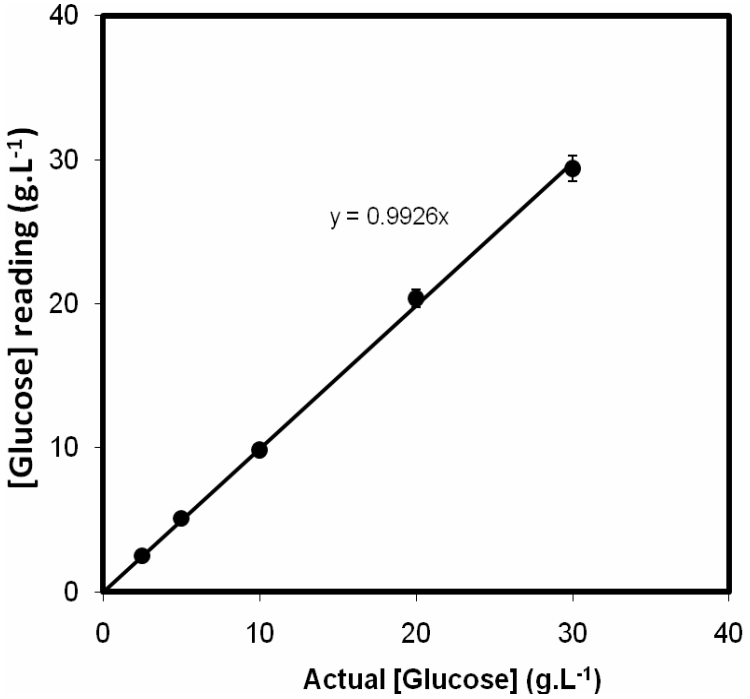

Figure 2.8 Measurement of glucose concentration using the glucose analyser. Error quoted represent one standard deviation about the mean (n=3)

2.2.6.4 Organic acids analysis

The concentration of the several organic acids used in this work was measured by HPLC using an Aminex ion-exchange column (7.8 x 300 mm; model HPX-87H; Bio-Rad Laboratories, Hertfordshire, UK). Assays were performed on a HPLC (UVD-1700, Dionex UK Ltd, Leeds UK) with UV detection at 210 nm under acidic conditions with 0.05 M sulphuric acid at pH 2.2 as the mobile phase at a flow rate of 0.6 $mL.min^{-1}$. The retention time for malic, lactic, acetic and fumaric acids were at approximately 11, 14, 15, 16 min, respectively. The calibration curves are shown in Figure 2.9.

2.2.6.5 Assay kits

Alternatively, the concentrations of ethanol, acetic and L-malic acids were determined using their specific assay kit (Megazyme International Ireland Ltd., Wicklow, Ireland). These were used when HPLC was not a suitable analytical tool, such as when the acidic nature of the mobile phase would cause hydrolysis of ethyl acetate. Appendix B1 shows all calibration curves using assay kits with error bars from at least triplicate determinations.

The quantification of ethanol is completed through two enzyme reactions. Reaction 2.1 is catalysed by alcohol dehydrogenase (ADH) where ethanol is oxidised to acetaldehyde by nicotinamide-adenine dinucleotide (NAD^+). The equilibrium of reaction 2.1 is in favour of ethanol and NAD^+, so a further reaction is require to trap the products. Reaction 2.2 is achieved by the quantitative oxidation of acetaldehyde to acetic acid in the presence of aldehyde dehydrogenase (Al-DH) and NAD^+. The amount of NADH formed is stoichiometric with twice the amount of ethanol. It is the

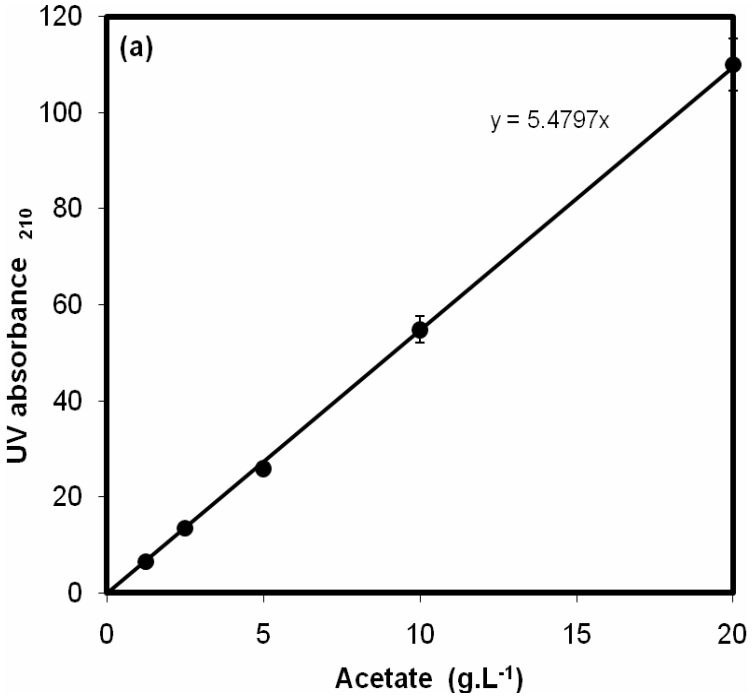

Figure 2.9(a) HPLC analysis of acetate concentration. Error quoted represent one standard deviation about the mean (n=3)

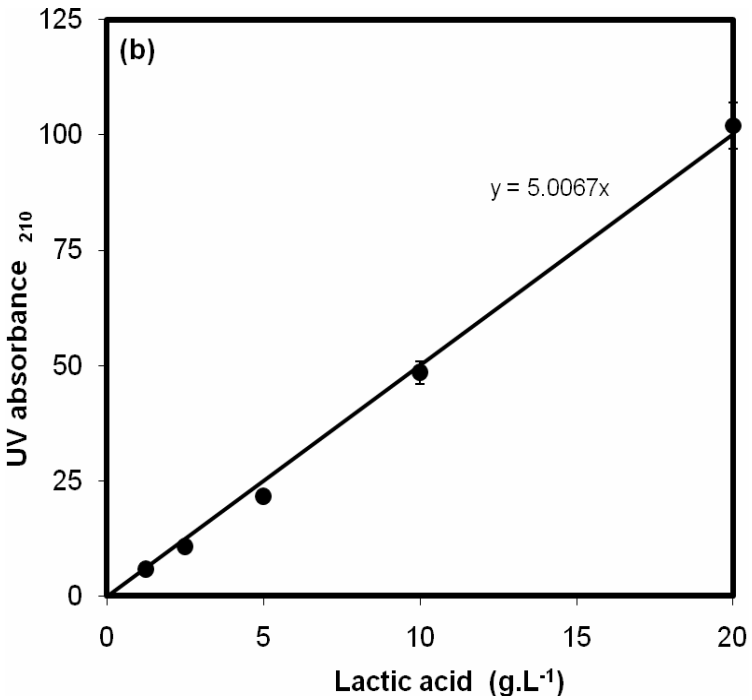

Figure 2.9(b) HPLC analysis of lactic acid concentration. Error quoted represent one standard deviation about the mean (n=3)

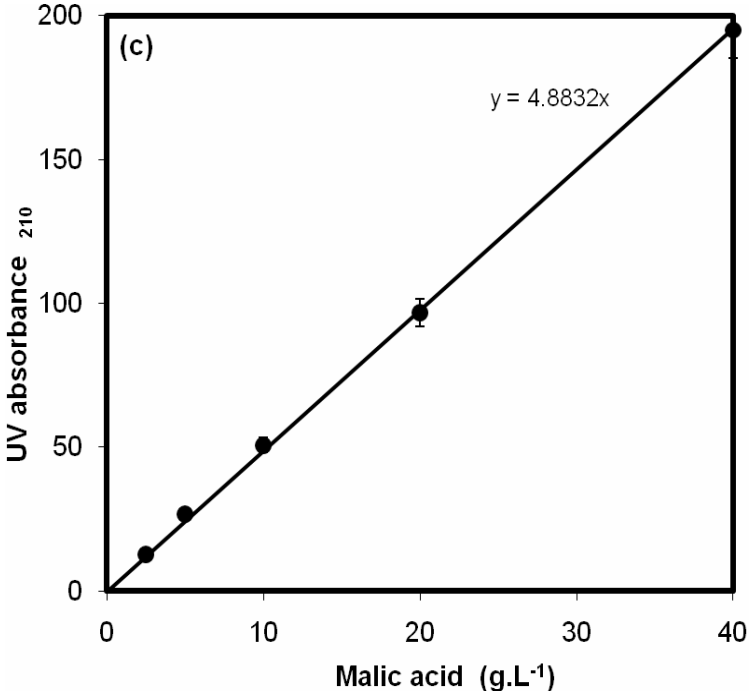

Figure 2.9(c) HPLC analysis of malic acid concentration. Error quoted represent one standard deviation about the mean (n=3)

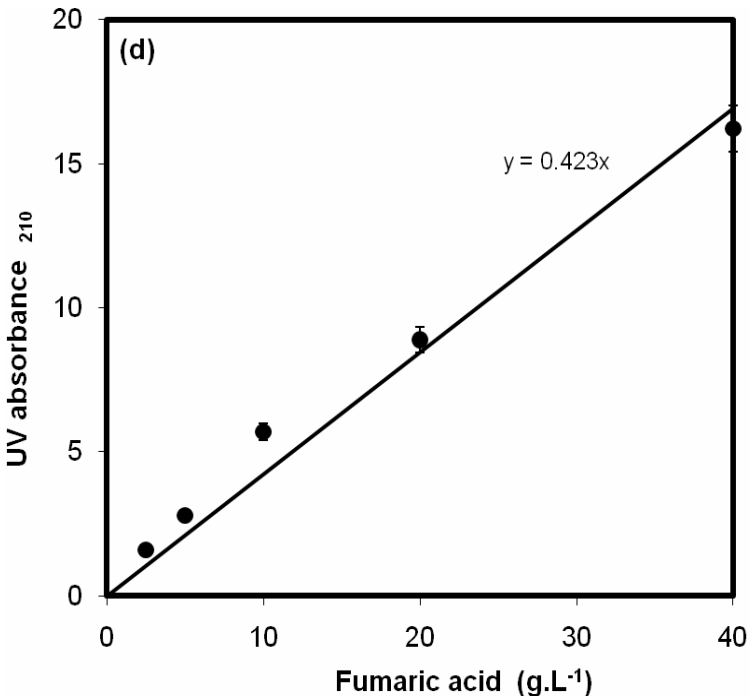

Figure 2.9(d) HPLC analysis of fumaric acid concentration. Error quoted represent one standard deviation about the mean (n=3)

NADH which is measured by the increase in absorbance at 340 nm. (Figure B.1)

(ADH)

$$\text{Ethanol} + NAD^+ \rightarrow \text{acetaldehyde} + NADH + H^+ \quad 2.1$$

(Al-DH)

$$\text{Acetaldehyde} + NAD^+ + H_2O \rightarrow \text{acetic acid} + NADH + H^+ \quad 2.2$$

Acetic acid was analysed through three reactions. Reaction 2.3 is the conversion of acetate to acetyl-CoA in the presence of the enzyme acetyl-CoA synthetase (ACS), adenosine triphosphate (ATP) and coenzyme A (CoA). In reaction 2.4, acetyl-CoA reacts with oxaloacetate to citrate in the presence of citrate synthase (CS). The oxaloacetate required for reaction 2.4 is formed from L-malate and NAD in the presence of L-malate dehydrogenase (L-MDH) in reaction 2.5. This test is based on the formation of NADH which is measured by the increase in absorbance at 340 nm. (Figure B.1)

(ACS)

$$\text{Acetic acid} + ATP + CoA \rightarrow \text{acetyl-CoA} + AMP + \text{pyrophosphate} \quad 2.3$$

(CS)

$$\text{Acetyl-CoA} + \text{oxaloacetate} + H_2O \rightarrow \text{citrate} + CoA \quad 2.4$$

(L-MDH)

$$\text{L-Malate} + NAD^+ \rightarrow \text{oxalacetate} + NADH + H^+ \quad 2.5$$

The detection of L-malic acid requires two enzyme reactions. Reaction 2.6 catalysed by L-malate dehydrogenase (L-MDH), L-malic acid is oxidised to oxaloacetate by NAD^+. The equilibrium of reaction 2.6 favours L-malic acid and NAD^+, so in order to drive the equilibrium backward, a further reaction was required. In reaction 2.7, oxalacetate is converted to L-aspartate and 2-oxoglutarate in the presence of a large excess of L-glutamate, by glutamate-oxaloacetate transaminase (GOT). This test is based on the formation of NADH which is measured by the increase in absorbance at 340 nm. (Figure B.1)

$$\text{L-Malate} + NAD^+ \xrightarrow{\text{(L-MDH)}} \text{oxalacetate} + NADH + H^+ \qquad 2.6$$

$$\text{Oxaloacetate} + \text{L-glutamate} \xrightarrow{\text{(GOT)}} \text{L-aspartate} + \text{2-oxoglutarate} \qquad 2.7$$

Chapter 3

Electrodialysis module design and operation: Solute mass transfer studies

3.1 Introduction

As described in Section 1.1 electrodialysis involves the transport of charged molecules and their separation through a selection ion exchange membrane (Xu and Huang, 2008). The applications of ion exchange membranes and electrodialysis have been used since 1890 for demineralisation of sugar syrup (Xu, 2005). The technique has since been widely used as an *in situ* product removal tool for the continuous separation of many organic acids, such as carboxylic (Huang *et al.,* 2007), citric (Ling *et al.,* 2002) and lactic (Choi *et al.,* 2002; Wee *et al.,* 2005) acids as they are produced during microbial fermentation. The principle of electrodialysis and integrated membrane system of this study has been discussed in detail in Section 1.1. Sections 2.1.1 and 2.2.1 have described the membrane module designed and fabricated for this study.

The aim of this chapter is to investigate the design parameters of the newly built electrodialysis module and to establish its robustness. For these initial studies a model extraction system is used comprising electrodes and ion exchange membranes in a four compartmented module. The specific objectives include:

- Quantification of the mass transfer rate of acetic acid as a function of module operational parameters e.g. voltage applied, flow rates of electrolyte circulation, ion exchange membrane area per unit volume, concentration of electrolyte and the initial feed concentration of acetic acid in compartment F.
- Investigation of the effect on solute mass transfer rate by the addition of culture medium.
- Maximising the performance of the electrodialysis module by optimisation of the design parameters.
- Establishment of reproducible data and the applicability of the electrodialysis module for other organic acids such as lactic acid and malic acid.

3.2 Results and discussions

3.2.1 Design and operational parameters

3.2.1.1 Voltage

The magnitude of the potential applied between the two electrodes in Figure 2.1 induces the strength of the electric field within the electrodialysis module and hence it is one of the key operational parameters. Figures 3.1a and 3.1b show the profile of acetate ions transferred from a model feed stream comprising of 5 $g.L^{-1}$ acetic acid at 40 V and 20 V, respectively. At 40V, 3.4 $g.L^{-1}$ of acetate was transferred from the feed compartment F to the product recovery compartment R in 180 min. In contrast at 20 V, over the same time period only 2.4 $g.L^{-1}$ of acetate was removed from compartment F. In both cases there is a good mass balance between the acetate ions transferred between

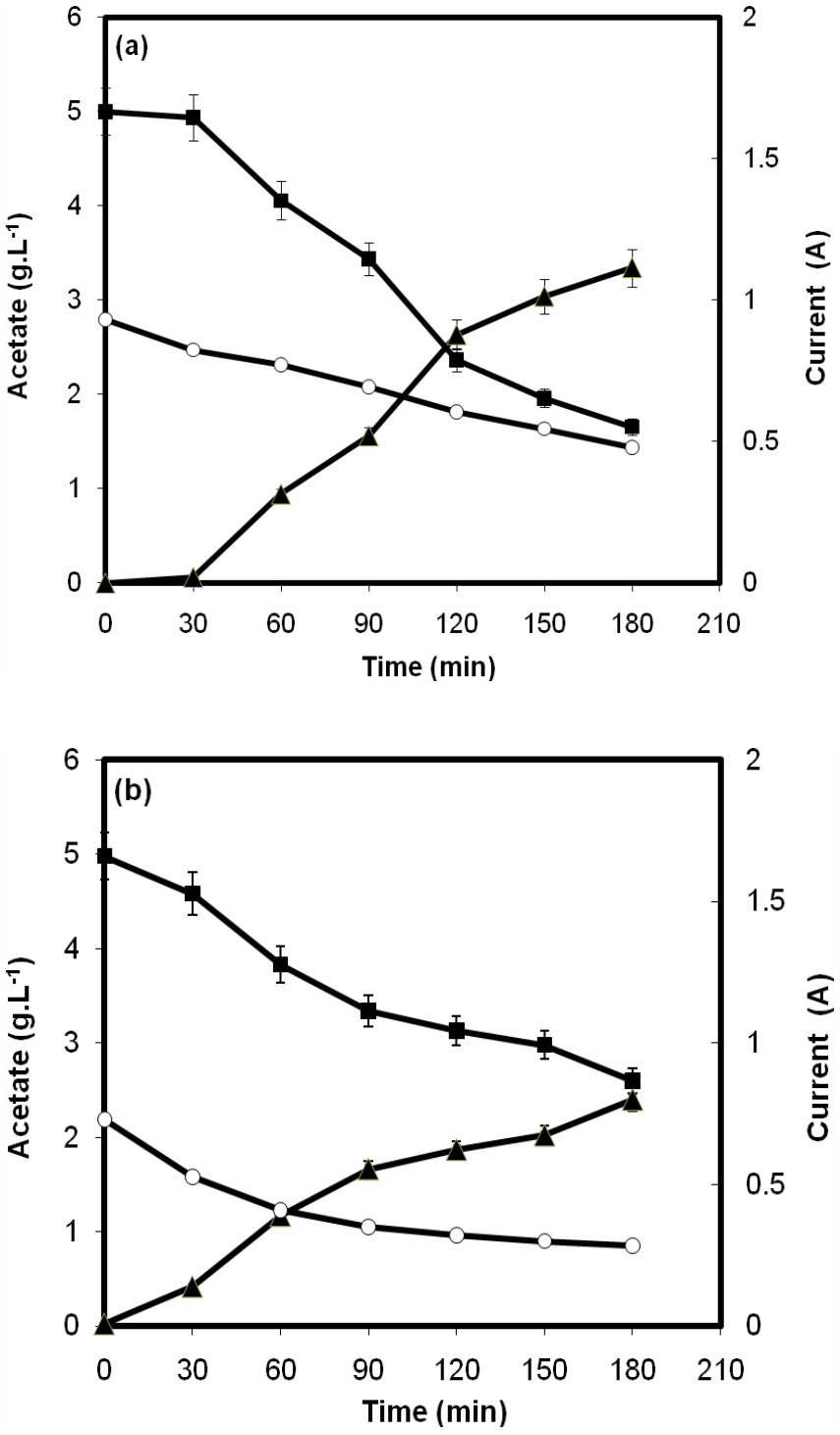

Figure 3.1. Mass transfer of acetate ions from model feed streams between feed compartment F (■) and product recovery compartment R (▲) at voltages of **(a)** 40 and **(b)** 20 V. Current ouput (○) during the experiemnt is also shown. Error bars represent one standard deviation about the mean (n=3). Experiments performed as described in Section 2.2.1.1 at initial feed concentration of 5 $g.L^{-1}$, feed flow rate of 300 $ml.min^{-1}$, ion exchange membrane per unit volume of 100 $cm^2.L^{-1}$ and electrolyte concentration of 0.2M.

the two compartments suggesting little, if any, acetate accumulation on the membrane surface. Also shown in Figure 3.1 is the measured current output during each experiment. This drops with the continuous removal of acetate from compartment F. Equation 1.1 suggests voltage is directly proportional to acetate transfer rate. However, in practice, this was not the case, because conductivities across the four compartments were constantly changing and process efficiency was below 100%.

3.2.1.2 Feed flow rate

The feed flow rate determines the residence time of feed in the membrane module as well as the solute mass transfer coefficient on the feed side of the membrane (Yu *et al.,* 2003). Figure 3.2 indicate the rate of acetate ion transfer at feed flow rates of 500, 300 and 100 $mL.min^{-1}$, respectively. At 500 and 300 $mL.min^{-1}$, the module performance is similar with 3.2 $g.L^{-1}$ of acetate being transferred to the product recovery compartment in 180 min. In contrast at the lowest flow rate studied at 100 $mL.min^{-1}$ the transfer of acetate ions was 20% lower. Therefore, the minimum flow rate to obtain an acceptable transfer rate is around 300 $mL.min^{-1}$. However, in relation to later bioreactor studies (Section 4.2) when active microbial culture will be circulated through the feed compartment it will also be desirable to minimise the broth residence time to limit any possibility of oxygen depletion hence the highest flow rate of 500 $mL.min^{-1}$ was used in the subsequent experiments.

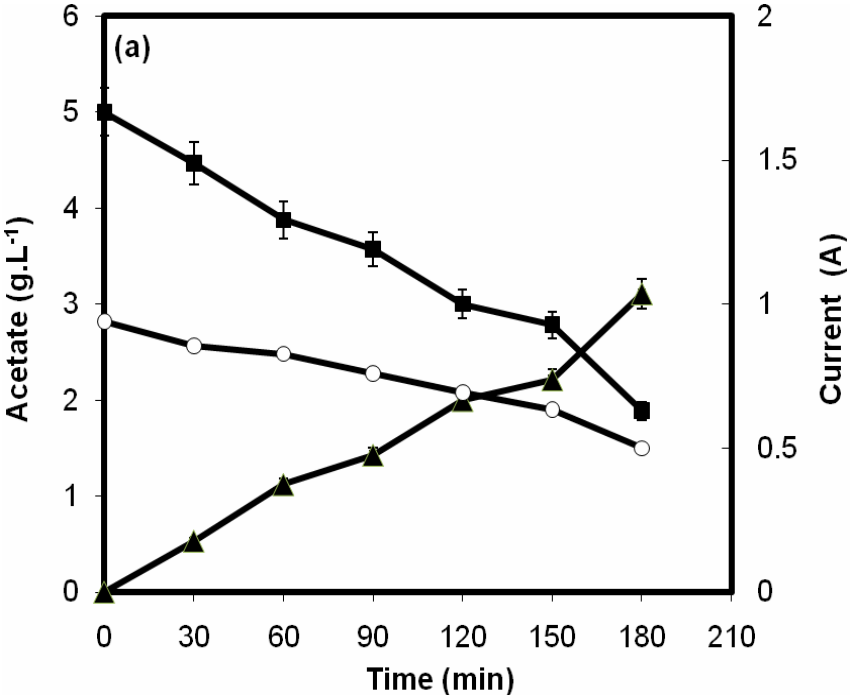
(a)
Acetate (g.L-1)
Current (A)
Time (min)
0
30
60
90
120
150
180
210
0
1
2
3
4
5
6
0
0.5
1
1.5
2

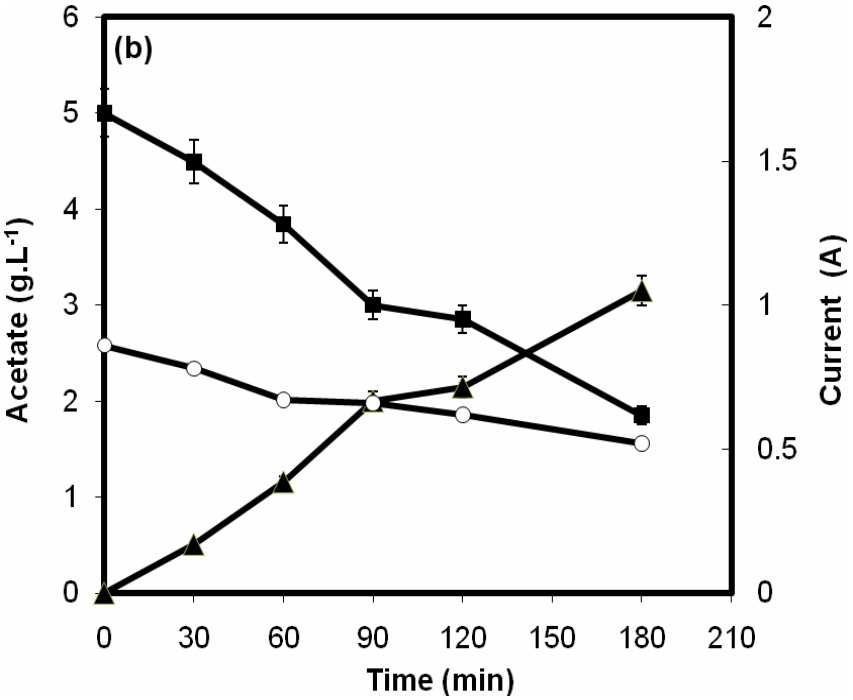
(b)
Acetate (g.L-1)
Current (A)
Time (min)
0
30
60
90
120
150
180
210
0
1
2
3
4
5
6
0
0.5
1
1.5
2

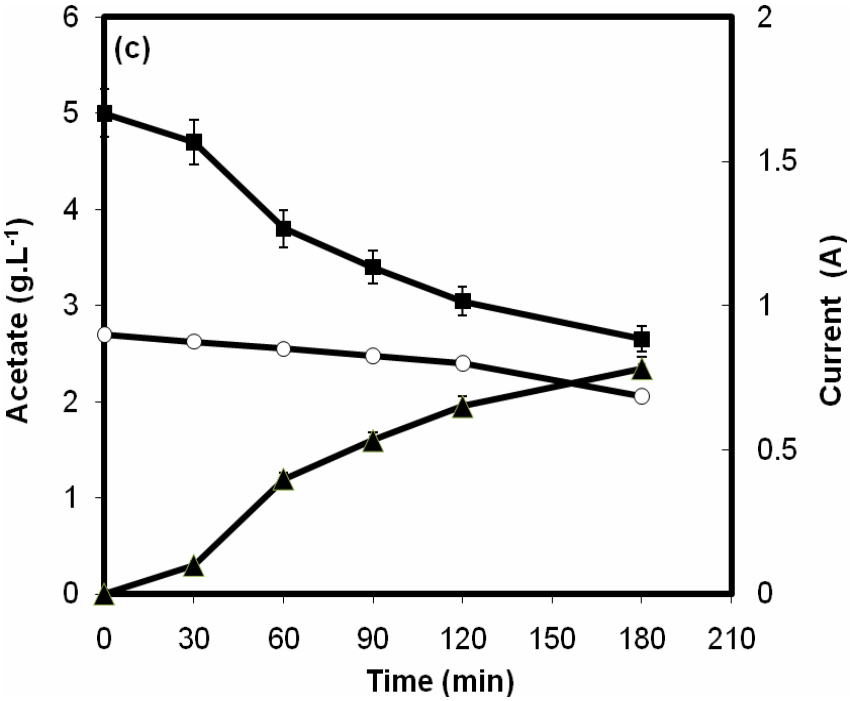

Figure 3.2. Mass transfer of acetate ions from model feed streams between feed compartment F (■) and product recovery compartment R (▲) at flow rates of **(a)** 500, **(b)** 300 and **(c)** 100 mL.min^{-1}. Current ouput (○) during the experiemnt is also shown. Error bars represent one standard deviation about the mean (n=3). Experiments performed as described in Section 2.2.1.1 at initial feed concentration of 5 g.L^{-1}, voltage of 40 V, ion exchange membrane per unit volume of 100 cm^2.L^{-1} and electrolyte concentration of 0.2M.

3.2.1.3 Membrane area per unit volume

The area of ion exchange membrane per unit volume of feed solution directly influences the rate of ions migration from compartment F to R. Figure 3.3 demonstrates the rate of acetate ion transfer with membrane area per unit volume of 50, 100 and 200 $cm^2.L^{-1}$, respectively. Figure 3.3c clearly indicates the greater the ratio of membrane area to unit volume, the greater the mass transfer of acetate. Also, in this experiment the current output also decreased rapidly, as all 5 $g.L^{-1}$ of acetate was transferred in 180 min. However at pilot scale, it is unlikely to operate with such high ratio of 200 $cm^2.L^{-1}$ because limitation of designed module. Typical industrial units have a membrane area to unit volume ratio of 0.5 $m^2.L^{-1}$ (Xu. 2005). Equation 1.1 suggests membrane area per unit volume is directly proportional to acetate transfer rate. However, in practice, this was not the case, because conductivities across the four compartments were constantly changing and process efficiency was below 100%.

3.2.1.4 Concentration of electrolyte

As described in Section 1.1, the concentration of electrolyte is directly linked to conductivity which is proportional to the current output. Figure 3.4 illustrates acetate ion transfer at different concentrations of sodium sulphate of 0.4, 0.2 and 0.1 M, respectively. Sodium sulphate was added for ED application because of high conductance at low concentration (Park *et al.*, 2006). At all three added concentrations of sodium sulphate, similar current output and mass transfer rates were obtained. However, as shown by the current data, at higher concentrations, the system would consume energy in transferring the electrolyte between compartments.

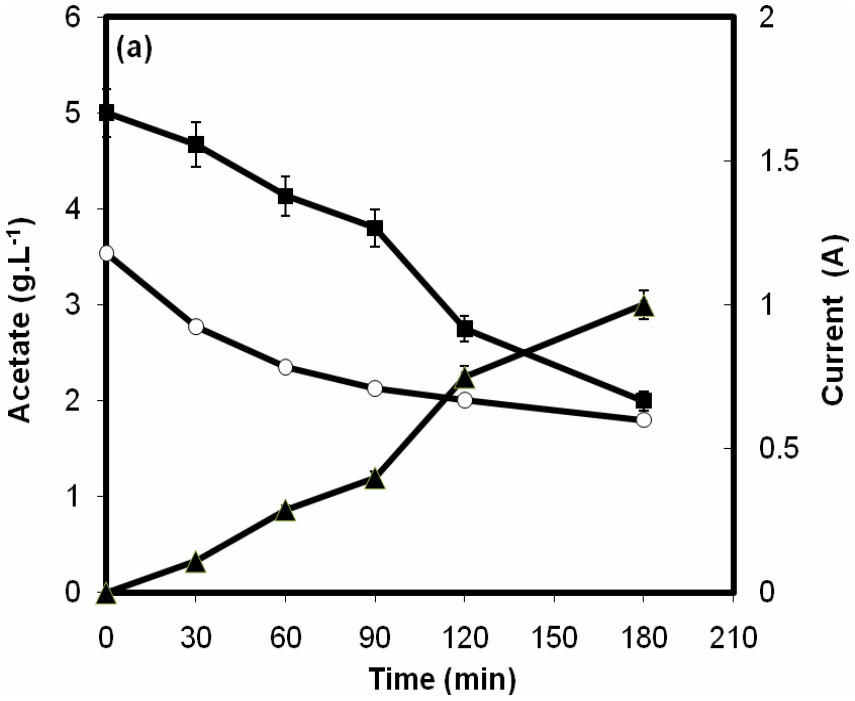
(a)
Acetate (g.L-1)
Current (A)
Time (min)
0
30
60
90
120
150
180
210
0
1
2
3
4
5
6
0
0.5
1
1.5
2

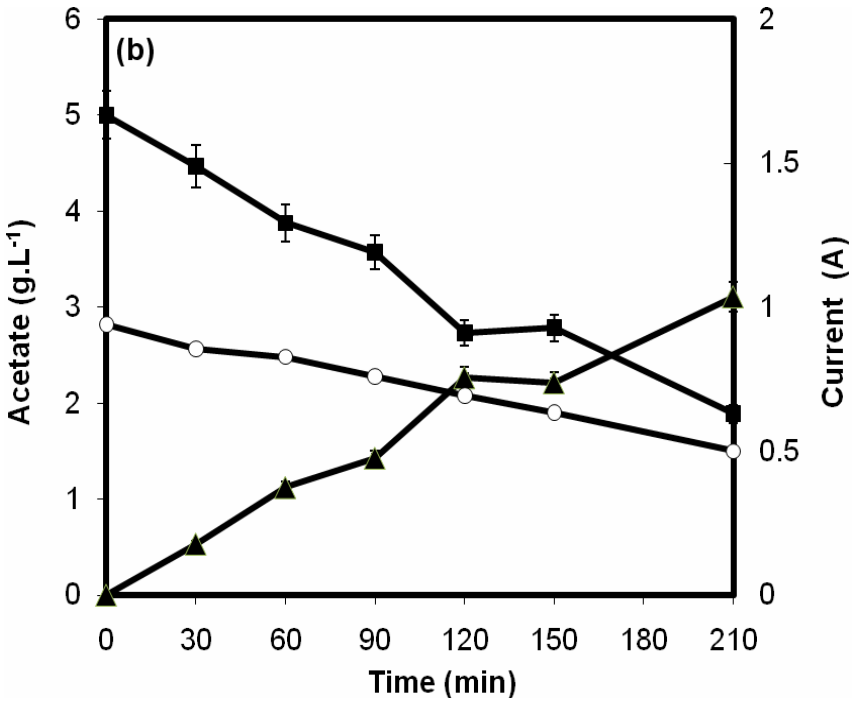
(b)
Acetate (g.L-1)
Current (A)
Time (min)
0
30
60
90
120
150
180
210
0
1
2
3
4
5
6
0
0.5
1
1.5
2

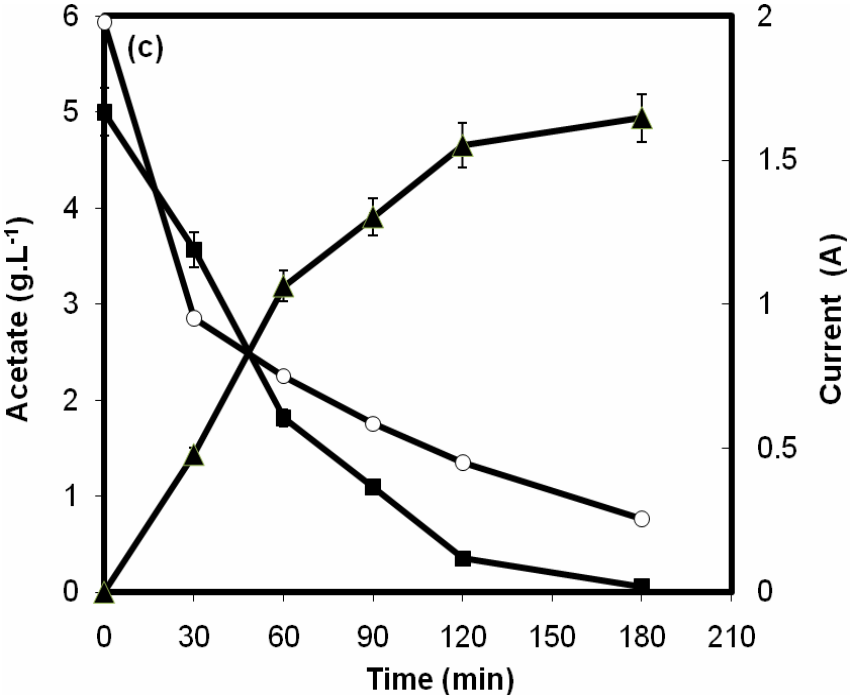

Figure 3.3. Mass transfer of acetate ions from model feed streams between feed compartment F (■) and product recovery compartment R (▲) at membrane area per unit volume of **(a)** 50, **(b)** 100 and **(c)** 200 $cm^2.L^{-1}$ Current ouput (○) during the experiemnt is also shown. Error bars represent one standard deviation about the mean (n=3). Experiments performed as described in Section 2.2.1.1 at initial feed concentration of 5 $g.L^{-1}$, voltage of 40 V, flow rate of 300 $mL.min^{-1}$ and electrolyte concentration of 0.2M.

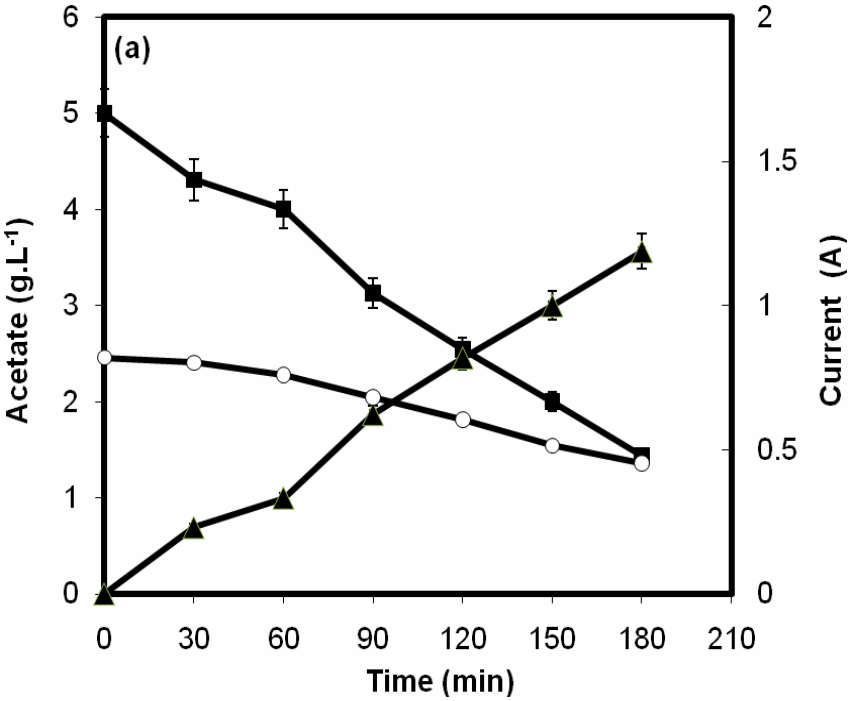
(a)
Acetate (g.L-1)
Current (A)
Time (min)
0
30
60
90
120
150
180
210
0
1
2
3
4
5
6
0
0.5
1
1.5
2

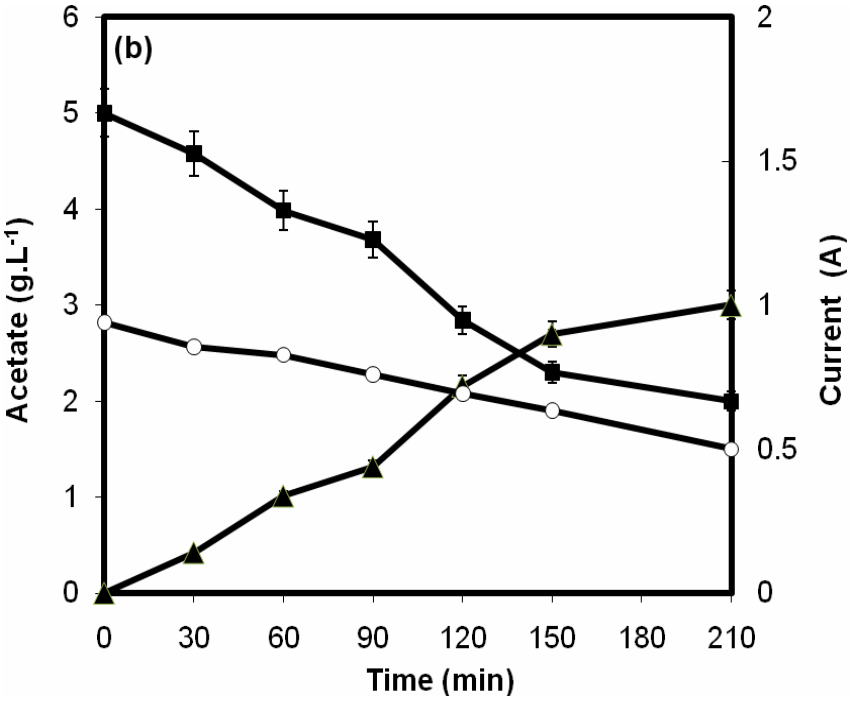
(b)
Acetate (g.L-1)
Current (A)
Time (min)
0
30
60
90
120
150
180
210
0
1
2
3
4
5
6
0
0.5
1
1.5
2

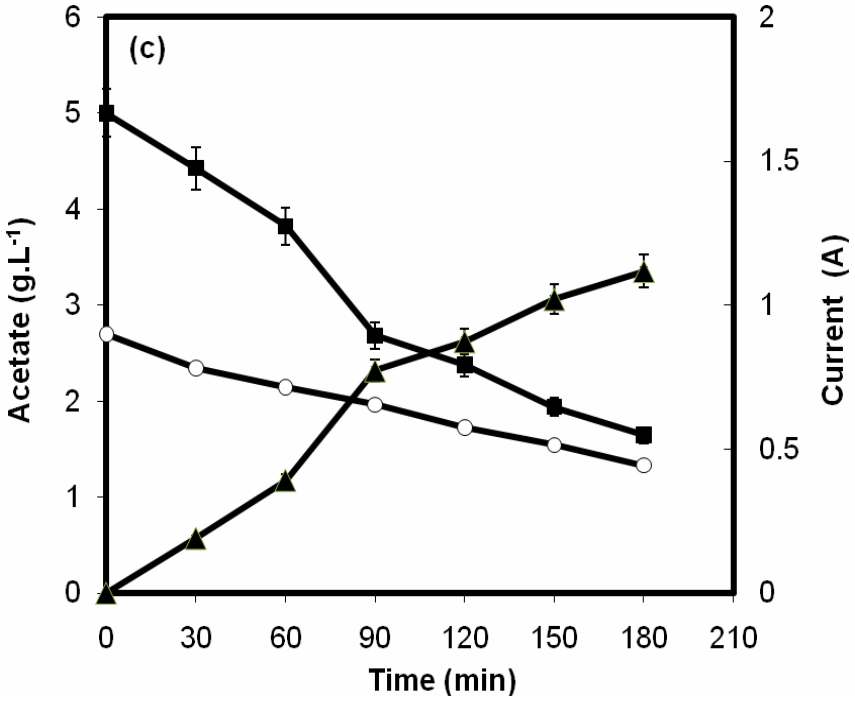

Figure 3.4. Mass transfer of acetate ions from model feed streams between feed compartment F (■) and product recovery compartment R (▲) at concentrations of electrolyte of **(a)** 0.4, **(b)** 0.2 and **(c)** 0.1 M. Current ouput (○) during the experiemnt is also shown. Error bars represent one standard deviation about the mean (n=3). Experiments performed as described in Section 2.2.1.1 at initial feed concentration of 5 $g.L^{-1}$, feed flow rate of 300 $ml.min^{-1}$, ion exchange membrane per unit volume of 100 $cm^2.L^{-1}$ and voltage of 40V.

3.2.1.5 Initial acetate concentration

Varying the initial concentration of acetate in compartment F will simulate the different levels of this fermentation by-product (Section 1.2.2) that can be removed within given time periods by the ED module used here. Figures 3.5a and 3.5b show the comparison of solute mass transfer at initial acetate concentrations of 5 and 20 $g.L^{-1}$, respectively. After 210 min operation a maximum 50 % of the initial acetate is removed from a starting concentration of 5 $g.L^{-1}$ and 50 % from the starting concentration of 20 initial $g.L^{-1}$. This suggests that in the fermentation experiments if acetate is produced at these levels then ED module used here will be unable to completely remove the accumulated acetate. At this point in the project it was not possible to build a larger ED module due to lack of available funding and so it is estimated that the maximum rate of acetate formation during a fermentation that could be removed into compartment R is 2.5 $g.L^{-1}.h^{-1}$.

3.2.1.6 Acetate extraction from real fermentation medium

In a real *in situ* product/by-product removal situation acetate must be removed from a complex, multi-component fermentation medium. This creates competition of ion transfer across the ion-selective membrane while the larger proteinaceous components may also bind or cause progressive membrane fouling over time (Koter, 2007). Figure 3.6 shows the difference in current output and acetate migration rate from the model feed stream used in earlier experiments and from the Korz medium (composition as in Table 2.1) that will be used in the later fermentation experiments described in Chapter 4. The extra ions in compartment F with the Korz medium will increase the medium conductivity and so as shown in Figure 3.6 the measured current output was two times higher and also constant at 2 A. However, in terms of the acetate transfer rates these

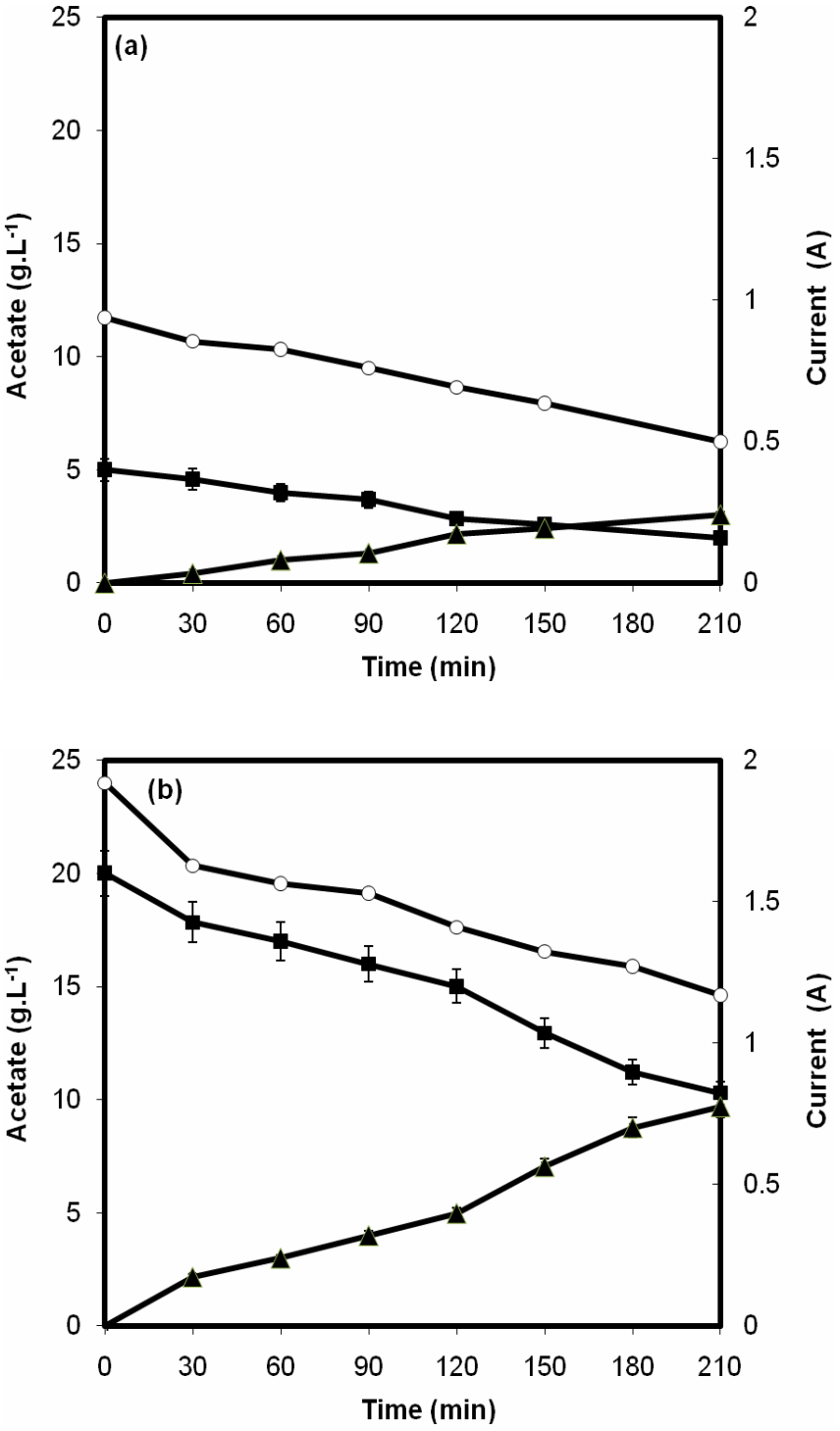

Figure 3.5. Mass transfer of acetate ions from model feed streams between feed compartment F (■) and product recovery compartment R (▲) at initial concentrations of acetate of **(a)** 5, **(b)** 20 $g.L^{-1}$. Current ouput (○) during the experiemnt is also shown. Error bars represent one standard deviation about the mean (n=3). Experiments performed as described in Section 2.2.1.1 at electrolyte concetration of 0.2 M, feed flow rate of 300 $ml.min^{-1}$, ion exchange membrane per unit volume of 100 $cm^2.L^{-1}$ and voltage of 40V.

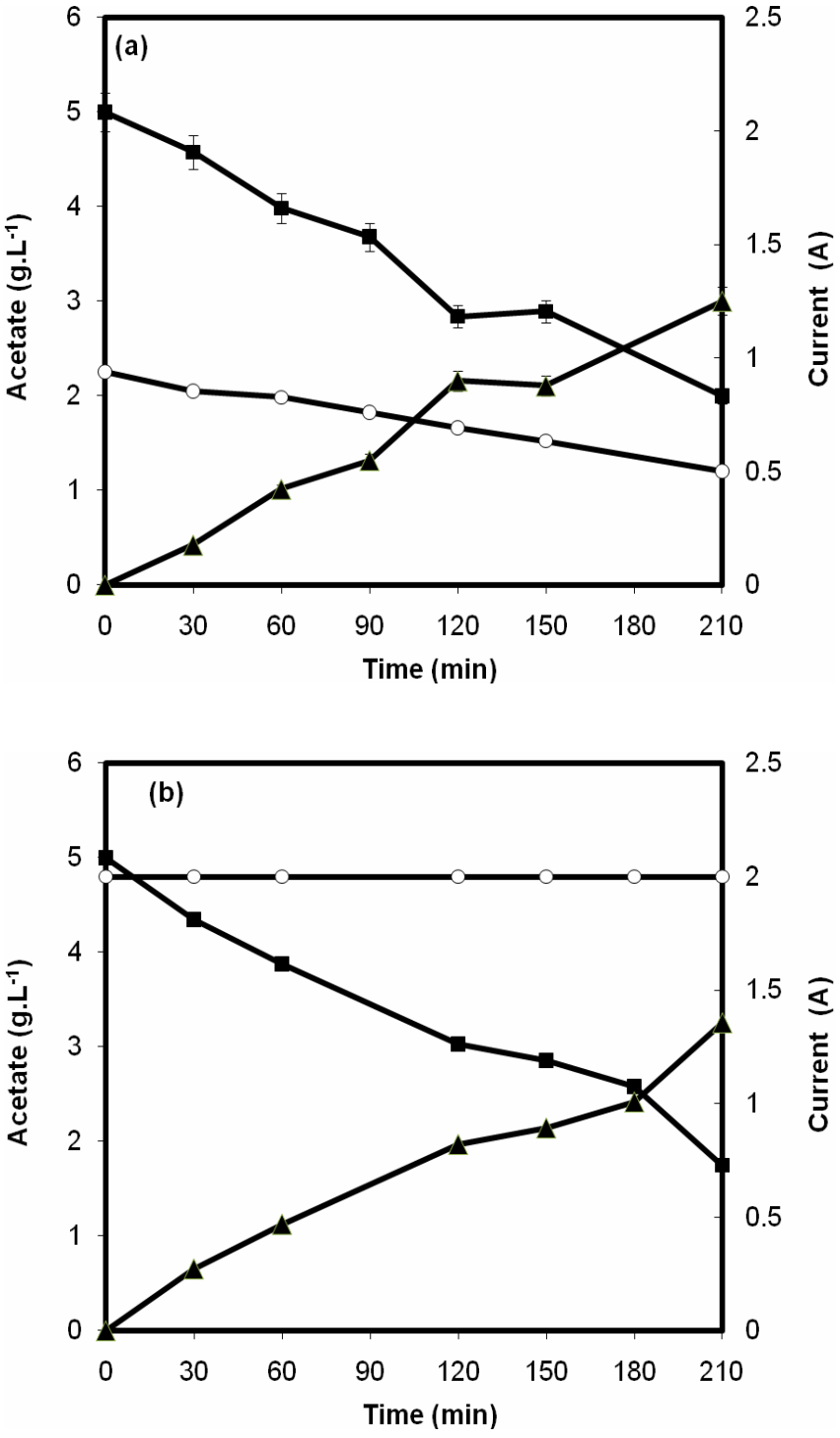

Figure 3.6. Mass transfer of acetate ions from model feed streams between feed compartment F (■) and product recovery compartment R (▲) **(a)** without and **(b)** with medium addition. Current ouput (○) during the experiemnt is also shown. Error bars represent one standard deviation about the mean (n=3). Experiments performed as described in Section 2.2.1.1 at electrolyte concetration of 0.2 M, feed flow rate of 300 $ml.min^{-1}$, ion exchange membrane per unit volume of 100 $cm^2.L^{-1}$ and voltage of 40V and initial concentrations of acetate of 5 $g.L^{-1}$.

were found to be very similar. The fact that the transfer rate is relatively constant over time also suggests there was no protein fouling of the membrane at least over 3 hours duration of this experiment.

These results suggest that while the transfer rate remain unaltered more energy is required in transferring acetate ions in the presence of the Korz medium from compartment F to R. In actual electrodialysis fermentation, medium ions will be undesirably removed and have an adverse effect on the fermentation performance. Therefore, this will be compensated by operational mode of ED as discussed in Section 2.2.3.

3.2.2 Comparison of acetate mass transfer rate with other organic acids

In Section 3.2.1, several ED module design and operational parameters were investigated for the mass transfer of acetate ions. Using these conditions, the mass transfer of lactic acid and malic acid were performed to establish reproducible mass transfer rate and the electrodialysis module to withstand other organic acids. Figure 3.7 show a comparison of mass transfer rate for acetic, lactic and malic acid under the operating conditions of 40V at 500 $mL.min^{-1}$ with membrane per unit volume of 100 $cm^2.L^{-1}$ and electrolyte concentration of 0.2M. In all three separate experiments, 3.2-3.4 $g.L^{-1}$ of organic acid was removed from compartment F to R in 180 min suggesting the mass transfer rates (2.5 $g.L^{-1}.h^{-1}$) of these ions were very similar. Kim and Moon (2001) achieved 50 $g.L^{-1}.h^{-1}$ of lactic acid removal with an industrial ED unit (TS3B-2-5, Tokuyama Corp, Japan) of 1200 cm^2 effective IE membrane area and operating current of 12 A. A ratio of mass transfer rate and membrane are of 0.0416 $(g.L^{-1}.h^{-1}).cm^{-2}$, compared to 0.025 $(g.L^{-1}.h^{-1}).cm^{-2}$ used in this study

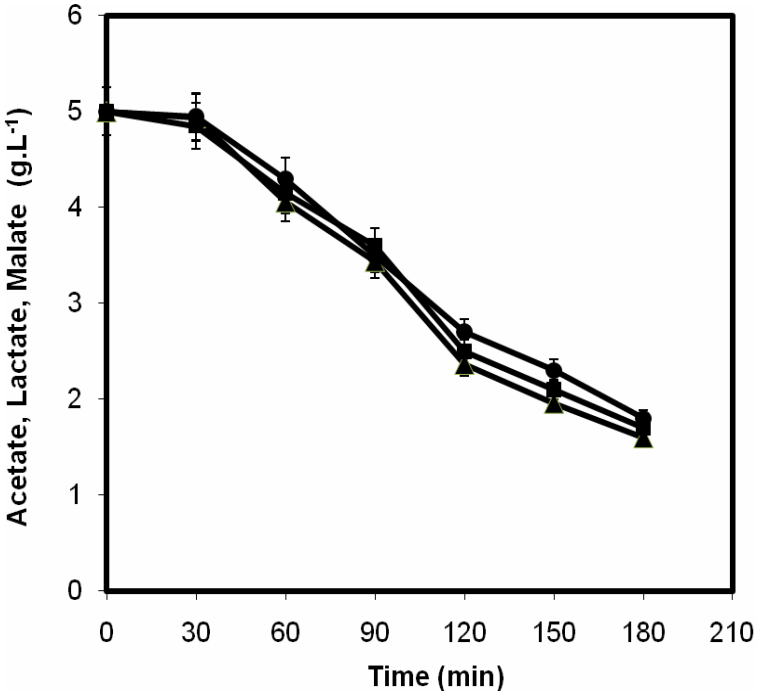

Figure 3.7. Comparison of solute mass transfer rates from model solutions for acetate (▲), lactate (■) and malate (●) ion concentrations depleted from compartment F. Error bars represent one standard deviation about the mean (n=3). Experiments performed as described in Section 2.2.1.1 at electrolyte concetration of 0.2 M, .feed flow rate of 300 ml.min^{-1}, ion exchange membrane per unit volume of 100 cm^2.L^{-1} and voltage of 40V and initial concentrations of acetate of 5 g.L^{-1}.

3.3 Summary

In this chapter, the basic design of the ED module has been described and its performance evaluated as a function of key operational parameters. The results indicate that the optimum operating conditions of the ED module for acetate mass transfer. These include an applied voltage of 40 V (Figure 3.1) and recirculation flow rate of 500 $mL.min^{-1}$ (Figure 3.2). However, there are certain parameters such membrane area per unit volume of 200 $cm^2.L^{-1}$ (Figure 3.3) and concentration of electrolyte of 0.4 M (Figure 3.4), which are not feasible to operate at the maximal rate at pilot scale. So less optimised conditions of 100 $cm^2.L^{-1}$ and 0.2M would be considered, but still provides an effective ion transfer rate. The limit of the electrodialysis module was also tested with a range of initial acetate concentration (Figure 3.5) and the addition of culture medium (Figure 3.6). Overall, under these design parameters, an organic acid transfer rate of 1.5 $g.L^{-1}.h^{-1}$ was achieved (Figure 3.7).

The reproducibility of all the data presented in this chapter also helps confirm the reliability of this newly-built ED module and the associated Standard Operating Procedures (SOPs) described in Section 2.2.1. Having established the ED module design and confidence in its performance its application to *in situ* product removal applications for both microbial fermentation (Chapters 4 and 5) and enzymatic bioconversion (Chapter 7) will next be investigated.

Chapter 4

Impact of electrodialysis on acetate removal and recombinant protein synthesis in *E.coli* fermentation: Late protein induction[1]

4.1 Introduction

E.coli is one of the most important host organisms for biochemical synthesis (Varma *et al*., 1993), in particular for the production of recombinant enzymes and therapeutic proteins (Pavlou and Reichert, 2004). One of the challenges in achieving high product yield is the accumulation of metabolic by-products such as acetate (Han *et al*., 1992). Acetic acid is undesirable because it retards cell growth (Han *et al*., 1992; Luli and Strohl, 1990), and is known to inhibit recombinant protein synthesis (Jensen and Carlsen, 1990; Koh *et al*., 1992; Turner *et al*., 1994). Formation of acetic acid in *E.coli* fermentation occurs under fully aerobic growth conditions and its production rate is directly associated with the rate of cell growth, substrate uptake and oxygen consumption (Han *et al*., 1992). One explanation for acetate accumulation is that at

[1]The majority of results presented in this chapter have previously been published as Wong M, Wright M, Woodley JM, Lye GJ (2009) Enhanced recombinant protein expression in batch and fed-batch *Escherichia coli* fermentation based on removal of inhibitory acetate by electrodialysis. Journal of Chemical Technology and Biotechnology 84: 1284-1291

high glucose uptake rate, the flux of acetylCoA is high and so it is directed to acetate (via acetyl phosphate) instead of entering the TCA cycle. At this point further increases in glucose uptake result in overflow metabolism of acetyl-CoA to acetate (Eiteman and Altman, 2006). The problem becomes more severe in high cell concentration cultivation (Kleman and Strohl, 1994), where high oxygen and substrate uptake rates generally result in a much greater production of acetic acid (Delisa *et al*., 1999).

A number of strategies have been developed to overcome the problem of acetate inhibition. These have been reviewed recently (Eiteman and Altman, 2006). One of the most widely used methods is the implementation of a controlled carbon feeding strategy. This can be carried out at a pre-determined feeding rate to keep the growth of the cells beneath a threshold rate (Xu *et al*., 1999). However, the feed rates used must be lower than the optimal glucose uptake rate for maximum cell growth, thus limiting productivity. Other feeding strategies include feedback control of glucose addition via acetate detection (Akesson *et al*., 2001), and on-line glucose measurement to maintain a low glucose level (Kleman *et al*., 1991). High cell densities up to 190 $g.L^{-1}$, have also been obtained by removal of the inhibitory acetate via dialysis (Fuchs *et al*., 2002; Nakano *et al*., 1997). These studies, however, were carried out using wild type *E. coli*, in the absence of recombinant protein synthesis and productivity was assessed solely on the basis of biomass production. Electrodialysis is another potential technique for acetate removal as described in Section 1.1.3. The configuration of a potential electrodialysis module for application to acetate removal from fermentation broths and the principle of operation are shown in Figure 2.3.

Similar inhibitory problems can also arise due to small molecule product synthesis which has led to the use of *in-situ* product removal techniques to increase reactor productivity (Lye and Woodley, 1999; Stark and von Stockar, 2003; Woodley *et al*., 2008). ISPR has previously been applied to remove toxic or inhibitory products. One particular case is lactic acid fermentation, where the productivity is inhibited by lactic acid accumulation (Kumar Dutta *et al*., 1996). To overcome this inhibition, electrodialysis was employed during fermentation to remove lactic acid as it was produced and thus increased product yield (Gao *et al*., 2004; Hirata *et al*., 2005; Li *et al*., 2004). Elsewhere, electrodialysis (ED) is primarily used as a desalting technique, where charged compounds can be recovered from solution (Wang *et al*., 2006).

In the previous chapter it was shown that electrodialysis could satisfactorily remove acetate from aqueous solution at rates comparable to acetate formation during microbial fermentation. The aim of this chapter is to examine the application of electrodialysis to acetate removal and recombinant protein production in batch and fed-batch *E.coli* fermentations. The specific objectives include:

- Selection of an *E.coli* strain and medium which are most suitable for high cell density fermentation and production of a model recombinant protein production.
- Determination of the acetate inhibition level and the target concentration of acetate to minimise inhibition in the chosen expression system.
- Establishment of reproducible 7L batch and fed-batch fermentations (without electrodialysis) in order to benchmark the rate and yields of biomass, acetate and recombinant protein production.

- Investigation of electrodialysis to batch and fed-batch *E.coli* fermentations and its impact on acetate removal, biomass growth and recombinant protein production.

For these first fermentation studies the induction of recombinant protein expression will be fixed toward the end of the cell growth phase. Subsequent studies described in Chapter 5 will explore the relationship between time of protein synthesis induction and electrodialysis application in more detail.

4.2 Results and discussions

4.2.1 Shake flask fermentations

4.2.1.1 Selection of *E.coli* strain and culture medium

The initial objection of the fermentation studies was to choose a suitable *E.coli* host strain and to investigate the influence of medium composition on cell growth. Figure 4.1 illustrates the biomass concentrations of *E.coli* TG1, HB101 and DH5α for growth on both complex and defined medium. These three strains were chosen because they have been used for pGLO transformation and are commercially available. The two different media compositions were selected because they are widely used medium for *E.coli* fermentation.

The biomass profiles for the three *E.coli* strains obtained, using LB medium are indicated in Figure 4.1(a). Each strain showed typical batch growth kinetics over a 9 h growth period and achieved a final biomass concentration between 7.5 and 8.5 g DCW.L^{-1}. However, *E.coli* TG1 had the highest specific growth rate reaching a peak

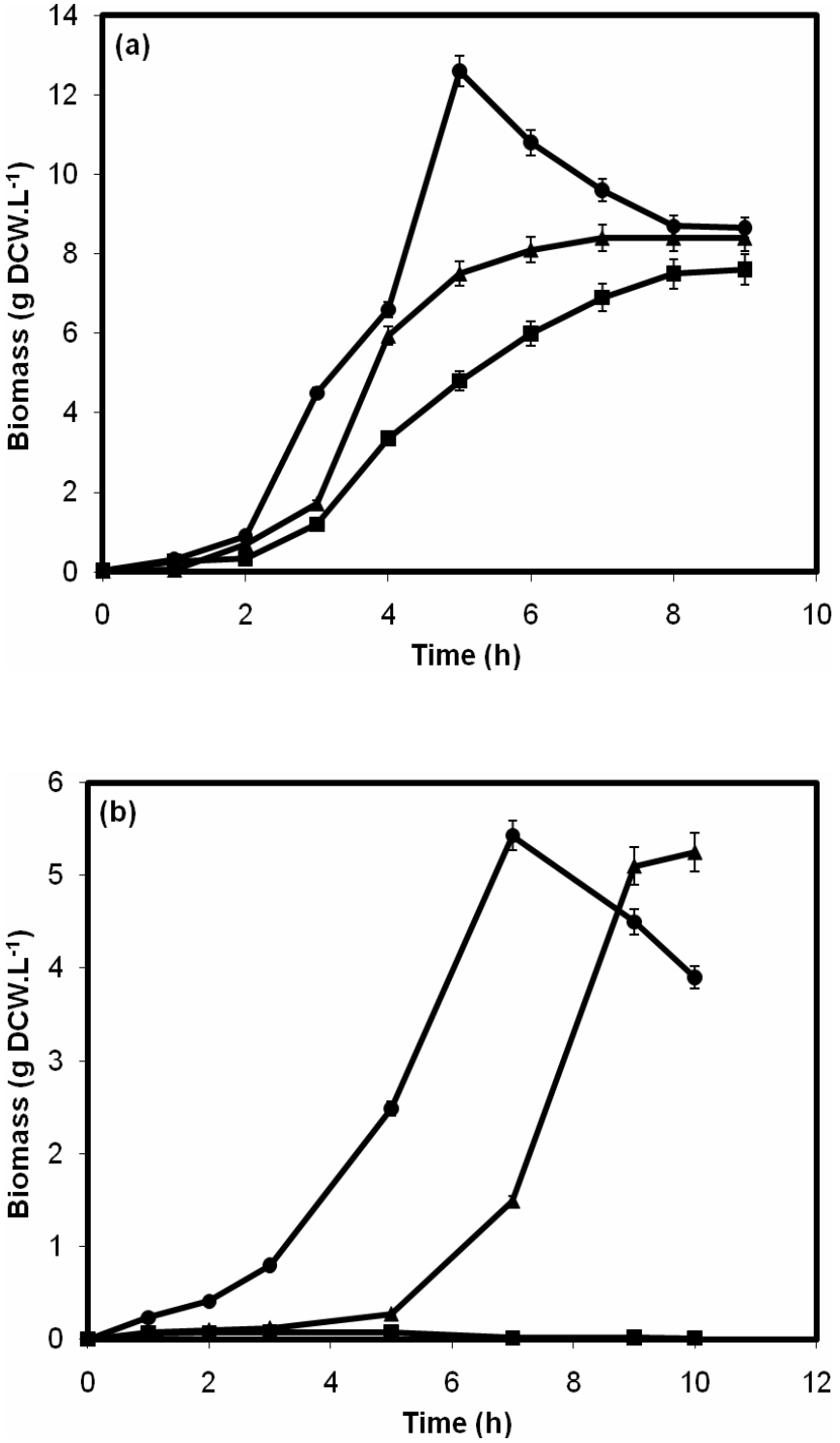

Figure 4.1. **(a)** Shake flask cultivation of *E.coli* TG1 (●), HB101 (▲) and DH5α (■) using LB medium. **(b)** Shake flask cultivation of *E.coli* TG1 (●), HB101 (▲) and DH5α (■) using Korz medium. Error quoted represent one standard deviation about the mean (n=3). Experiments performed as described in Section 2.2.2.3.

biomass concentration of up to 13 g DCW.L^{-1} at 5 h, before entering death phase. Similar experiments were carried out using a defined medium (Table 2.1), as described by Korz *et al.,* 1995, and results are shown in Figures 4.1(b). Both *E.coli* TG1 and HB101 reached biomass concentrations of up to 5.5 g DCW.L^{-1}, but *E.coli* DH5α did not grow using this medium. The genotype of DH5α was studied and it was found that leucine and proline which were required for the growth of *E.coli* DH5α are missing in this defined medium. The genotypes of TG1 and HB101 were then also studied and it was also found that *E.coli* HB101 would resist against arabinose, the inducer for the protien production this particular fermentation.

Using both media, *E.coli* TG1 demonstrated better performance than the other two strains and has a genotype more suitable for the desired transformation and induction required for recombinant protein production (Section 2.2.2.6). Consequently *E.coli* pGLO is the strain selected to be transformed with the plasmid pGLO for the production of a recombinant GFP.

LB medium, in general, provides a rich but complex nutrient source which enhances biomass concentration and protein production. However the Korz medium is more suitable when good control and reproducibility are essential at pilot scale and provides a better base medium for fed-batch studies. Also, defined medium, in most cases, presents fewer problems during downstream processing. Therefore, the defined medium was chosen to perform all subsequent *E.coli* TG1 pGLO fermentations.

4.2.1.2 Determination of *E.coli* TG1 pGLO acetate inhibition level

Acetate inhibition has been reported in the literature for many different *E. coli* strains as

described in Section 1.2.2. Inhibition levels are strain specific but generally in the range of 0.8-5.1 $g.L^{-1}$ (Luli and Strohl, 1990). In order to establish a basis for the design of electrodialysis fermentations with *E.coli* TG1 (Mosher, 2002), a range of known acetate additions was initially made to shake flask cultures. The results are shown in Figure 4.2. In the absence of added acetate, fermentations yielded a maximum biomass concentration of 4 $g.L^{-1}$. The maximum level of acetate secreted into the fermentation broth by the growing culture in this case was just 0.75 $g.L^{-1}$. Addition of 1, 3 and 5 $g.L^{-1}$ of sodium acetate at 6h, led to reduced final biomass concentrations of 2.8, 1.5 and 1.1 $g.L^{-1}$, respectively. Hence like other *E.coli* strains, the biomass yield of *E.coli* TG1 (Mosher, 2002) was inhibited by the presence of acetate at concentrations around 0.75-1.0 $g.L^{-1}$. In electrodialysis fermentations then, this is the level to which acetate concentration must be reduced if enhancements are to be seen in cell growth and potentially in recombinant protein synthesis.

4.2.2 Standard batch and fed-batch fermentations

In order to demonstrate the benefits of electrodialysis fermentations, it is first necessary to establish the benchmark biomass and recombinant protein yields obtained in standard batch and fed-batch cultures of *E.coli* Tg1 pGLO. Aerobic batch cultivations were consequently performed with a constant aeration rate and agitation speed as described in Section 2.2.2.4. Synthesis of recombinant GFP was induced during the late stages of the growth phase in all cases.

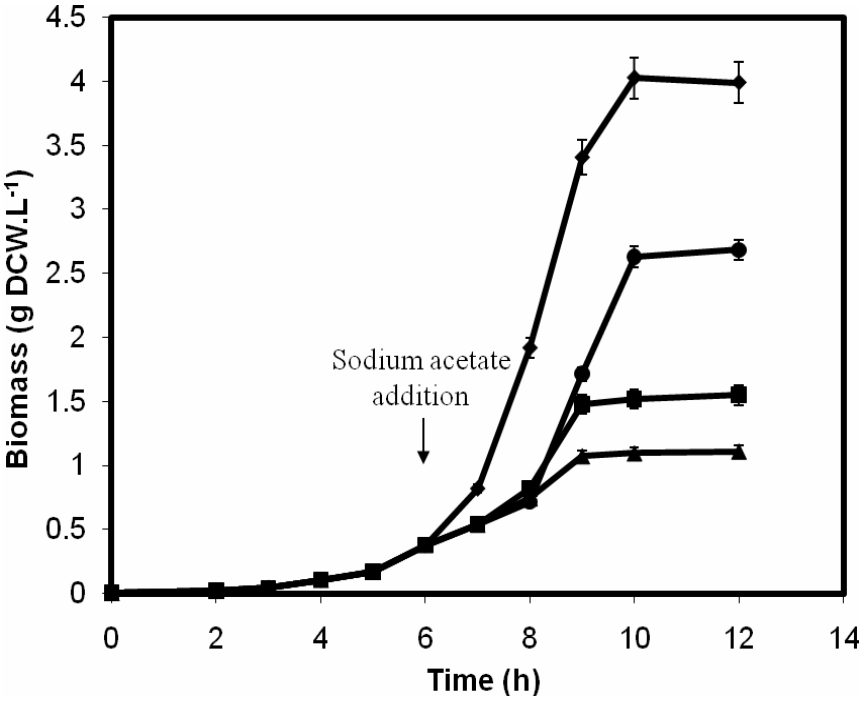

Figure 4.2. Effect of acetate inhibition on growth of *E.coli* TG1 pGLO in shake flask fermentations with additions of 0 (♦), 1 (●), 3 (■) and 5 (▲) g.L-1 of sodium acetate to establish inhibition levels. The arrow indicates the time of acetate addition. Error quoted represent one standard deviation about the mean (n=3). Experiments performed as described in Section 2.2.2.3.

Figure 4.3a shows typical measured values for cell growth, GFP synthesis and acetate accumulation based on triplicate batch fermentations. Figure 4.3b indicates the corresponding glucose consumption, dissolved oxygen tension (DOT) and the cumulative amount of base added to counteract the formation of acetate and other acidic metabolic by-products. After an initial lag phase a maximum growth rate of 0.45 h^{-1} was calculated and a final biomass concentration of 11.2 $g.L^{-1}$ was achieved which coincided with glucose exhaustion. At the maximum specific growth rate, the DOT dropped to a minimum of 10% while the acetate concentration in the broth reached a peak value of 5.7 $g.L^{-1}$, after which it was seen to be reabsorbed into the cells. Arabinose was added to induce GFP synthesis at 10h during the late growth phase of the culture. GFP expression subsequently increased sharply leading to a final GFP concentration of 0.085 $g.L^{-1}$ at 14 h. The maximum specific growth rate, glucose consumption rate and oxygen uptake rate shown in Figure 4.3 coincide with values previously published for this particular strain (Korz *et al*., 1995).

It has been reported in the literature that acetate inhibition is more severe in fed-batch mode, because depending on the *E.coli* strain used, up to 5 times more acetate is produced even when controlled glucose feeding is employed (Luli and Strohl, 1990). Moreover, the majority of industrial fermentation processes are operated in this way in order to achieve high cell densities. Consequently fed-batch fermentations were also performed in which the glucose feeding rate was matched to the maximum glucose uptake rate previously reported for the *E.coli* strain used here (Korz *et al*., 1995). In the absence of acetate inhibition, this condition would be expected to give rise to maximum bioreactor productivity in terms of cell growth.

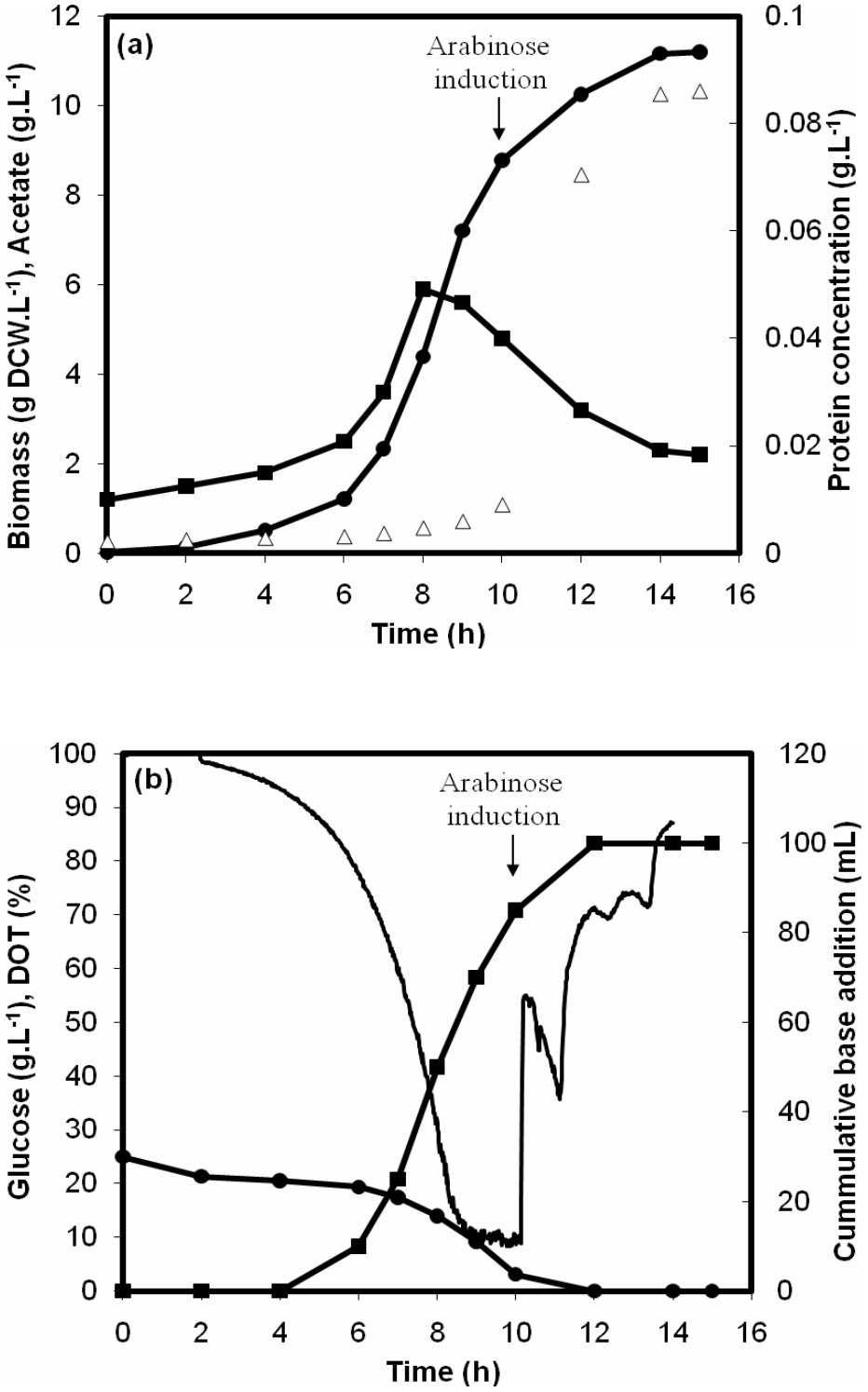

Figure 4.3. Batch fermentation kinetics of *E.coli* TG1 pGLO with late exponential phase GFP induction. **(a)** Offline data for biomass (●), acetate (■) and recombinant protein, GFP, (Δ) concentration. **(b)** On-line measurements of glucose (●), dissolved oxygen tension (-) and base addition (■). The arrow indicates the time of induction. Results show a typical profile from triplicate fermentations. Experiments performed as described in Section 2.2.2.4.

The results of high cell density *E.coli* Tg1 pGLO fermentations with exponential feeding of glucose are shown in Figure 4.4. After unlimited growth during the batch mode ($\mu=\mu_{max}$), glucose became limiting at around 12 h. The cell growth rate began to decline and glucose feeding was commenced. During this period the DOT remained constant at around 10% and the majority of glucose was rapidly consumed coinciding with an exponential increase in the volumetric biomass concentration. The feeding led to an increase in fermenter working volume from 4 L to 6 L with induction taking place at 24 h. By the end of the culture, the final biomass concentration obtained was 24.3 $g.L^{-1}$, while acetate production, which coincided with cell growth, reached a maximum of 26.9 $g.L^{-1}$. A maximum concentration of 0.09 $g.L^{-1}$ of GFP was obtained for the fed-batch culture. The total volume of base added was 0.8L, compare to 0.1 L for the corresponding batch fermentation indicating the higher level of acidic metabolic by-product produced.

Table 4.1 provides a summary of the results for these initial batch and fed-batch fermentations. In the fed-batch culture a slightly higher maximum specific growth rate was achieved but over twice the final biomass concentration was obtained. However, this was matched by as much as 5 times the concentration of acetate in the fed-batch fermentation in agreement with previous studies (Luli and Strohl, 1990). While a greater total amount of GFP was produced in the fed-batch culture this was with significantly higher biomass levels and so the specific GFP yield was lower. This suggests a possible link between acetate formation and recombinant protein synthesis level which will be explored further in the next section when ED is applied for the *in situ* removal of acetate.

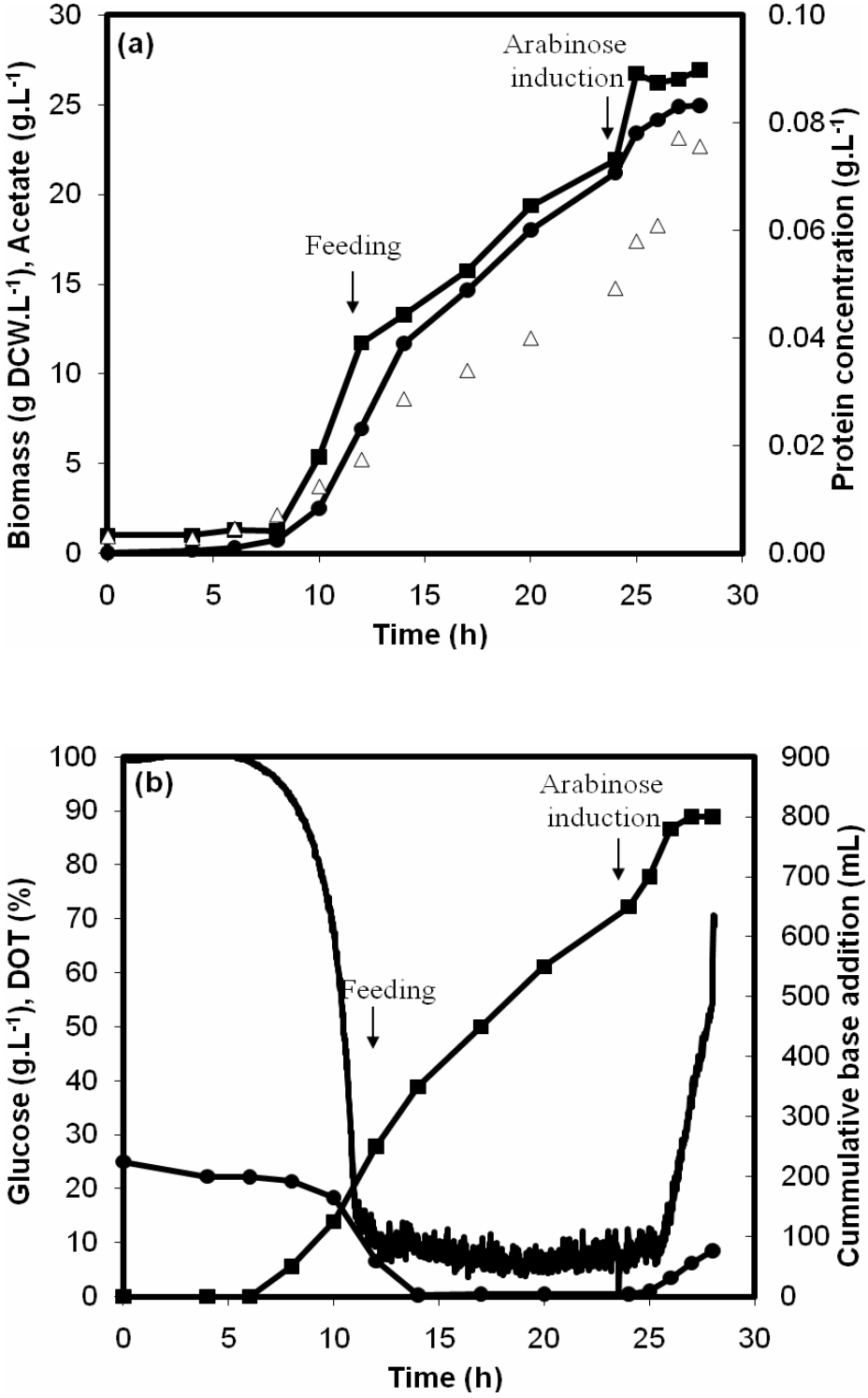

Figure 4.4. Fed-batch fermentation kinetics of *E.coli* TG1 pGLO with late GFP induction. **(a)** Offline data for biomass (●), acetate (■) and recombinant protein, GFP, (Δ) concentration. **(b)** On-line measurements of glucose (●), dissolved oxygen tension (-) and base addition (■). The arrows indicate the times of induction and feeding. Results show typical profile from triplicate fermentations. Experiments performed as described in Section 2.2.2.5.

Table 4.1. Summary of biomass yield, maximum specific growth rate, GFP yield and bioreactor acetate concentration with late induction of recombinant protein synthesis. Error quoted represents one standard deviation about the mean (n=3).

Experiment	Maximum [biomass] ($g.L^{-1}$)	Maximum growth rate, μ (h^{-1})	Maximum [GFP] ($g.L^{-1}$)	Maximum [acetate] ($g.L^{-1}$)	Total biomass (g)	Total GFP (g)	GFP/ biomass yield ($g.g^{-1}$)
Batch	11.2 ± 0.2	0.45 ± 0.03	0.09 ± 0.01	5.9 ± 0.2	44.8	0.34	7.6×10^{-3}
Fed-batch	24.3 ± 0.3	0.55 ± 0.02	0.08 ± 0.01	26.9 ± 0.7	145.8	0.48	3.3×10^{-3}
ED batch (control)	10.7 ± 0.3	0.43 ± 0.03	0.08 ± 0.01	5.1 ± 0.2	42.8	0.30	7.0×10^{-3}
ED batch	10.3 ± 0.2	0.66 ± 0.04	0.35 ± 0.03	2.5 ± 0.2	41.2	1.40	34.0×10^{-3}
ED fed-batch	17.4 ± 0.4	0.61 ± 0.03	0.17 ± 0.02	19.2 ± 0.6	104.4	1.02	9.8×10^{-3}

4.2.3 Batch and fed-batch electrodialysis fermentations

Having established the benchmark biomass and protein synthesis levels in conventional fermentation processes with *E.coli* Tg1 pGLO (Section 4.3.2), equivalent fermentations were performed with the electrodialysis module in place as shown in Figure 2.3. However, before operating electrodialysis fermentations, two control experiments were carried out as described in Section 2.2.3, to investigate any potential adverse effects of the EDF set-up on cell growth as described earlier. The first experiment investigated the possible effect of oxygen deficiency, due to the circulation of culture between the fermenter and the electrodialysis module in the absence of any applied current. In this control fermentation the levels of biomass, acetate and GFP achieved were 10.7 $g.L^{-1}$, 5.1 $g.L^{-1}$ and 0.08 $mg.L^{-1}$, respectively. As shown in Table 4.1 these concentrations are similar to those obtained in standard batch fermentations. The slightly reduced maximum specific growth rate of 0.42 h^{-1} suggests only a negligible impact of oxygen depletion with culture recirculation on fermentation performance. The second control experiment examined the influence of the applied electric field on cell growth and protein synthesis in the absence of any transport of acetate through the ED module (as described in Section 2.2.3 this was achieved by replacing the anion exchange membrane with a cation exchange membrane). The results of this second control experiment (data shown in Appendix B Figure B.3) indicated that the applied electric field had no measurable influence on the culture performance. Typical results from replicate ED batch fermentations are shown in Figure 4.5. In terms of cell growth a similar biomass concentration to the standard batch

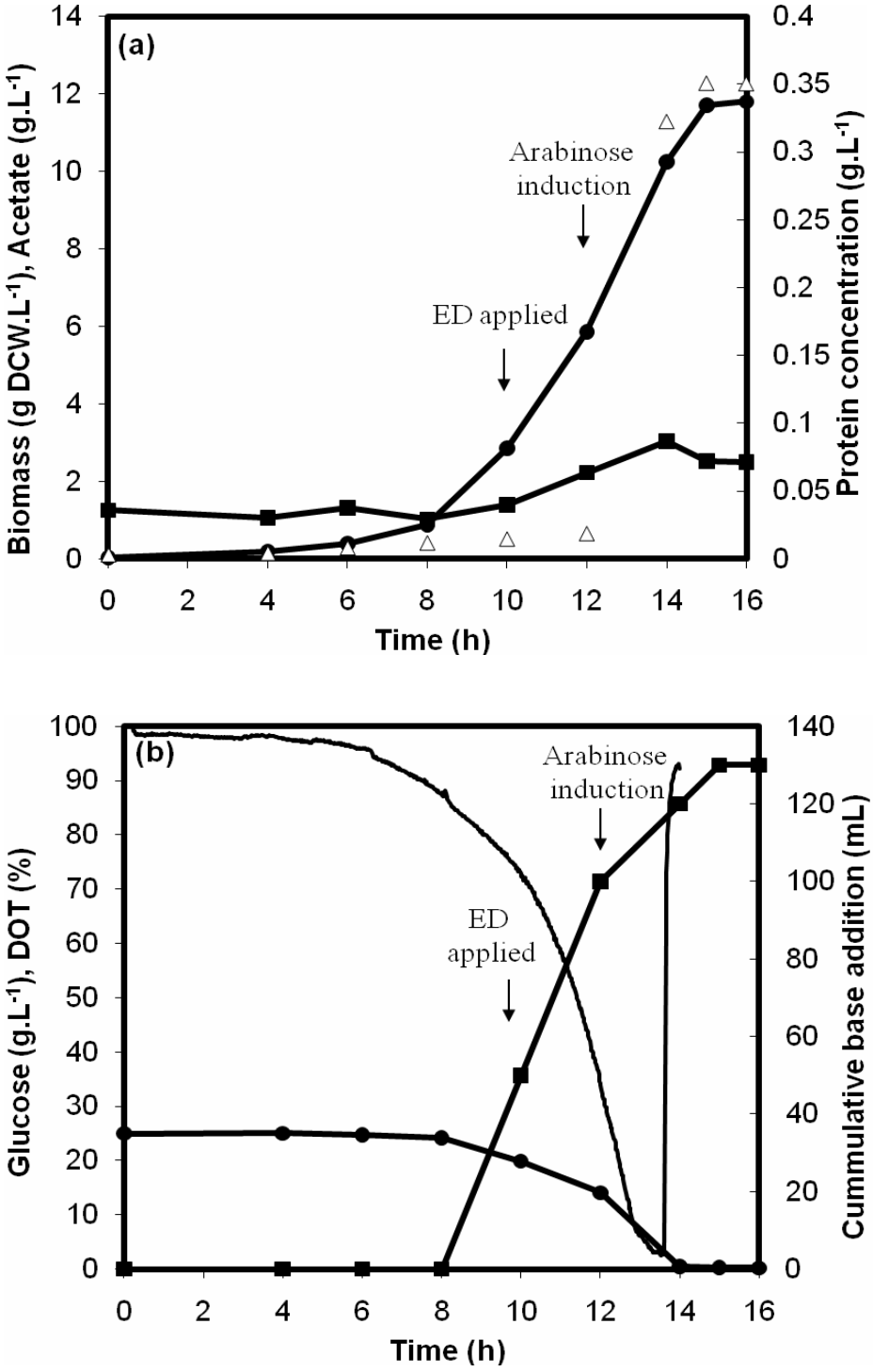

Figure 4.5. Electrodialysis batch fermentation kinetics of *E.coli* TG1 pGLO with late exponential phase GFP induction. **(a)** Offline data for biomass (●), acetate (■) and recombinant protein, GFP, (Δ) concentration. **(b)** On-line measurements of glucose (●), dissolved oxygen tension (-) and base addition (■). The arrows indicate the times of induction and ED application. Results show typical profile from triplicate fermentations. Experiments performed as described in Section 2.2.3.

fermentation of 10.3 $g.L^{-1}$ was obtained although there was a significant increase in the maximum specific growth rate to 0.66 h^{-1}. This is most likely due to the removal of acetate by the ED module since by implementation of ED between 10 to 12 h (during exponential growth phase), a maximum 2.5 $g.L^{-1}$ of acetate accumulated in the culture medium. The fact that this is still above the inhibitory level of approximately 0.75 $g.L^{-1}$ determined in Section 4.2 suggests that the limited membrane area in the ED module used was insufficient to cope with the rate of acetate production by the cells. Further improvements in culture performance may thus be possible if a larger ED module were available. Based on acetate analysis in compartment R of the ED module a further 3.0 $g.L^{-1}$ of acetate was produced by the cells but then removed via ED. The addition of base was 0.13L, slightly more than the volume used in a batch fermentation.

Most importantly however, after induction at 12 h there was a significant increase in the level of GFP synthesis resulting in a maximum concentration of 0.35 $g.L^{-1}$. This corresponds to a nearly 4-fold increase in specific GFP production. This increase in recombinant protein production occurred in all replicate fermentations to a similar extent. These results confirm others in the literature suggesting that acetate removal in batch fermentation leads to an increase in cell growth (Fuchs *et al*., 2002). However this work shows for the first time that acetate removal can also lead to an increase in recombinant protein synthesis. This could have wide implications given the number of enzymes and biopharmaceuticals produced in *E.coli* fermentations.

The results of a typical ED fed-batch fermentation are shown in Figure 4.6. The biomass concentration achieved, 17.4 $g.L^{-1}$, was slightly lower than the standard fed-

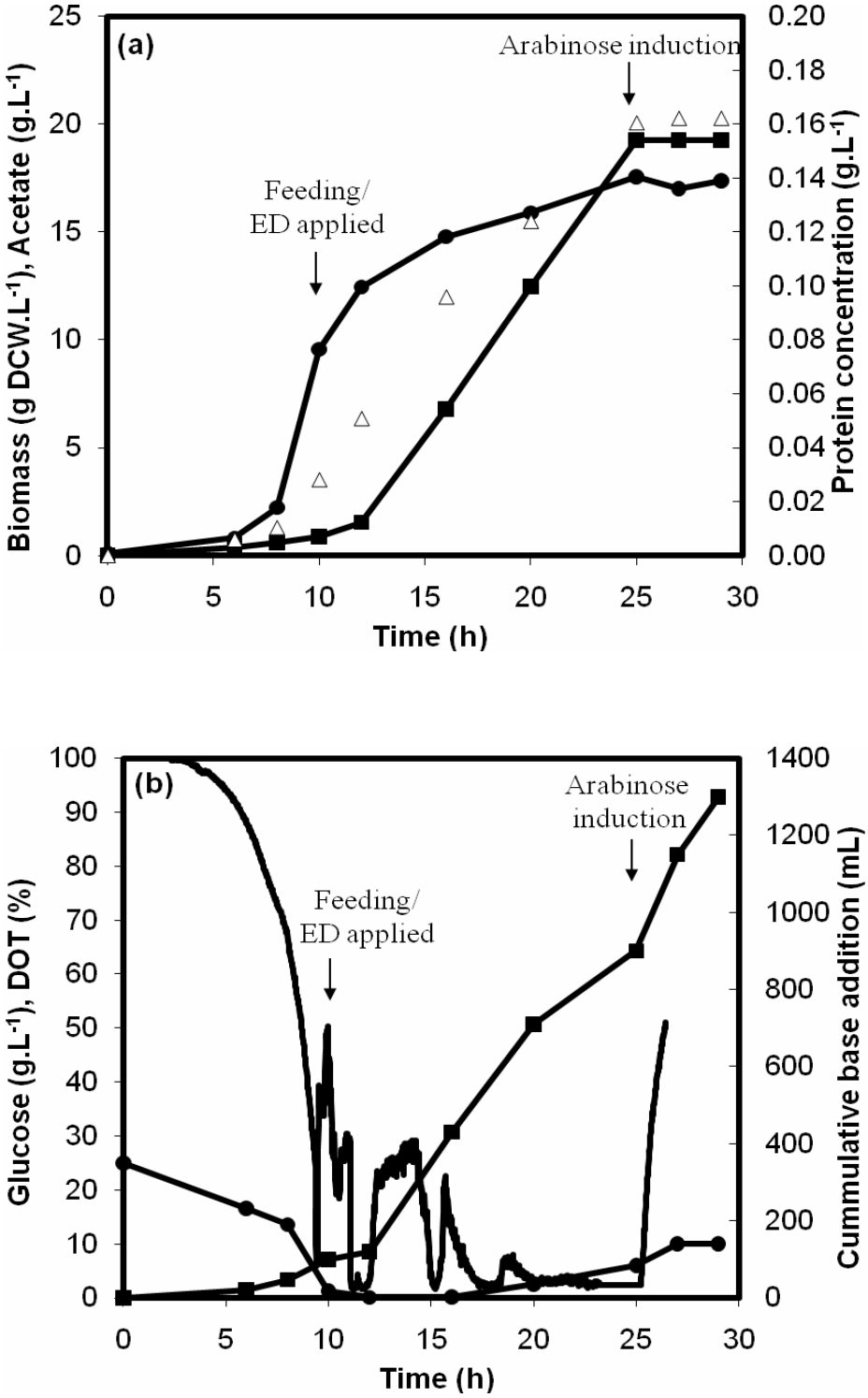

Figure 4.6. Electrodialysis fed-batch fermentation kinetics of *E.coli* TG1 pGLO with late GFP induction. **(a)** Offline data for biomass (●), acetate (■) and recombinant protein, GFP, (Δ) concentration. **(b)** On-line measurements of glucose (●), dissolved oxygen tension (-) and base addition (■). The arrows indicate the times of induction, feeding and ED application. Results show typical profile from triplicate fermentations. Experiments performed as described in Section 2.2.3.

batch culture but the calculated maximum specific growth rate of 0.61h^{-1} was a little higher. Given the increased level of acetate production in the fed-batch culture and the limited area of the ED module available, a high level of acetate accumulation was still measured in the culture medium of 19.2 $g.L^{-1}$. As a result, the maximum GFP concentration measured was 0.17 $g.L^{-1}$. While this was still over twice the level recorded in the standard fed-batch fermentation it was significantly lower than the 0.35 $g.L^{-1}$ measured in ED-batch fermentation where there was a greater level of acetate removal by ED. The amount of acetate collected in compartment R during the fed-batch culture was 12.8 $g.L^{-1}$ and a total of 1.3 L of base was added. Therefore, the limited membrane area of the electrodialysis device is seen as the limiting factor preventing further acetate removal.

A summary of the performance of all the late protein synthesis induction fermentations is provided in Table 4.1. Similar conclusions can be drawn between both sets of batch and fed-batch experiments, with or without the application of electrodialysis. Generally, fed-batch fermentations led to greater biomass production
levels but this was concomitant with greater levels of acetate accumulated. Thus the specific yield of GFP produced was lower. In terms of the significance of the ED technology, the results of both the ED batch and ED fed-batch cultures demonstrate that ED was capable of removing inhibitory acetate *in situ* leading to at least a 4-fold increase in the level of GFP synthesis. It may be possible to increase this further by the use of an ED module with a larger membrane area capable of keeping acetate levels in the fermentation medium to below the inhibitory level of 0.75 $g.L^{-1}$ determined earlier for the particular *E.coli* strain used here.

4.2.4 Comparison of electrodialysis with controlled feeding methods

To overcome the acetate inhibition effect on *E.coli*, both dialysis (Fuchs *et al*., 2002) and controlled feeding approaches (Akesson *et al*., 2001) offer enhanced fermentation performance either by *in situ* removal of acetate or restricting the production of acetate respectively. However, both approaches have their advantages and disadvantages and so it is worth briefly discussing these in light of the results presented in Section 4.2.2 and 4.2.3. A rigorous comparison though is complicated by the fact that while the work in this thesis has focussed on the levels of recombinant protein synthesis, most of the controlled feeding work reported has focussed solely on achieving the greatest amount of biomass rather than recombinant protein production.

The main advantage of electrodialysis would appear to be the instant removal of acetate from the culture medium once it is formed (Figure 4.5(a)). With an appropriately sized ED module this would enable the acetate concentration to be maintained below the inhibitory level for any particular strain. The application of electrodialysis would then overcome the need to limit glucose feeding rate in high cell density cultivation, such that the cells can take up the carbon source at an unrestricted rate leading to maximum cell growth rates and overall space-time yields. Furthermore, as shown here, this may also lead to enhance levels of recombinant protein synthesis through biochemical mechanisms that remain to be determined. A further advantage might be the generic nature of this approach in that once an ED module is available it can readily be applied to a wide range of organisms and culture conditions. However, this may involve problems such as compatibility of ED module to the existing production method, shearing and oxygen shortage on cell and the removal of medium ions.

In contrast, the commonly used controlled feeding method can be operated more easily and does not involve complicated set-up. But it is based on the restricted feeding of the carbon source to a rate that limits cell growth below the threshold of high levels of acetate production (Nomura *et al.,* 1988). Compared to ED, this would appear to be a more conservative approach providing lower maximum specific growth rates and hence overall space-time yields. In addition, for optimum performance with feedback control of the carbon source feed rate, complicated online measurement of acetate levels and a controlled feeding device fitted to the fermenter are necessary.

4.3 Summary

This chapter presents, for the first time, successful enhancements in recombinant protein synthesis in both batch and fed-batch electrodialysis fermentations with induction occurring during the late phase of cell growth. As a basis for these studies a model expression system was established for GFP expression explained in Section 2.2.2.1 and 4.2.1.1. It was subsequently shown for this strain that acetate inhibition occurred at around the 0.75 $g.L^{-1}$ level (Figure 4.2). To facilitate ED fermentations a 7L laboratory fermentation system was first constructed to enable electrodialysis application in both batch and fed-batch cultures (Figure 2.3a). This was shown to enable *in situ* removal of the negatively charged and inhibitory acetate ions during fermentation (Figure 4.4). Overall, the removal of acetate via ED led to a significant improvement in recombinant protein synthesis, demonstrated by results using both batch (Figure 4.3) and ED batch fermentations (Figure 4.4). However, in the case of fed-batch mode, enhancements reported were limited by the membrane area of the ED module used suggesting that still further improvements would be possible.

In these studies the induction of recombinant protein expression was fixed toward the end of the cell growth phase. In the next chapter the relationship between time of protein synthesis induction and electrodialysis application will be studies in more detail.

Electrodialysis has shown potential to be a useful *in-situ* product removal technique, and could be offered as an alternative to the feeding strategy in solving acetate accumulation problems in *E.coli* fermentation. However, further understanding of the technology and improvement of the electrodialysis module is required, especially to address mass transfer of ions across the membrane and membrane fouling in order to optimise ED module performance. Further studies are also required with alternative systems to show the generic nature of the process.

Chapter 5

Impact of electrodialysis on acetate removal and recombinant protein synthesis in *E.coli* fermentation: Early protein induction[2]

5.1 Introduction

In the previous chapter the potential of the electrodialysis application to enhance recombinant protein production during *E.coli* fermentation was established. However, another major influence on the level of cell growth and recombinant protein synthesis is the time of induction. The optimum time for induction of recombinant protein synthesis is generally system specific. Panda *et al* (1999) have shown the benefit of late induction to minimise the extra metabolic burden of protein synthesis which can cause a reduction in cell growth. Alternatively, Yuan *et al* (2004) have reported that greater recombinant protein synthesis was achieved when *E.coli* was induced at the early exponential phase of growth.

[2]The majority of results presented in this chapter have previously been published as Wong M, Wright M, Woodley JM, Lye GJ (2009) Enhanced recombinant protein expression in batch and fed-batch *Escherichia coli* fermentation based on removal of inhibitory acetate by electrodialysis. Journal of Chemical Technology and Biotechnology 84: 1284-1291

The aim of this chapter is to investigate the effect of early exponential phase induction on recombinant protein synthesis. The specific objectives include:

- The examination of performance of standard and electrodialysis *E.coli* TG1 pGLO fermentations under batch and fed-batch mode at early exponential phase induction.
- Comparisons between data obtained here and the results from Chapter 4 for late protein induction, in particular the level and enhancement of recombinant protein production.

5.2 Results and discussions

5.2.1 Early phase induction fermentations

As described in Section 5.1 the induction of recombinant protein synthesis can occur either early or late in the cell growth phase. In general the optimum time for induction is system specific and depends on the metabolic burden that heterologous protein synthesis induction may cause (Panda *et al*., 1999; Yuan *et al*., 2004). Consequently a further series of batch and fed-batch fermentations, with and without ED, were performed similar to those shown in Figures 4.3 to 4.6 but with induction of GFP synthesis during the early exponential phase of *E.coli* Tg1 pGLO growth. Figure 5.1 to 5.4 show typical profiles of offline and online measurements from triplicate experiments. By inducing at an earlier exponential phase, up to 5 $g.L^{-1}$ of GFP was achieved.

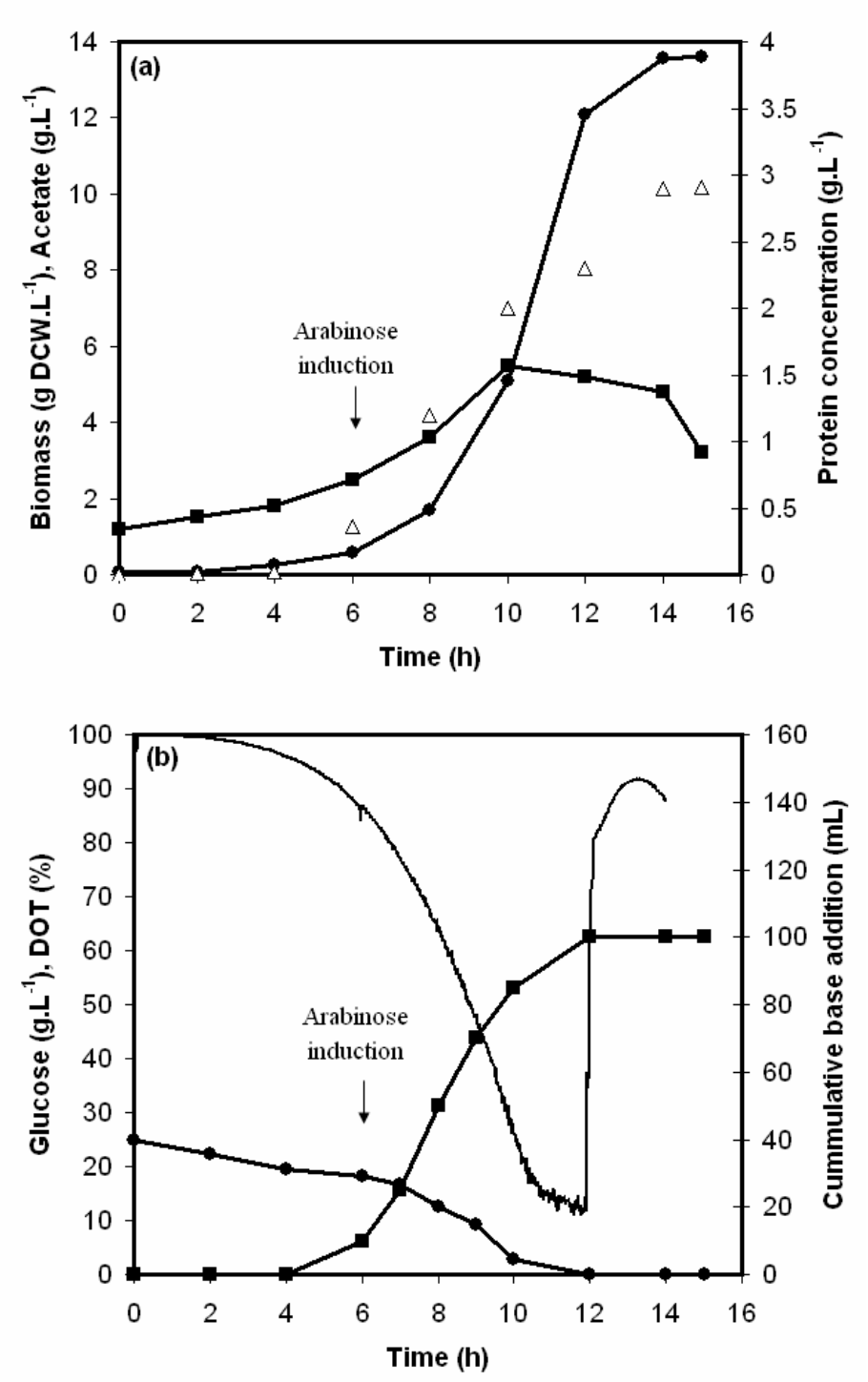

Figure 5.1. Batch fermentation kinetics of *E.coli* TG1 pGLO with early exponential phase GFP induction. **(a)** Offline data for biomass (●), acetate (■) and recombinant protein, GFP, (Δ) concentration. **(b)** On-line measurements of glucose (●), dissolved oxygen tension (-) and base addition (■). The arrow indicates the time of induction. Results show typical profile from triplicate fermentations. Experiments performed as described in Section 2.2.2.4.

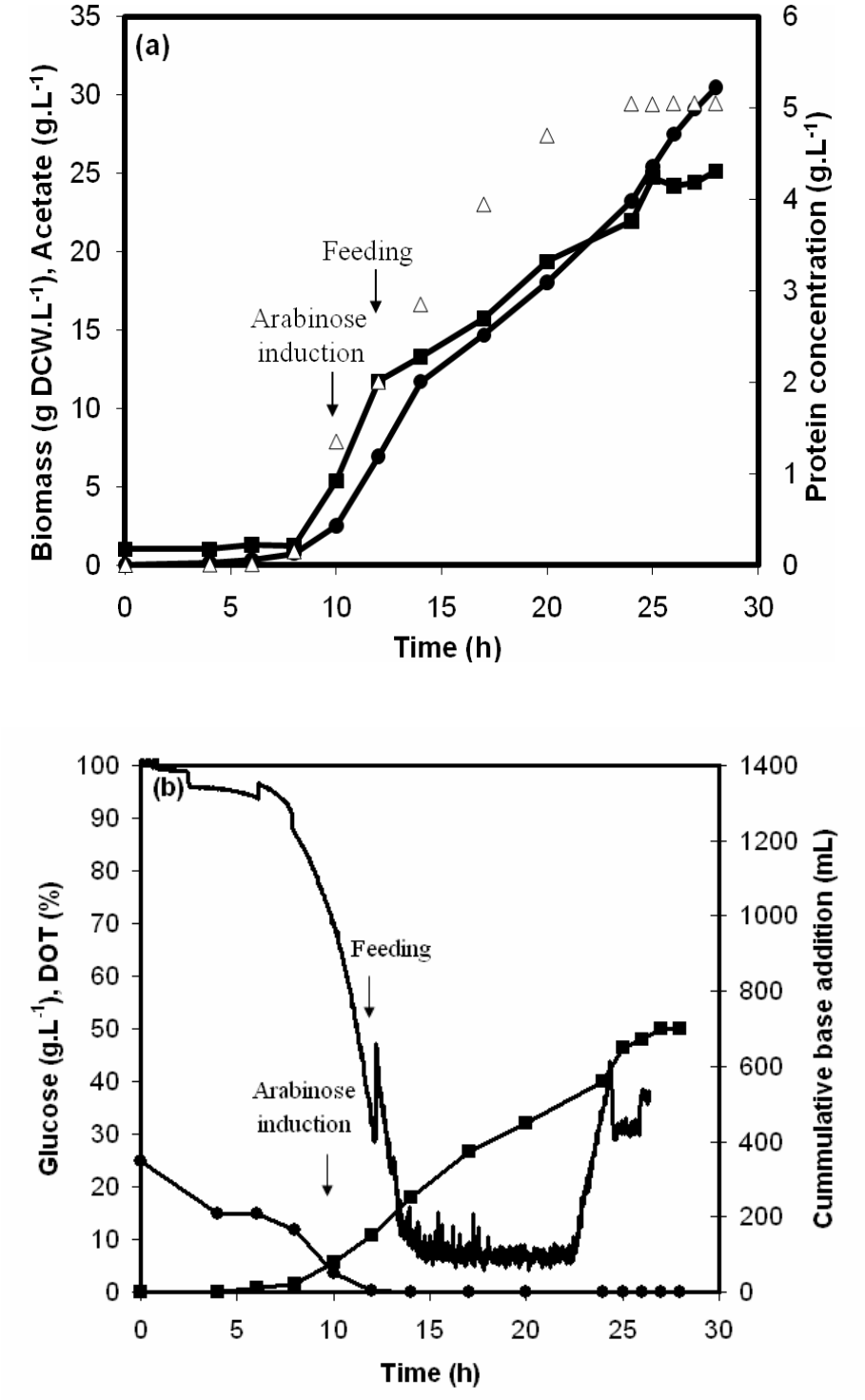

Figure 5.2. Fed-batch fermentation kinetics of *E.coli* TG1 pGLO with early GFP induction. **(a)** Offline data for biomass (●), acetate (■) and recombinant protein, GFP, (Δ) concentration. **(b)** On-line measurements of glucose (●), dissolved oxygen tension (-) and base addition (■). The arrows indicate the times of induction and feeding. Results show typical profile from triplicate fermentations. Experiments performed as described in Section 2.2.2.5.

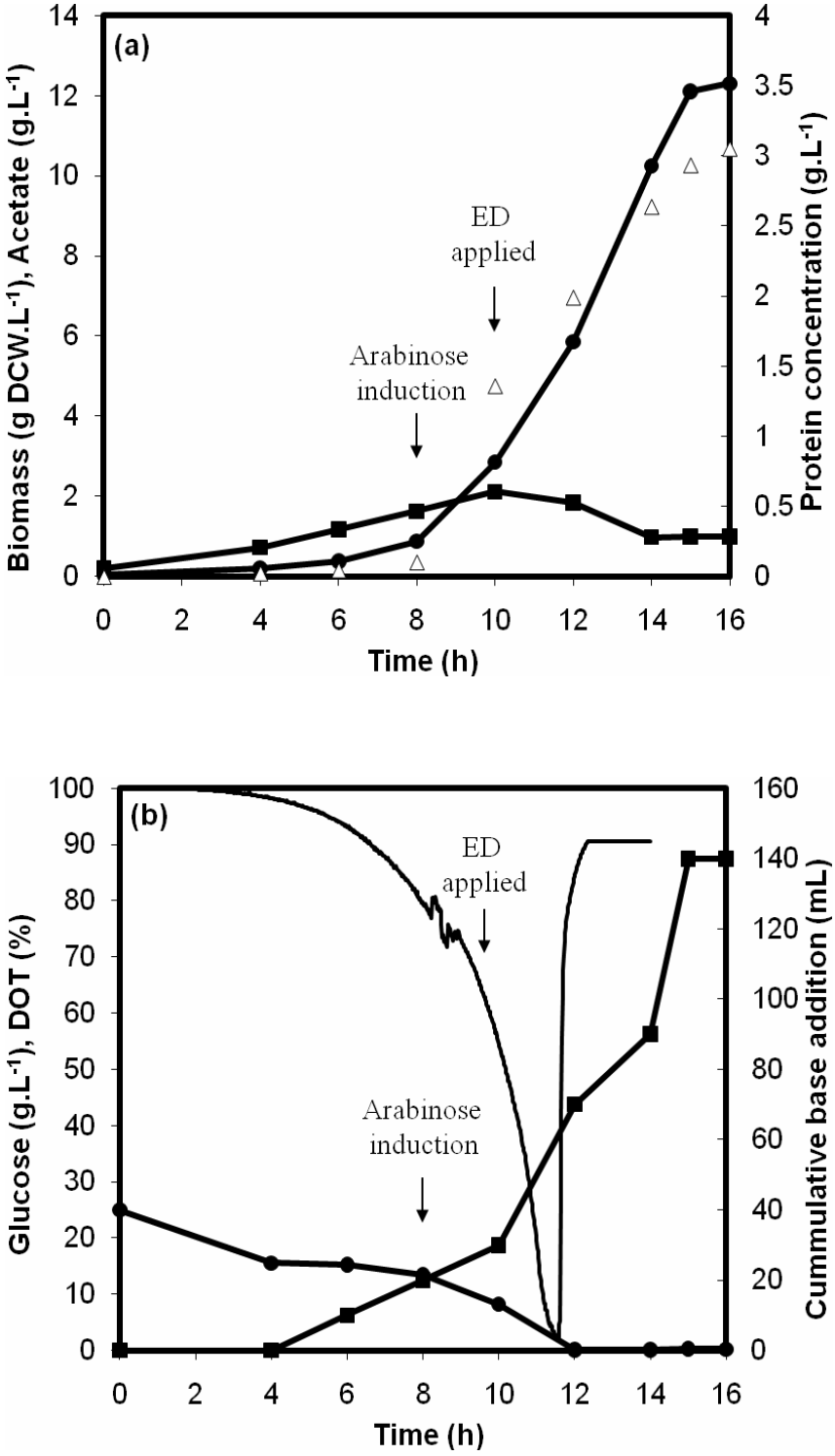

Figure 5.3. Electrodialysis batch fermentation kinetics of *E.coli* TG1 pGLO with early exponential phase GFP induction. **(a)** Offline data for biomass (●), acetate (■) and recombinant protein, GFP, (Δ) concentration. **(b)** On-line measurements of glucose (●), dissolved oxygen tension (-) and base addition (■). The arrows indicate the times of induction and ED application. Results show typical profile from triplicate fermentations. Experiments performed as described in Section 2.2.3.

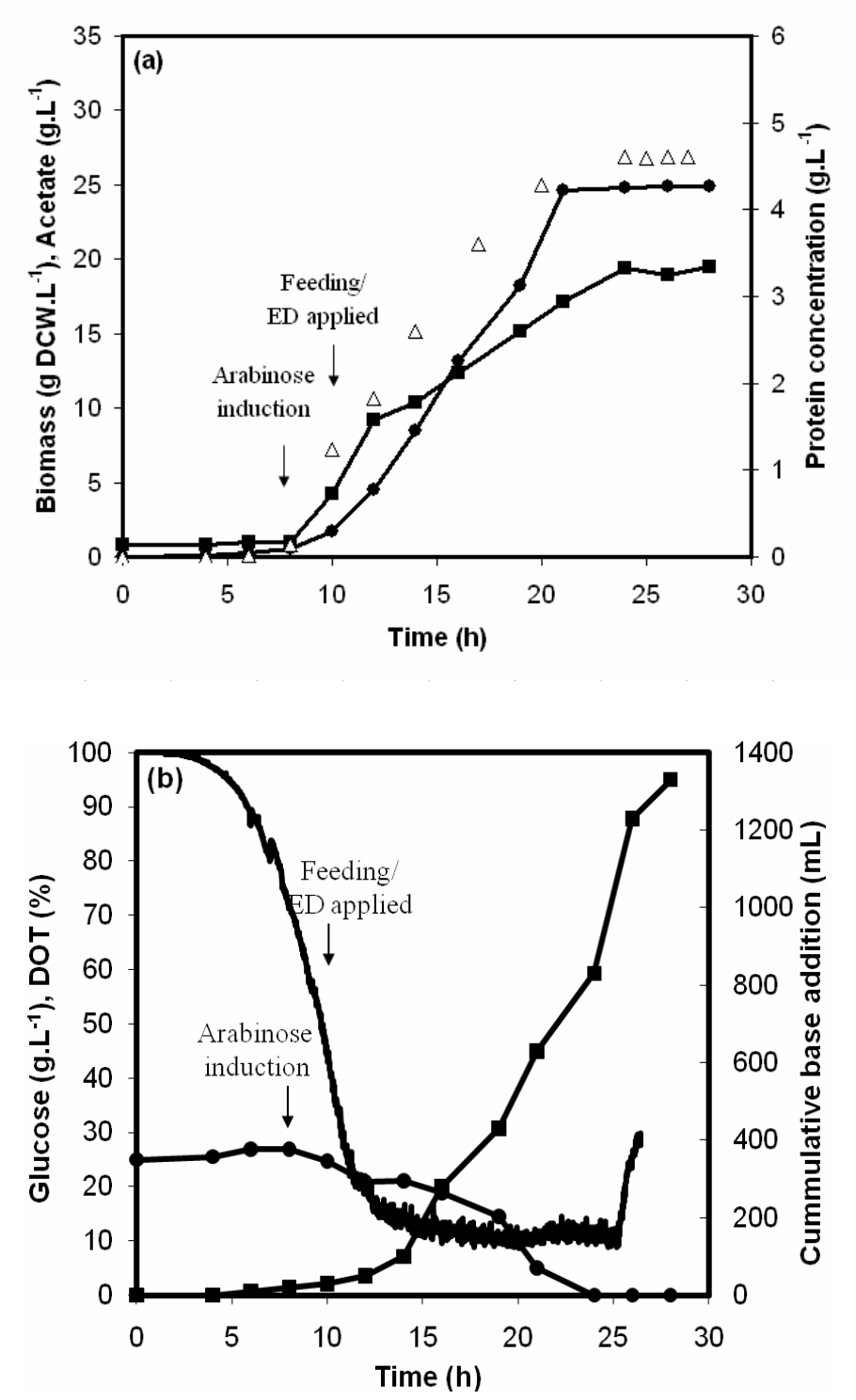

Figure 5.4. Electrodialysis fed-batch fermentation kinetics of *E.coli* TG1 pGLO with early GFP induction. **(a)** Offline data for biomass (●), acetate (■) and recombinant protein, GFP, (Δ) concentration. **(b)** On-line measurements of glucose (●), dissolved oxygen tension (-) and base addition (■). The arrows indicate the times of induction, feeding and ED application. Results show typical profile from triplicate fermentations. Experiments performed as described in Section 2.2.3.

Figure 5.1a shows typical measured values for cell growth, GFP synthesis and acetate accumulation based on triplicate batch fermentations. Figure 5.1b indicates the corresponding glucose consumption, dissolved oxygen tension (DOT) and the cumulative amount of base added to counteract the formation of acetate and other acidic metabolic by-products. After an initial lag phase a maximum growth rate of 0.46 h^{-1} was calculated and a final biomass concentration of 13.6 $g.L^{-1}$ was achieved which coincided with glucose exhaustion. At the maximum specific growth rate, the DOT dropped to a minimum of 10% while the acetate concentration in the broth reached a peak value of 5.5 $g.L^{-1}$, after which it was seen to be reabsorbed into the cells. Arabinose was added to induce GFP synthesis at 6 h during the early growth phase of the culture. GFP expression subsequently increased sharply leading to a final GFP concentration of 2.91 $g.L^{-1}$ at 14 h. The results of high cell density *E.coli* Tg1 pGLO fermentations with exponential feeding of glucose are shown in Figure 5.2. By the end of the culture, the final biomass concentration obtained was 30.5 $g.L^{-1}$, while acetate production, which coincided with cell growth, reached a maximum of 25.1 $g.L^{-1}$. A maximum concentration of 5.01 $g.L^{-1}$ of GFP was obtained for the fed-batch culture.

Typical results from replicate ED batch fermentations are shown in Figure 5.3. In terms of cell growth a similar biomass concentration to the standard batch fermentation of 12.3 $g.L^{-1}$ was obtained although there was a significant increase in the maximum specific growth rate to 0.44 h^{-1}. This is most likely due to the removal of acetate by the ED module, a maximum 2.1 $g.L^{-1}$ of acetate accumulated in the culture medium
Most importantly however, after induction at 6 h there was a significant increase in the level of GFP synthesis resulting in a maximum concentration of 3.05 $g.L^{-1}$. The results of a typical ED fed-batch fermentation are shown in Figure 5.4. The biomass concentration achieved, 24.9 $g.L^{-1}$, was slightly lower than the standard fed-

batch culture but the calculated maximum specific growth rate of $0.47h^{-1}$ was a little higher. Given the increased level of acetate production in the fed-batch culture and the limited area of the ED module available, a high level of acetate accumulation was still measured in the culture medium of 18.8 $g.L^{-1}$. As a result, the maximum GFP concentration measured was 4.56 $g.L^{-1}$.

5.2.2 Influence of early versus late recombinant protein synthesis induction

Table 5.1 provides a summary of the key parameters determined from the measured culture kinetics which in general terms were similar to those shown in Table 4.1 for early induction experiments. Overall the measured biomass concentrations, cell growth rates and level of acetate accumulation and removal for both sets of fermentations were in a similar range. However, for the early induction of recombinant protein synthesis there was an order of magnitude increase in the level of GFP synthesis for all experiments (compare GFP levels in Table 4.1 and Table 5.1). This suggests that for this particular *E.coli* strain (Tg1), the extra metabolic burden caused by induction of recombinant protein synthesis is insignificant and early induction is preferred as also seen by (Yuan *et al*., 2004).

Comparing the benefits of ED application in Table 5.1 there is still an improvement in specific GFP levels comparing both standard and ED batch and fed-batch fermentations although the levels of enhancement (5%) are much less than for the late induction fermentations described in Table 4.1. These results are still promising, given the limited ED membrane area available for this study, but suggests that like recombinant protein synthesis the benefits of ED application will be system specific and operating conditions must be optimised for each particular fermentation process.

Table 5.1. Summary of biomass yield, maximum specific growth rate, GFP yield and bioreactor acetate concentration with early induction of recombinant protein synthesis. Error quoted represents one standard deviation about the mean (n=3).

Experiment	Maximum [biomass] ($g.L^{-1}$)	Maximum growth rate, μ (h^{-1})	Maximum [GFP] ($g.L^{-1}$)	Maximum [acetate] ($g.L^{-1}$)	Total biomass (g)	Total GFP (g)	GFP/ biomass yield ($g.g^{-1}$)
Batch	13.6 ± 0.1	0.46 ± 0.03	2.91 ± 0.04	5.5 ± 0.3	54.4	11.6	0.21
Fed-batch	30.5 ± 0.3	0.49 ± 0.02	5.01 ± 0.08	25.1 ± 0.6	183.0	30.1	0.16
ED batch	12.3 ± 0.2	0.44 ± 0.03	3.05 ± 0.05	2.1 ± 0.2	49.2	12.2	0.25
ED fed-batch	24.9 ± 0.3	0.47 ± 0.04	4.56 ± 0.04	18.8 ± 0.5	149.4	27.4	0.18

5.3 Summary

This chapter presents evidence to demonstrate the importance of induction time for recombinant protein production in *E.coli* fermentation. Induction took place at an earlier phase of growth at 6 h for batch (Figure 5.1 and 5.3) and 10 h for fed-batch (Figure 5.2 and 5.4) fermentations, instead of a later phase of 12 h (Figure 4.3 and 4.5) and 25 h (Figure 4.4 and 4.6). Tables 4.1 and 5.1 compare the significant increases of up to 8 times greater in batch and 14 times greater in fed-batch fermentations for the production of recombinant protein. Moreover, by running 12 more experiments here with reproducible data, it establishes the robustness of the integrated 7 L fermenter and electrodialysis module.

Considering Chapters 4 and 5 together the key factors influencing the design of an ED process would be the time of induction for protein synthesis and duration of ED operation. Bipolar membrane is next introduced to ED application and will be studied in Chapter 6.

Chapter 6

Application of bipolar electrodialysis (BPED) to *E.coli* fermentation for simultaneous acetate removal and pH control[3]

6.1 Introduction

As described previously in Section 1.2, *E.coli* fermentation is widely used for the production of recombinant enzymes and therapeutic proteins. One of the factors limiting the productivity of *E.coli* fermentation is the formation of acetate, as shown in Section 4.2, which causes inhibition of cell growth and recombinant protein synthesis (Han *et al,*. 1992). A number of approaches exist to overcome this problem (Eiteman and Altman. 2006), the most widely used being controlled feeding of the carbon source (Akesson *et al,*. 2000). As shown in Chapters 4 and 5 benefits of ED applied to *E.coli* fermentation led to a reduction of the concentration of acetate in the media and hence increases in both cell growth and the specific recombinant protein production. Concerns remain however regarding the volume of NH_4OH added for pH control which could also be toxic to the cells (Muller *et al,*. 2006). A potential solution is the

[3] The results presented in this chapter have previously been published as Wong M, Woodley JM, Lye GJ (2010) Application of bipolar electrodialysis to *E.coli* fermentation for simultaneous acetate removal and pH control. Biotechnology Letter 32: 1053-1057

use of bipolar electrodialysis (BPED), which can hydrolyse an aqueous salt solution under the influence of electrical current to produce pure hydrogen and hydroxide ions. In principle this approach could be used to directly acidify or basify the fermentation broth without the addition of extraneous chemicals. From an operational perspective, the cost of acid or base could be reduced and the process could have reduced requirements with regard to treatment of the spent broth.

The aim of this chapter is therefore to demonstrate the principle of BPED fermentations and compare cell growth and protein production to the earlier studies in Chapters 4 and 5 on batch and fed-batch fermentations with or without ED application (Wong et al. 2009). The specific objectives include:

- Investigation of the effect of ammonia on the growth of *E.coli* TG1 pGLO.
- Examination of the performance of reproducible 7L batch and fed-batch bipolar electrodialysis fermentations.
- Comparison of ED and BPED fermentations on biomass growth, recombinant protein synthesis and volume of base used.

6.2 Results and discussions

6.2.1 Principle of BPED

A bipolar (BP) membrane is a cation exchange membrane laminated together with an anion exchange membrane through an intermediate layer. In the presence of electric field, water molecules are split into hydrogen and hydroxyl ions. The principle of

BPED and its application in *E.coli* fermentation were explained in Section 2.2.4 and Figure 2.4.

6.2.2 Ammonium toxicity

To demonstrate the impact of ammonium toxicity on the cells, a small scale preliminary experiment was performed involving additions of 10, 20 and 30 $g.L^{-1}$ of NH_4Cl to separate 100 mL shake-flask cultivations. These amounts were indicative of the quantity of ammonium used for pH control in our previous batch and fed-batch fermentations in Section 5.2. Figure 6.1 gives an indication of ammonium toxicity on growth of the *E.coli* TG1 cells. Once NH_4Cl was added at mid-exponential phase, there was an immediate effect on the cells resulting in a reduction of cell growth rate. Addition of 30 $g.l^{-1}$ NH_4Cl led to a 50% reduction in the final biomass concentration. These data suggest that the ammonium concentrations in the broth should be maintained below 10 $g.L^{-1}$.

6.2.3 Batch and fed-batch BPED fermentations

The results of batch and fed-batch BPED fermentations are presented in Figure 6.2 and 6.3, respectively. Reproducible trends for cell growth, acetate accumulation and recombinant protein production were obtained in replicate independent experiments. In batch BPED fermentations, BPED was applied after the lag phase at 6 h and arabinose was added to induce GFP synthesis at early exponential phase. The biomass and protein concentrations continued to increase to 15.4 and 3.3 $g.L^{-1}$ respectively at 18 h. Similar trends can be observed for the initial phase of the fed-batch BPED fermentation. When exponential feeding started at 10 h, biomass and protein

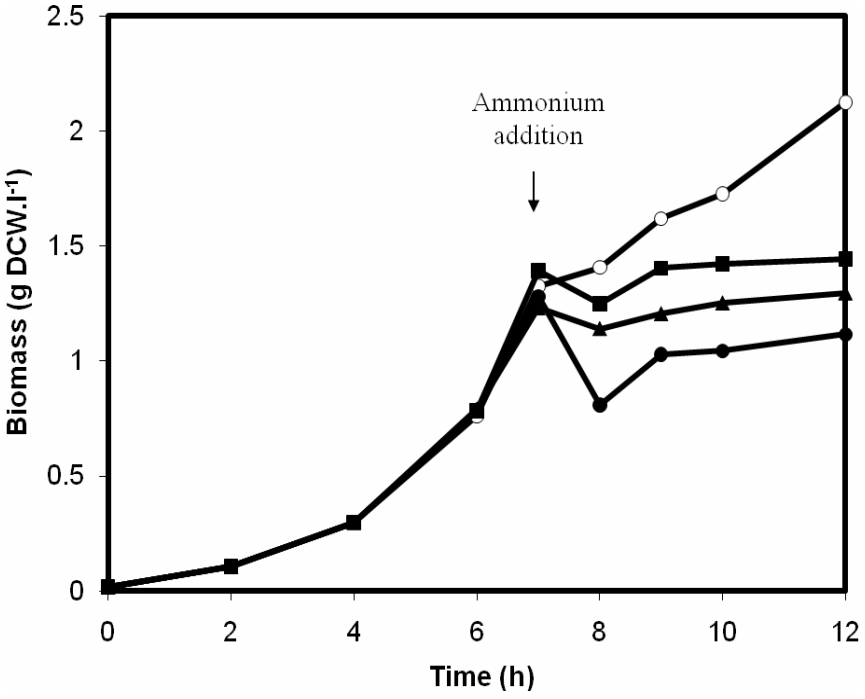

Figure 6.1. Effect of ammonium ion addition on growth of E.coli TG1 pGLO in shake-flask fermentations with additions of 0 (○), 10 (■), 20 (▲) and 30 (●) g.L-1 of NH4Cl. Arrow indicates time of ammonium chloride addition. Error quoted represent one standard deviation about the mean (n=3). Experiments performed as described in Section 2.2.2.3.

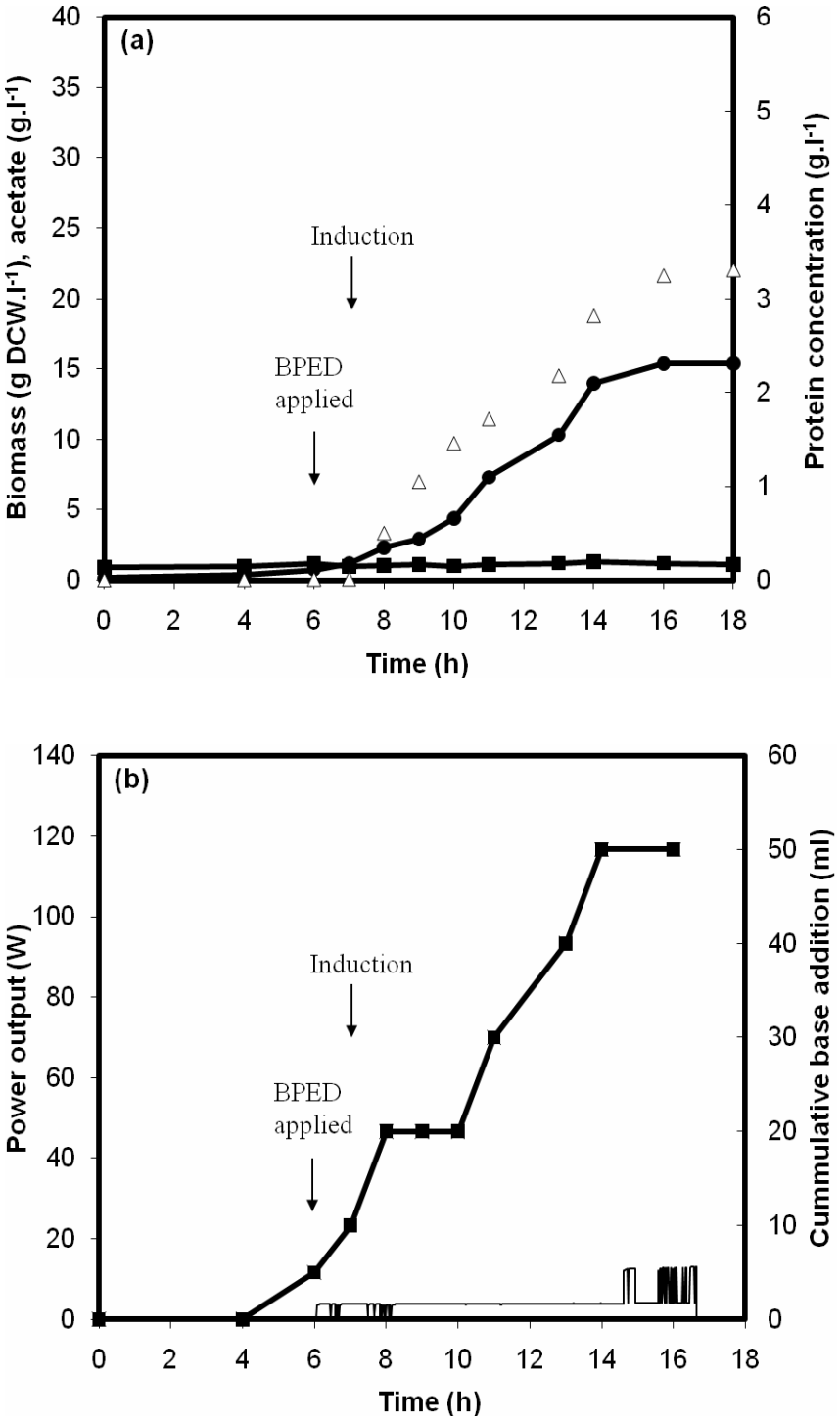

Figure 6.2. Bipolar electrodialysis batch fermentation kinetics of *E.coli* TG1 pGLO. (a) Off-line data for biomass (●), acetate (■) and recombinant protein, GFP, (Δ) concentration. (b) Power output (-) and base addition (■). Arrows indicate times of induction and BPED application. Results show typical profile from triplicate fermentations. Experiments performed as described in Section 2.2.4

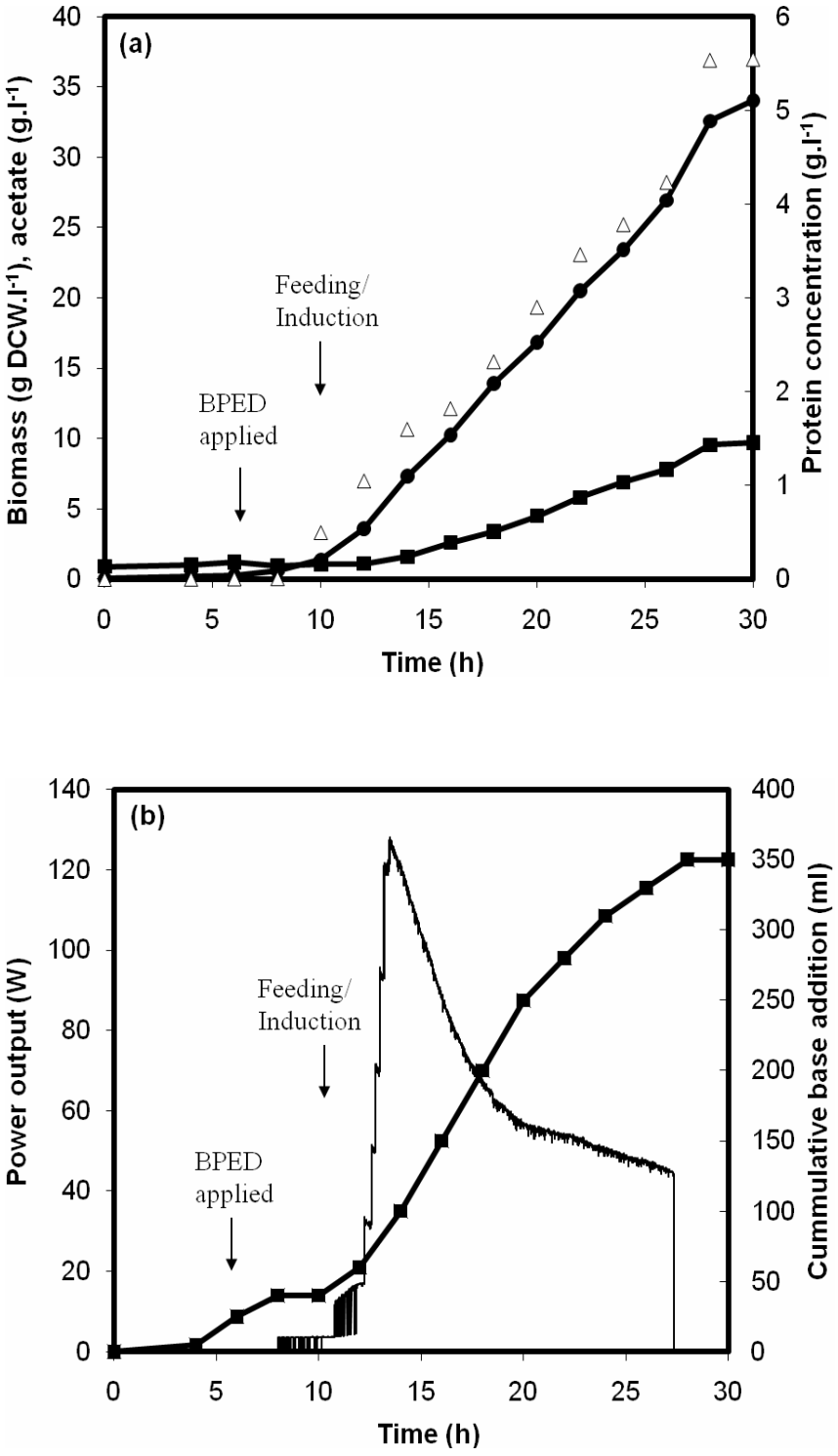

Figure 6.3. Bipolar electrodialysis fed-batch fermentation kinetics of *E.coli* TG1 pGLO. (a) Off-line data for biomass (●), acetate (■) and recombinant protein, GFP, (Δ) concentration. (b) Power output (-) and base addition (■). Arrows indicate times of induction, feeding and BPED application. Results show typical profile from triplicate fermentations. Experiments performed as described in Section 2.2.4

concentrations increased linearly up to 30 h, reaching final concentrations of 34.2 $g.L^{-1}$ and 5.5 $g.L^{-1}$ respectively. Figures 6.3b and 6.4b indicate the corresponding base additions and power output of each experiment. These are important parameters of BPED performance and are discussed further in the Section 6.2.4.

6.2.4 Comparison of ED and BPED fermentations

Table 6.1 summarises the results of the BPED fermentations performed here and compares them to previous results (Section 5.2.1) from batch and fed-batch fermentations with or without application of conventional electrodialysis. The presence of acetic acid retards cell growth and inhibits recombinant protein production (Han *et al*,. 1992). Consequently it was shown that the application of conventional ED for *in situ* acetate removal enhanced cell growth and recombinant protein synthesis (Section 5.2). A limitation of the earlier ED studies was that the anion exchange membrane area was limited to 100 cm^2. It is evident in this work that by doubling the anion exchange membrane area to 200 cm^2 (Section 2.2.4), the rate of acetate ion removal is increased and so the accumulated acetate concentrations were reduced by up to 50%.

In addition to removal of acetate, however, ED also removed hydroxyl ions from compartment F to R and as much as 50% extra base addition was required for pH control. In contrast to the ED fermentations, the additional PID controller used in the BPED system led to the rate of ion removal being proportional to the amount of acetate present so fewer hydroxyl ions were removed. This conservation of hydroxyl ions in compartment F and simultaneous generation of hydroxyl ions for pH control from the bipolar membrane resulted in reduction of base addition volume by up to 60% in batch

Table 6.1. Comparison of batch and fed-batch *E.coli* TG1 pGLO fermentation kinetics with standard electrodialysis (ED) application and application of bipolar electrodialysis (BPED). Error quoted represents one standard deviation about the mean (n=3).

Fermentation conditions	**[Biomass] (g DCW.L^{-1})**	**[Protein] (g.L^{-1})**	**[Acetate] (g.L^{-1})**	**Volume of base addition (mL)**	**References**
Batch	13.6 ± 0.1	2.91 ± 0.04	5.5 ± 0.3	100 ± 3	Section 5.2
ED batch	12.3 ± 0.2	3.05 ± 0.05	2.1 ± 0.2	125 ± 4	Section 5.2
BPED batch	15.4 ± 0.2	3.31 ± 0.05	1.33 ± 0.2	50 ± 2	Section 6.2
Fed-batch	30.5 ± 0.2	5.01 ± 0.08	25.1 ± 0.6	800 ± 8	Section 5.2
ED fed-batch	24.9 ± 0.3	4.56 ± 0.04	18.8 ± 0.5	1200 ± 15	Section 5.2
BPED fed-batch	34.2 ± 0.5	5.50 ± 0.08	9.70 ± 0.4	370 ± 6	Section 6.2

and 71% in fed-batch mode respectively. In addition, by providing a less toxic environment for cell growth and further reductions in acetate accumulation, there was an increase in biomass yield of up to 37% in fed-batch fermentation and an increase in recombinant protein production of up to 20%.

With respect to operation of the ED/BPED units reduced energy consumption is important as it leads to a reduction in operating cost and reduced environmental footprint of the process. ED fermentations operated at a fixed current of 2 A with a voltage range of 35-40 V, so the power output was fixed at 70-80 W. From Figure 6.3b and 6.4b, the calculated average power output for BPED batch and BPED fed-batch fermentations were 6.5 W and 59 W, respectively. Based on the ED power consumption data there appears to be a specific power consumption of the order of 10 $kW.m^{-3}$. However, this is due to the small scale and experimental nature of the ED device used. The lower energy consumption is a major advantage of BPED over ED. Furthermore, due to the lower power output with BPED, electromigration only took place when acetate was present, so energy was not wasted in the removal of other ions. This is even more significant at industrial scale where energy consumption and base used can be major cost factors.

Overall, the main advantages of BPED over ED were the production of hydroxyl ions and the PID controlling system, resulting in less undesirably removal of ions such as medium ions and hydroxyl ions from base. Therefore, BPED system reduced base addition and decreased ammonium toxicity.

6.3 Summary

This chapter has demonstrated for the first time the use of a PID controller system for

bioreactor pH control and simultaneous *in situ* removal of inhibitory acetate by BPED. As a basis for these studies, the adverse effect of ammonium toxicity was proven (Figure 6.1). BPED was able to remove up to 75% of acetate formed from the fermentation broth (Figure 6.2 and 6.3). Furthermore, it served to provide base pH control and therefore the total volume of base addition was decreased by 50%. Consequently, there were increases in biomass yield of up to 37% in fed-batch fermentation and in recombinant protein production of up to 21% (Table 6.1). It is therefore concluded that this approach could in principle be applied beneficially to a wide range of *E.coli* fermentations for production of recombinant enzymes and therapeutic proteins.

Chapter 7

Utilisation of electrodialysis to enhance the performance of hydrolytic enzymatic bioconversions

7.1 Introduction

Bioconversion has now become a standard technology in the fine chemicals industry (Straathof *et al.,* 2002). This is reflected by the increasing number of processes running on commercial scale. However, there are two common challenges to implementing bioconversion processes that meet the required levels of productivity (or space-time yield. One frequent limitation on productivity is product inhibition of enzymatic catalysis (Lye and Woodley, 1999). This problem lead to the invention of *in situ* product removal (ISPR) techniques, where the product is removed from the vicinity of the enzyme as soon as it is formed in the reactor (Freeman *et al.,* 1993). A second challenge is the addition of acid or base for pH control which is necessary since most enzyme display a defined pH optimum and reactants can equally be unstable outside a narrow pH range. Acid or base addition in this case results in the formation of organic salts instead of the desired free organic acids (Yazbeck *et al.,* 2004).

Having already shown the benefits of ED (Chapter 4) for (by-) product removal and BPED (Chapter 6) for simultaneous pH control, the technology is evaluated here for

application to bioconversion processes. The aim of this chapter, therefore, is to quantitatively investigate the potential uses of these electrodialysis techniques in enzymatic bioconversion processes. The specific objectives include:

- The application of ED as an *in situ* product removal tool for the stereospecific hydrolysis of ethyl acetate to increase the productivity of acetate formation.
- Demonstration of utility of BPED for pH control in an attempt to reduce the usage of acid and base in the bioconversion of fumaric acid.
- Evaluation of ED to remove sodium ions from sodium malate molecules and form free malic acid and so aid bioconversion product recovery and purification.

7.2 Results and discussions

7.2.1 Hydrolysis of ethyl acetate

7.2.1.1 Shake flask bioconversion

In order to demonstrate the advantages of electrodialysis to the hydrolysis of ethyl acetate, it is first necessary to establish the benchmark lipase concentration and product yield at shake flask scale. The reaction scheme is shown in Figure 2.5 and background to the bioconversion was described earlier in Section 1.3. For these initial shake flask experiments Figure 7.1 presents the kinetic profiles of ethyl acetate hydrolysis and the formations of ethanol and acetate. Addition of 20, 10 and 5 $g.L^{-1}$ of lipase at the start of each experiment, led to decreases in the percentage of substrate hydrolysed after 300 min from 50, to 40 to 25%, respectively. Hence at the highest lipase concentration used, the greatest productivity was obtained and the theoretical maximum conversion

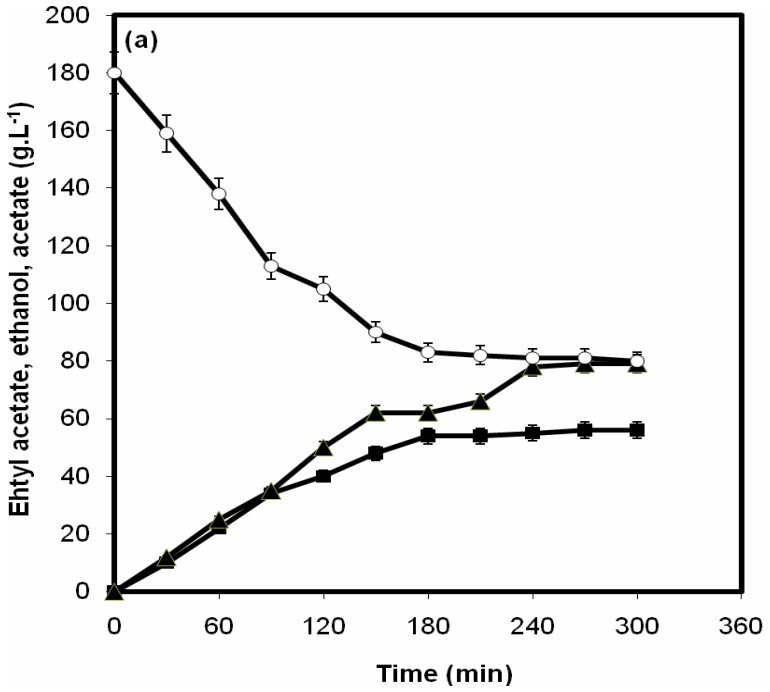
(a)
Ehtyl acetate, ethanol, acetate (g.L-1)
Time (min)
0
20
40
60
80
100
120
140
160
180
200
0
60
120
180
240
300
360

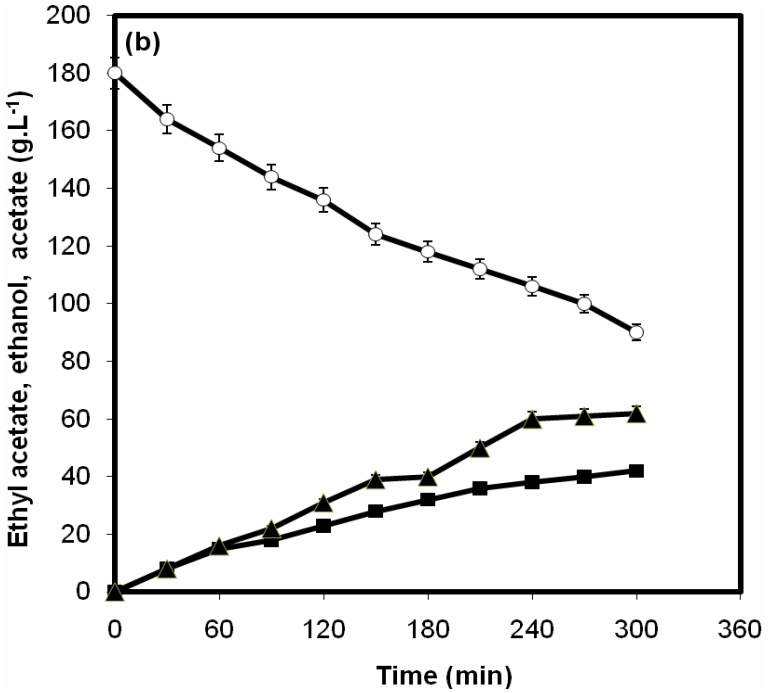
(b)
Ethyl acetate, ethanol, acetate (g.L-1)
Time (min)
0
20
40
60
80
100
120
140
160
180
200
0
60
120
180
240
300
360

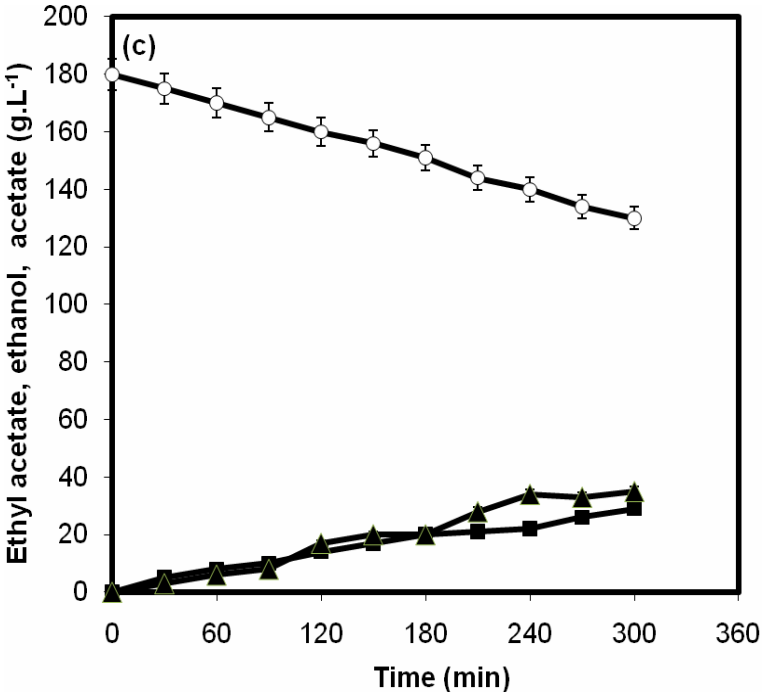

Figure 7.1. Shake flask hydrolysis kinetics of ethyl acetate (○) bioconversion into ethanol (■) and acetate (▲) at lipase concentrations of **(a)** 20 **(b)** 10 and **(c)** 5 $g.L^{-1}$. Error bars represent one standard deviation about the mean (n=3). Experiments performed as described in Section 2.2.5.1.

of 50% was obtained. However, at larger scale, it may not be feasible to operate at such high enzyme concentration of 20 $g.L^{-1}$ or if this much enzyme is used it would need to reused over many cycles. At this highest enzyme concentration of 180 $g.L^{-1}$ of ethyl acetate was hydrolysed yielding 56 $g.L^{-1}$ of ethanol and 79 $g.L^{-1}$ of acetate formed, complementary to the dissociation of ethyl acetate.

7.2.1.2 Quantification of acetate inhibition level

Inhibition of lipase by the acetate product is a recognised problem in this bioconversion (Bevilaqua *et al.,* 2004). Figure 7.2 shows the effect of acetate inhibition in a reaction, where 20 $g.L^{-1}$ of acetate was added at the start of a standard hydrolysis of ethyl acetate at 20 $g.L^{-1}$ of lipase concentration. In the presence of acetate, there was only 50 $g.L^{-1}$ of ethyl acetate hydrolysed in 300 min. Compared to Figure 7.1a , this led to a 50 % decrease in product yield with the formation of ethanol and acetate were also reduced to 28 and 30 $g.L^{-1}$, respectively.

7.2.1.3 3L STR bioconversion

After demonstrating the small scale bioconversion kinetic (Figure 7.1) and showing the effect of acetate inhibition (Figure 7.2), the bioconversion was next scaled-up to a 3L STR scale where the ED module developed in Section 2.2.1 could be applied. Figure 7.3 indicates the dissociation rate of ethyl acetate with addition of 3.33 $g.L^{-1}$ of lipase at 3 L scale in a STR (without ED application). The lower concentration of enzyme used reflects the cost contribution of the enzyme to the overall process and a more realistic example of the enzyme loading level that could be used industrially. At 600 min, the concentration of ethyl acetate decreased from 180 to 140 $g.L^{-1}$ which led to 22.2% w/w product yield. The specific bioconversion rate was 8 $g.L^{-1}.h^{-1}$ coincides with

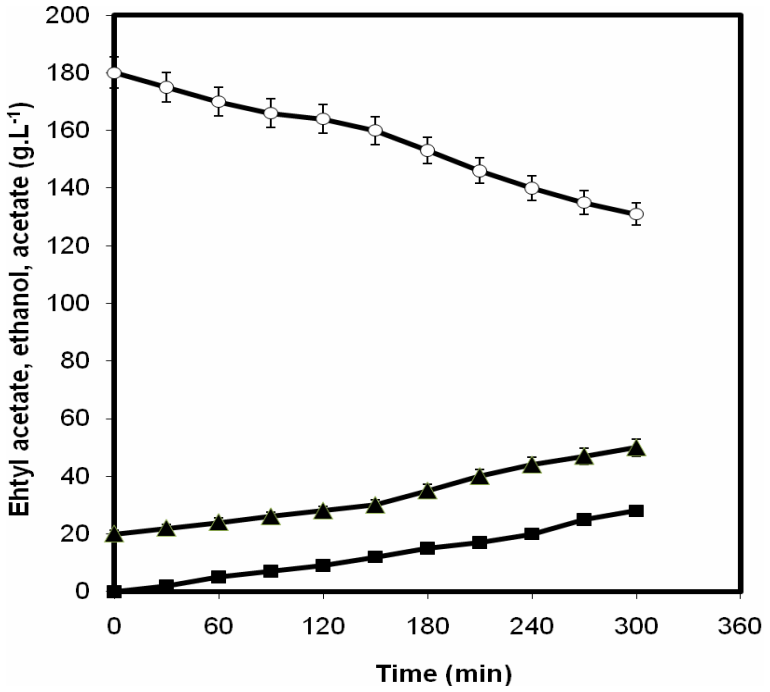

Figure 7.2. Shake flask hydrolysis kinetics of ethyl acetate (○) bioconversion into ethanol (■) and acetate (▲) to investigate acetate product inhibition. Lipase concentrations of 20 $g.L^{-1}$ with the addition of 20 $g.L^{-1}$ of acetate at the start of experiment. Error bars represent one standard deviation about the mean (n=3). Experiments performed as described in Section 2.2.5.1.

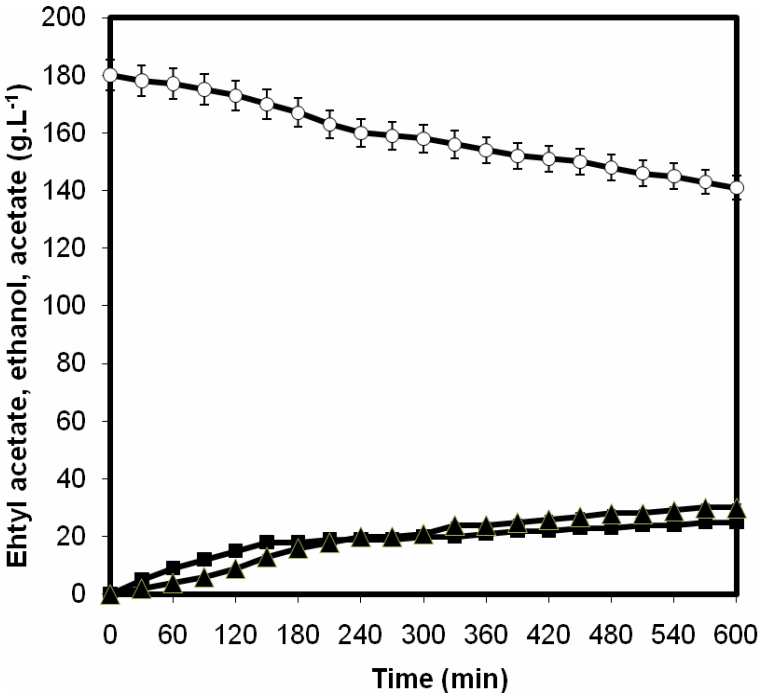

Figure 7.3. 3 L STR hydrolysis kinetics of ethyl acetate (○) bioconversion into ethanol (■) and acetate (▲) at a lipase concentrations of 3.33 $g.L^{-1}$. Error bars represent one standard deviation about the mean (n=3). Experiments performed as described in Section 2.2.5.1.

bioconversion performed at shake flask scale in Figure 7.1c.

7.2.1.4 3L STR bioconversion with electrodialysis

Having established the benchmark product yield and kinetic data in a conventional bioconversion with a biocatalyst concentration of 3.33 $g.L^{-1}$ of lipase (Section 7.2.1.3), the equivalent bioconversion was next performed with the electrodialysis module in place. Figure 2.5c shows the ED module configuration used in this work where acetate is expected to migrate through an anion exchange membrane from compartment F to compartment R.

Figure 7.4 shows that in the ED-bioconversion up to 23 $g.L^{-1}$ of the acetate product was removed from compartment F to R by 600 min. The concentration of ethyl acetate reached 96 $g.L^{-1}$ representing 46.6% w/w product yield in 600 min. This result confirms the benefits of applying ED to overcome product inhibition since the measured rate of ethyl acetate hydrolysis is nearly double that measured (Figure 7.3) when ED was not applied. The formation of ethanol and acetate were correspondingly also increased to 51 and 42 $g.L^{-1}$, respectively. This showed an equal mass balance and there was no substrate and product loss on membrane. Also, the constant rate of hydrolysis measured suggests that the lipase retained its activity over time and was not denatured or lost onto the membrane surface.

7.2.1.5 3L STR bioconversion with bipolar electrodialysis

With the availability of the more advanced bipolar electrodialysis module described in Section 6.2.2, an attempt was made to further improve the ethyl acetate bioconversion rate by BPED application. In this case, BPED was applied to reduce base addition for pH control.

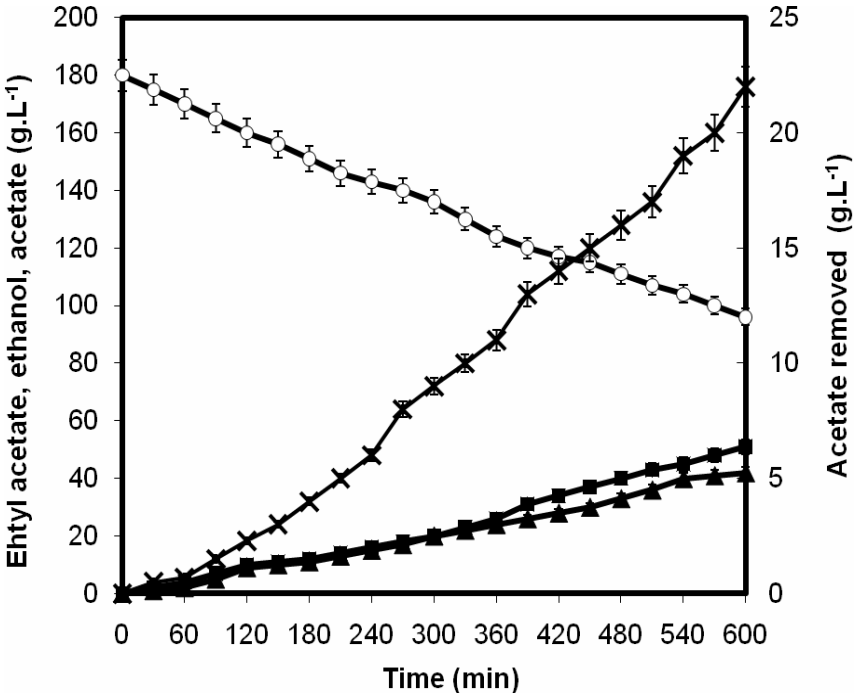

Figure 7.4. 3 L STR hydrolysis kinetics of ethyl acetate (○) bioconversion into ethanol (■) and acetate (▲) at a lipase concentrations of 3.33 $g.L^{-1}$. Electrodialysis is appplied from the start of the bioconversion to remove acetate (x) formed from compartment F to comparment R (Figure 2.5). Error bars represent one standard deviation about the mean (n=3). Experiments performed as described in Section 2.2.5.1.

Figure 7.5a shows the results of this BPED bioconversion which indicates a small improvement on the bioconversion rate seen previously with ED in Figure 7.4. In this case a similar concentration of acetate is removed and in which 10 $g.L^{-1}$ more of ethyl acetate was hydrolysed. Figure 7.5b shows the online pH profile throughout the experiment. The observed fluctuation of pH was most likely due to the low buffering capacity of the medium in compartment F which compromised of just ethyl acetate. Operation of the BPED was more complex and required extra equipments such as the bipolar membrane, PID controller and computerised control system. Given the limited additional benefits seen in the BPED results it would be more beneficially to run the hydrolysis of ethyl acetate only with the standard electrodialysis module.

7.2.2 Bioconversion of fumaric acid

7.2.2.1 Initial pH adjustment of fumaric acid

The reaction scheme for the second bioconversion studies is shown in Figure 2.5a and background to the bioconversion was described earlier in Section 1.3. In this case the application of ED is investigated in order to serve as a base provider by the splitting of water molecules through a bipolar membrane as explained in Section 2.2.4.

For the standard bioconversion Figure 7.6 shows that prior to the start of the experiment, 2 M sodium hydroxide was added to the fumaric acid powder until dissolved at pH 4. The BPED system (Figure 2.5a) was employed to adjust the pH of the fumaric acid solution to 7. This method reduced the presence of sodium ion, which subsequently would decrease the formation of sodium malate salt. For the similar reason of reducing unnecessary ions in the system, three phosphate buffer concentrations of 0,

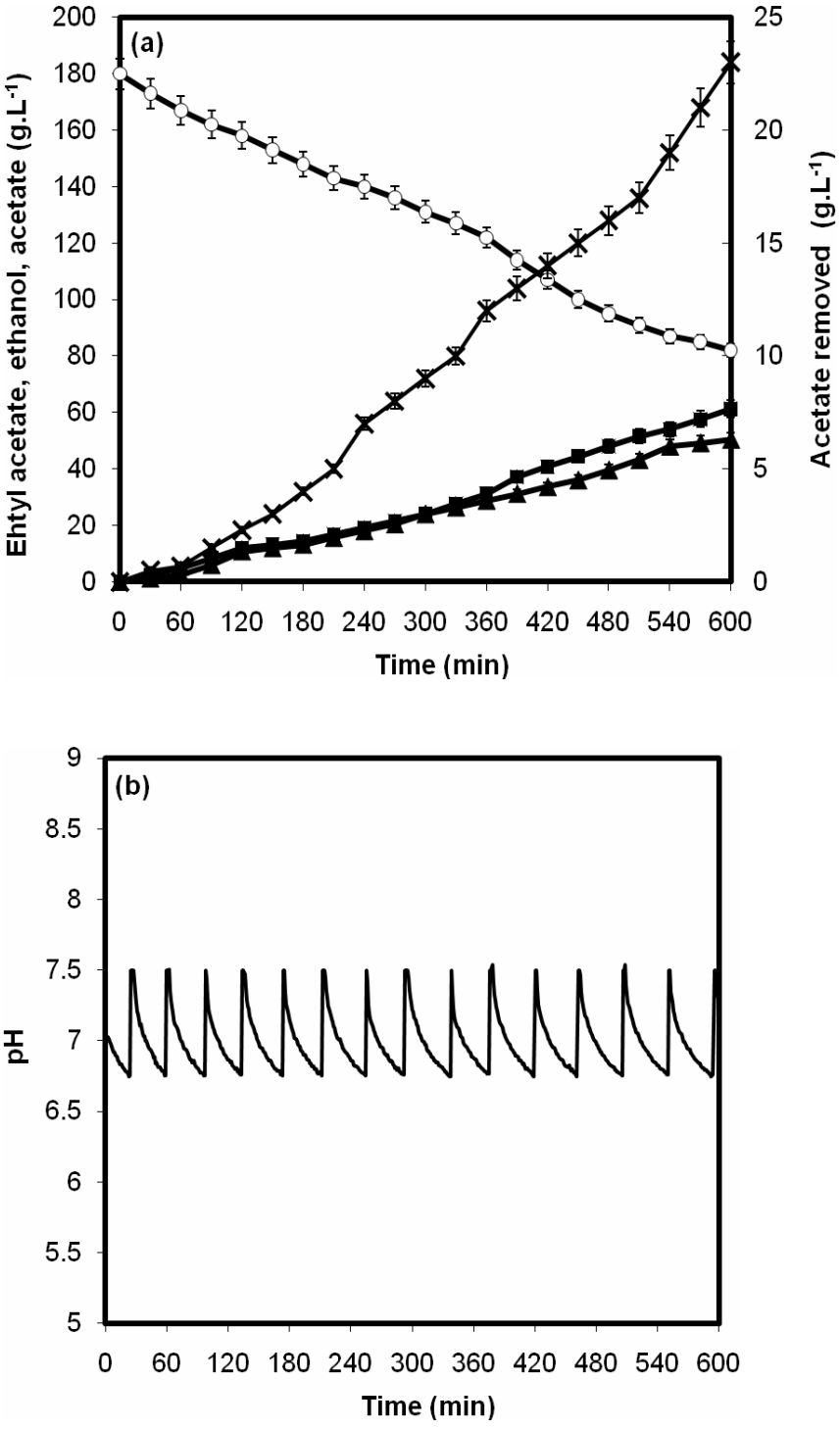

Figure 7.5. **(a)** 3 L STR hydrolysis kinetics of ethyl acetate (○) bioconversion into ethanol (■) and acetate (▲) at a lipase concentrations of 3.33 g.L-1. BPED is appplied from the start of the bioconversion to remove acetate (x) formed from compartment F to R. **(b)** Online pH mesurement during bipolar electrodialysis. Error bars represent one standard deviation about the mean (n=3). Experiments performed as described in Section 2.2.5.1.

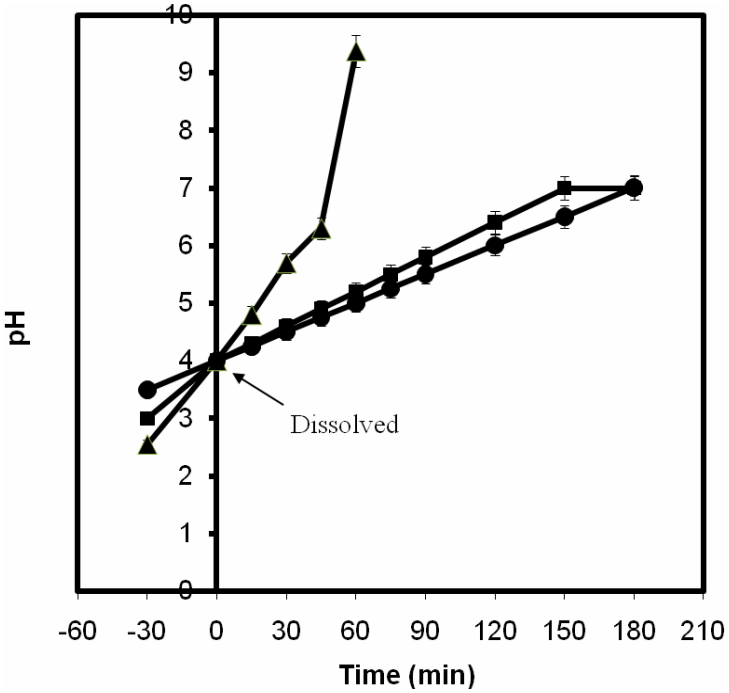

Figure 7.6. Initial pH adjustment of furmaric acid using BPED with buffer concentrations of 0 (▲), 0.01 (■) and 0.1 (●) M. Prior to 0 h, 2M sodium hydorxide was added for the dissolving fumaric acid powder as arrow indicates. Error bars represent one standard deviation about the mean (n=3). Experiments performed as described in Section 2.2.5.2.

0.01 and 0.1 M were used. Result indicates a minimum of 0.01 M of phosphate buffer was required, in order to aid the pH control by the BPED system.

7.2.2.2 Bioconversion of fumaric acid

Figure 7.7 shows the standard 3L STR bioconversion of fumaric acid (Figure 7.7a) and with the application of BPED (Figure 7.7b). In the case of the standard bioconversion solutions of 2M sodium hydroxide and 1M sulphuric acid were used for pH control. The use of BPED had a less stable pH control and gave a final malic acid concentration of 20.8 $g.L^{-1}$, compared to 19.2 $g.L^{-1}$ produced with addition of sodium hydroxide for pH control. Therefore, similar results were obtained by both methods. In the case of the standard pH control, there was up to 400 mL of extra sodium hydroxide added than under BPED which would result in dilution of the product stream by 13 %. Hence the excess of sodium would become critical in the subsequent process of producing free malic acid.

7.3 Summary

This chapter sought to extend the application of ED to enzymatic bioconversion and illustrated the application of ED to the bioconversions of ethyl acetate (Section 7.2.1) and fumaric acid (Section 7.2.2).Shake flask experiments of the lipase catalysed hydrolysis of ethyl acetate were initially carried out (Figure 7.1) to establish benchmark

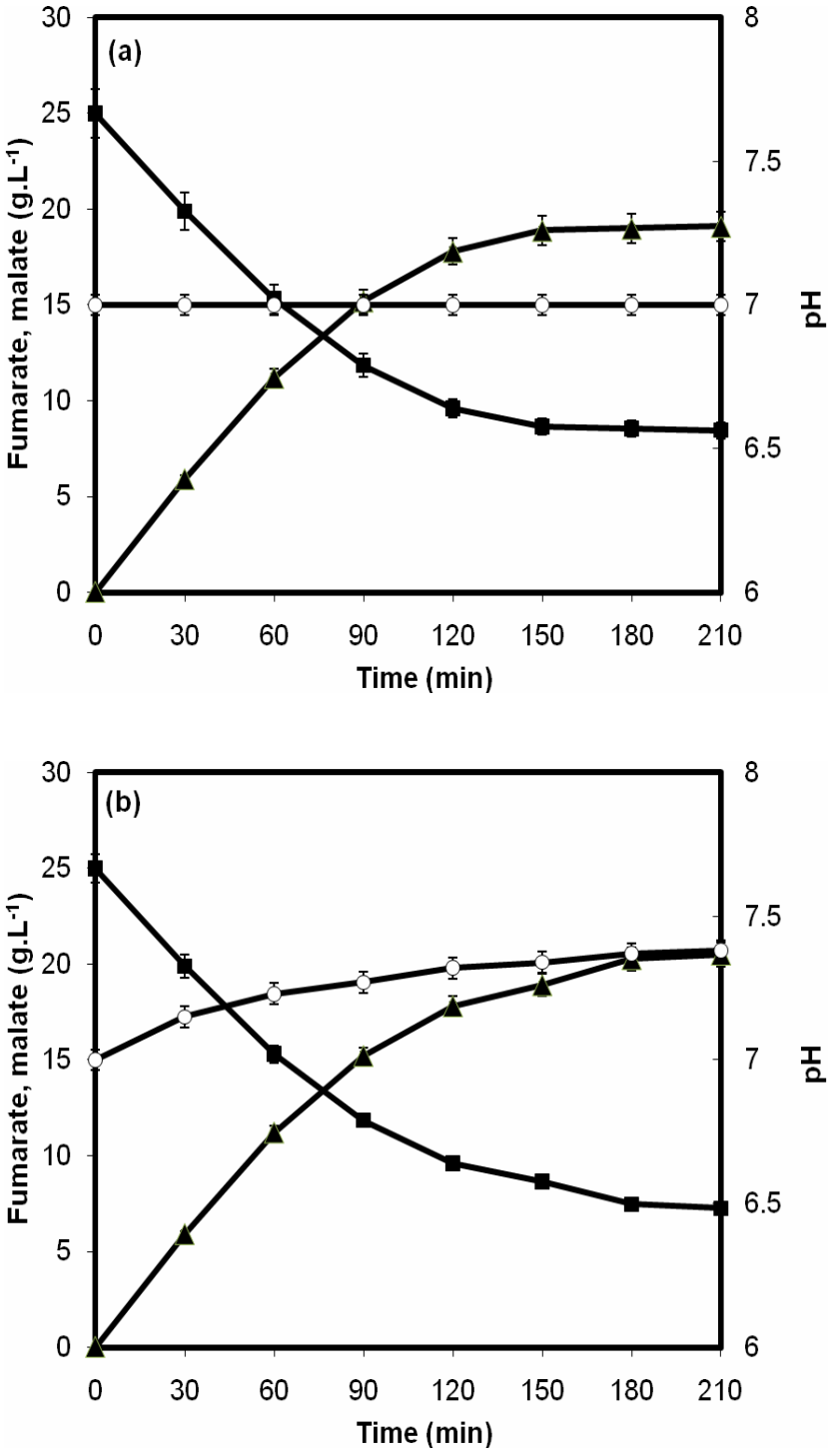

Figure 7.7. **(a)** Standard 3 L STR bioconversion kinetics of fumaric acid (■) into malic acid (▲) with 3.33 mg.L-1 of fumarase. Direct addition of acid/base used for pH (○) control. **(b)** 3 L BPED STR bioconversion kinetics of fumaric acid (■) into malic acid (▲) with 3.33 mg.L-1 of fumarase. Control of pH (○) achieved by controlled by the application of BPED. Error bars represent one standard deviation about the mean (n=3). Experiments performed as described in Section 2.2.5.2.

product yield and the adverse effect of acetate inhibition (Figure 7.2). The process was then scaled up to 3 L STR scale and the standard bioconversion (Figure 7.3) compared to both a 3 L ED bioconversion (Figure 7.4) and a 3L BPED bioconversion (Figure 7.5). Application of both ED and BPED led to enhancements in bioconversion performance as previously found in microbial fermentations (Chapters 4, 5 and 6). In this case the application of ED to *in situ* remove of inhibitory acetate increased the bioconversion product yield by over two times.

In the case of the fumarase bioconversion, prior to the bioconversion of fumaric acid, BPED system was applied for the pH adjustment of fumaric acid (Figure 7.6). It was then used again during the experiment for pH control (Figure 7.7b). Compare to the standard pH control method of acid/base addition (Figure 7.7a), there was up to 400 mL less of 2M sodium hydroxide added. This resulted an extra 14 $g.L^{-1}$ of sodium for the subsequent separation step.

Overall the work presented in this chapter has shown the additional potential of ED for application in enzymatic bioconversions to act as an *in situ* product removal in order to enhance productivity. The additional benefits of BPED for pH adjustment and pH control were also shown. Having now established the broad application and benefits of ED technology for both fermentation and bioconversion processes the following chapter will examine the industrial implementation and technology validation.

Chapter 8

ED Technology validation and industrial implementation[4]

8.1 Introduction

The work presented in this thesis has shown that ED can potentially be applied across a number of sectors within the bioprocess-using industries including enzyme and therapeutic protein manufacture as well as pharmaceuticals and fine chemicals. Each of these has its own regulatory requirements for technology implement and process operation. Those related to biopharmaceutical manufacture are currently the most stringent providing the greatest barrier to ED application. Consequently the requirements for ED application in this sector will be considered here.

Biopharmaceutical products need to be efficacious and economically viable to produce while satisfying regulatory requirements on their safety. Since they are biologically derived these drugs usually requires purification from a complex mixture of contaminating proteins, DNA, lipids and other metabolites. Throughout production, data must be collected that gives assurances that the process implies product quality under the regulatory bodies of FDA (USA) and MCA (UK/EU). The process must consistently meet these specifications. This includes a robust and well characterised process that can withstand inevitable variance in operating conditions including operator error. The aim of this EngD chapter is to review the set-up and operation of

[4] This chapter is included as part of the UCL requirement for the award of the EngD degree.

ED module in an industrial context and to make suggestions in the marketing of ED application. The specific objectives include:

- Validation requirements of ED technology comprising design, installation, operation and process, to provide assurance for reliable and reproducible results.
- Evaluation and justification of the ED module for industrial implementations and development issues.

8.2 Technology validation

Bioprocess validation is a sequential system of qualifications which provide assurance that a process will reliably and reproducibly result in a product meeting all critical quality acceptance criteria.

8.2.1 Design

Prior to the manufacturing of an ED module for a specific application, the engineering of design should be checked to ensure that it can meet the performance requirements for the intended application, such a by-product acetate removal (Chapter 4) during biopharmaceutical manufacture. The performance of ED is primarily determined by the required rate of solute ion removal (as shown in Section 3.2). At the designing stage, the specifications include the effective area of the plated electrodes and ion exchange membrane, volume of each compartment, the position of inlet and out to ensure both good mixing and efficient solute mass transfer within the ED module (Section 3.2.2). At high desired flow rate of above 1 $L.min^{-1}$ and specific pressure

limits, it is essential to prevent leakage from module and bursting of ion exchange membrane. Also, the distance between each membrane could be less than 1 mm so it is important to keep the membrane from contacting each other. This requires spacer to support membrane, while ensuring turbulent flow and enhance mass transfer Finally, uniform flow formation and even distribution of electrical current within the ED module are essential for .constant solute mass transfer. ED module is often made of PVC (Industrial ED module are made by Tokoyuma co, Japan and Eurodia Industre SA, France) due to its insulting properties which can withstand temperature of up to 100 ^{o}C and resistant for most chemical detergents. A unique material may be used to endure more extreme conditions of specific process

8.2.2 Installation

For small scale applications the assembling of an ED module (see Figure 2.1) is complicated and involves the fittings of electrodes, the placement of suitable ion exchange membranes and the o-ring sealing of these parts to prevent leakages during operation. The connections of the ED module to the rest of ED set-up include input and output streams of each compartment to the associated reservoir. Also, anode and cathode are connected at positive and negative terminals of the power supply, respectively, otherwise it would cause irreversible damaged to the electrodes. When installing a bipolar membrane (Chapter 6), the anodic and catholic sides must be facing the anode and cathode, respectively. At large scale, high voltage of up to 200V may be applied, so it is necessary to insulate electrodes and all other electrical contact points. At both scales the ion exchange membranes must be kept in moist condition to prevent them from drying, so operation should start within 3 hours after installation. Finally, the integration of ED module to another operation unit may require alteration to

apparatus and operation procedures to compromise both parts. At larger scales, it requires more sophisticated valves for by-pass operations, clean-in place and sterilisation of lines.

8.2.3 Operation

Sterilisation of ED module can be carried out chemically or through autoclaving at 121 ^{o}C. Chemical sterilisation involves circulating strong acid or base solution such as 2 M hydrochloric acid or sodium hydroxide through the ED module. It is then essential to rinse the channels with sterilised de-ionised water to remove any remaining acid or base. Autoclaving sterilisation requires placing the ED module under high pressure and temperature and this could cause drying of the ion exchange membranes.

During the operation of laboratory scale ED, current and voltage are kept below 5 A and 40V, respectively, to prevent overheating and increase in electrical resistance. This is likely to be a problem for the bioprocess product and the effectiveness of the ion exchange membrane. At large scale and high voltage, it may necessary to put a cooling system in place. Also, the circulation flow rate for all channels must be the same for constant solute mass transfer. Depending on the nature of feed and product, potential hydrodynamic shear damage caused by the flow should be considered.

8.2.4 Process

The benefits of ED application are quantitatively measured by the rate of desired solute ion removal and the level of product enhancement compared to a standard (non-ED) process (as shown in Chapters 4 and 5). Other criteria include contaminant free product and the re-usability of the ion exchange membranes.

Chapters 4, 5 and 6 demonstrated the benefits of ED to production of a model recombinant protein, GFP. It shows potentials for productions in biopharmaceutical and therapeutic uses. Barriers to the future commercialisation of ED technology is further discussed in Section 8.3.

8.3 Industrial implementation

In order to market ED for existing applications, a scaled-down version of a pilot or manufacturing scale ED unit would be highly desirable in order to allow industrial companies to quickly and cheaply evaluate the potential benefits and compatibility of ED module to their existing production method. Testing can be done rapidly because any ED module is externally integrated to the bioreactor (Figure 2.3a), so it does not require major alterations to the existing production set-up. After management approval of capital investment in ED, scaling-up for industrial production is essential. This requires larger cross sectional area of ED module and additions of compartment for increasing the effective ion exchange membrane area, greater circulation flow rate as well as the increased current applied to electrodes.

The main start-up costs of ED include the fabrication of module compartments, platinum and stainless steel electrodes, peristaltic pump and power supply. At industrial scale of up to 300 m^2 in effective membrane area, the cost of the whole set-up ranges from £75,000 to £250,000, depending on the materials and specifications of the module (Personal Communication from Eurodia Industrie SA, France). The operational cost of ED process includes the usage of electricity and the replacement of ion exchange membranes. These are system specified, as they depend on the duration of the process and the rate and extent of membrane fouling. Despite the expense of ED,

the market trends of recombinant protein for therapeutics have continuously increased over the past twenty years (Pavlou and Reichert. 2004). For example the manufacturing cost of heparinase I is up to $560,000 per kg (Ernst *et al.,* 1997) as discussed in Section 4.1. Chapters 4, 5 and 6 illustrated the application of ED enhanced the protein production level by up to four times. Therefore, given a suitable bioprocess application, ED would be a very profitable technology to be employed. A 5 % enhancement in recombinant protein production (achieved in Chapter 5) would provide extra $28,000 of profit per kg.

A number of issues relate to the further development ED technology need to be considered which may reduce its chance to be widely applied at industrial scale. The first obstacle is the limited selectivity of ion exchange membrane (Section 3.2) which only separates positively and negatively charged solute ion and this may affect on processes involving chargeable medium. Secondly when circulating feed or product through ED module, there may be a shortage of oxygen supply and electric current may cause an adverse effect.

8.4 Summary

This chapter has briefly reviewed ED technology including design, installation, operation and process qualifications related to commercial manufacture. The scaling up of ED to suit industrial production was also discussed. Finally the idea of commercialising was suggested and development issues of current ED module were raised for future work.

Chapter 9

General conclusions and recommendations for future work

9.1 General conclusions

In general terms the aims and objectives of this project (Section 1.4) have all been fully achieved. Solute mass transfer investigations (Chapter 3) of acetic, lactic and malic acids were carried out to investigate the design and operation of the laboratory scale ED module used here. It was discovered that the voltage applied and membrane area per unit volume were the most influencing parameters for ion removal rate. The application of ED (Chapter 4 and 5) was then used in *E.coli* TG1 pGLO for production of recombinant protein, GFP. The removal of inhibitory acetate ions led up to a four times enhancement in GFP synthesis under both early and late exponential phase inductions. Furthermore, bipolar membrane was introduced in ED as a proton and hydroxyl ion providers (Chapter 6). BPED reduced the base addition of a standard *E.coli* fermentation by up to 50% which decreased the level of ammonium toxicity to *E.coli* cells. Both ED and BPED were then employed in the bioconversions of ethyl acetate and fumaric acid (Chapter 7), showing the potentials of ED used in biotransformation.

In conclusion, this study demonstrates the robustness and benefits of ED technology to recombinant protein production and opens up the possibility of applying ED for other

industrial bioprocesses.

Although ED has the possibility of being applied to a number of fermentations and bioconversions, it is important keep in mind that every reaction represents a challenge because the design parameters may required optimising for each individual case. The next significant milestone would be the integration of ED with existing industrial process at large production scale, also increasing selectivity of ion exchange membrane for ions separations

9.2 Future Work

- The work presented in his thesis has focused on one preliminary ED module design (Figure 2.1) and has evaluated its mass transfer characteristics (Chapter 3). It would be desirable to study further how module designs impact on solute mass transfer and to consequently develop an operation model on ED module performance.
- The work presented in Chapters 4 and 5 have shown the benefits of ED for enhancing the production of a model heterologous protein GFP. An immediate next step would be to examine the potential of ED to a fermentation involving the production in *E.coli* of an industrial relevant protein.
- Chapters 4 and 5 can also be extended to study a 'high valued low volume' production' protein but in a system not limited by ED module area so that the true benefits of ED application can be quantified.
- Chapter 6 introduced the use of BPED to *E.coli* fermentation. Further work can

be carried to optimise the PID control system for pH control.

- Chapter 7 presented the application of ED and BPED to bioconversions. This can be explored to a wider range of bioconversions.
- As mentioned in Chapter 8, an improved module design would be appropriate for easier and automated operation. Also, to establish a scale-down model for rapid evaluation of ED technology.

References

Akesson M, Karlsson EN, Hagander P, Axelsson JP and Tocaj A. On-line detection of acetate formation in *Escherichia coli* culture using dissolved oxygen responses to feed transients. *Biotechnology and bioengineering* **64**:590-598 (1999)

Akesson M, Hagander P and Axelsson JP. Avoiding acetate accumulation in *Escherichia coli* cultures using feedback control of glucose feeding. *Biotechnology and bioengineering* **73**:223-230 (2001)

Armstrong DW, Martin SM and Yamazaki H. Production of ethyl acetate from dilute ethanol solutions by *Candida utilis*. *Biotechnology and bioengineering* **26**:1038-1041 (1984)

Banasiak LJ, Kruttschnitt TW and Schafer AI. Desalination using electrodialysis as a function of voltage and salt concentration. *Desalination* **205**:38-46 (2007)

Bazinet L and Farias MA. Electrodialysis of calcium and carbonate high concentration solutions and impact on composition in cations of membrane fouling. *Journal of Colloid and Interface Science* **286**:639-646 (2005)

Belafi-Bako K, Nemestothy N and Gubicza L. A study on applications of membrane techniques in bioconversion of fumaric acid to L-malic acid. *Desalination* **162**:301-306 (2004)

Bevilaqua JV, Pinto JC, Lima LM, Barreiro EJ, Alves T and Freire D. Enzymatic hydrolysis by immobilized lipase applied to a new prototype anti-asthma drug.

Biochemical Engineering Journal **21**:103-110 (2004)

Blayer S, Woodley JM and Lilly MD. Characterization of the chemoenzymatic synthesis of N-Acetyl-D-neuraminic acid (Neu5Ac). *Biotechnol.Prog* **12**:758-763 (1996)

Choi JH, Kim SH and Moon SH. Recovery of lactic acid from sodium lactate by ion substition using ion-exchange membrane. *Separation and Purification Technology* **28**:69-79 (2002)

Delisa MP, Li J, Rao G, Weigand WA and Bentley WE. Monitoring GFP-operon fusion protein expression during high cell density cultivation of *Escherichia coli* using an on-line optical sensor. *Biotechnology and bioengineering* **65**:54-64 (1999)

Demircioglu M, Kabay N, Ersoz E, Kurucaovali I, Safak C and Gizli N. Cost comparison and efficiency modeling in the electrodialysis of brine. *Desalination* **136**:317-323 (2001)

Dutta SK, Mukherjee A and Chakraborty P. Effect of product inhibition on lactic acid fermentation: simulation and modelling. *Appl microbiol biotechnol* **46**:410-413 (1996)

Eiteman MA and Altman E. Overcoming acetate in *Escherichia coli* recombinant protein fermentations. *Trends in Biotechnology* **24**:530-536 (2006)

Fidaleo M and Moresi M. Modeling of sodium acetate recovery from aqueous solutions by electrodialysis. *Biotechnology and bioengineering* **91**:556-568 (2005)

Fidaleo M and Moresi M. Assessment of the main engineering parameters controlling the electrodialytic recovery of sodium propionate from aqueous solutions. *Journal of food engineering* **76**:218-231 (2006)

Fuchs C, Koster D, Wiebusch S, Mahr K, Eisbrenner G and Markl H. Scale-up of dialysis fermentation for high cell density cultivation of *Escherichia coli*. *Journal of Biotechnology* **93**:243-251 (2002)

Gao M, Hirata M, Koide M, Takanashi H and Hano T. Production of L-lactic acid by electrodialysis fermentation (EDF). *Process Chemistry* **39**:1903-1907 (2004)

Gohil GS, Nagarale RK, Shahi VK and Rangarajan R. Micellar-enhanced electrodialysis: Influence of surfactants on the transport properties of ion-exchange membranes. *Separation and Purification Technology* **47**:1-9 (2005)

Habova V, Melzoch K, Rychtera M and Sekavova B. Electrodialysis as a useful technique for lactic acid separation from a model solution and a fermentation broth. *Desalination* **163**:361-372 (2004)

Han K, Lim HC and Hong J. Acetic acid formation in *Escherichia coli* fermentation. *Biotechnology and bioengineering* **39**:663-671 (1992)

Hari Krishna S and Karath NG. Lipases and lipase-catalyzed esterification reactions in non-aqueous media. *Catalysis review* **44**:499-591 (2002)

Hirata M, Gao M, Toorisaka E, Takanashi H and Hano T. Production of lactic acid by continuous electrodialysis fermentation with a glucose concentration controller.

Biochemical Engineering Journal **25**:159-163 (2005)

Hobbs GR, Mitra RK, Chauhan RP, Woodley JM and Lilly MD. Enzyme-catalysed carbon-carbon bond formation: Large-scale production of *Escherichia coli* transketolase. *Journal of Biotechnology* **45**:173-179 (1996)

Hu L, Harrison JD and Masliyah JH. Numerical model of electrokinetic flow for capillary electrophoresis. *Journal of Colloid and Interface Science* **215**:300-312 (1999)

Huang C, Xu T, Zhang Y, Xue Y and Chen G. Application of electrodialysis to the production of organic acids: State-of-the-art and recent developments. *Journal of membrane science* **288**:1-12 (2007)

Hwang SO and Park YH. Gas phase ethyl acetate production in a batch bioreactor. *Bioprocess Engineering* **17**:51-54 (1997)

Jackman SA, Maini G, Sharman AK and Knowles CJ. The effects of direct electric current on the viability and metabolism of acidophilic bacteria. *Enzyme and microbial technology* **24**:316-324 (1999)

Jensen EB and Carlsen S. Production of recombinant human growth hormone in *Escherichia coli*: expression of different precursors and phyiological effects of glucose, acetate, and salts. *Biotechnology and bioengineering* **36**:1-11 (1990)

Johnston WA, Stewart M, Lee P and Cooney MJ. Tracking the acetate threshold using DO-transient control during medium and high cell density cultivation of

recombinant *Escherichia coli* in complex media. *Biotechnology and bioengineering* **84**:314-323 (2003)

Junker B. Foam and its migration in fermentation systems. *Biotechnol.Prog* **23**:767-784 (2007)

Kim J and Cha HJ. Down-regulation of acetate pathway through antisense strategy in *Escherichia coli*: Improved foreign protein production. *Biotechnology and bioengineering* **83**:841-853 (2003)

Kim YH and Moon SH. Lactic acid recovery from fermentation broth using one-stage electrodialysis. *Journal of Chemical Technology and Biotechnology* **76**:169-178 (2001)

Kleman GL, Chalmers JJ, Luli GW and Strohl WR. A predictive and feedback control algorithm maintains a constant glucose concentration in fed-batch fermentations. *Applied and environmental microbiology* **57**:910-917 (1991)

Kleman GL and Strohl WR. Acetate metabolism by *Escherichia coli* in high-cell density fermentation. *Applied and environmental microbiology* **60**:3952-3958 (1994)

Ko YF, Bentley WE and Weigand WA. An integrated metabolic modeling approach to describe the energy efficiency of *Escherichia coli* fermentations under oxygen-limited conditions: cellular energetics, carbon flux and acetate production. *Biotechnology and bioengineering* **42**:843-853 (1993)

Koh BT, Nakashimada U, Pfeiffer M and Yap M. Comparison of acetate inhibition

on growth of host and recombinant *E.coli* K12 strains. *Biotechnology Letters* **14**:1115-1118 (1992)

Korz DJ, Rinas U, Hellmuth K, Sanders EA and Deckwer WD. Simple fed-batch technique for high cell density cultivation of *Escherichia coli*. *Journal of Biotechnology* **39**:59-65 (1995)

Koter S. Modeling of weak acid production by the EDB method. *Separation and Purification Technology* **406**:406-412 (2007)

Koter S. Separation of weak and strong acids by electro-electrodialysis - Experiment and theory. *Separation and Purification Technology* **60**:251-258 (2008)

Kumar Dutta S, Mukherjee A and Chakraborty P. Effect of product inhibition on lactic acid fermentation: simulation and modeling. *Appl microbiol biotechnol* **46**:410-413 (1996)

Leah RT, Brandon NP, Vesovic V and Kelsall GH. Numerical modeling of the mass transport and chemistry of a simplified membrane-divided chlor-alkali reactor. *Journal of the electrochemical society* **147**:4173-4183 (2000)

Lee EG, Moon SH, Chang YK, Yoo IK and Chang HN. Lactic acid recovery using two-stage electrodialysis and its modelling. *Journal of membrane science* **145**:53-66 (1998)

Lee HJ, Sarfert F, Strathmann H and Moon SH. Designing of an electrodialysis desalination plant. *Desalination* **142**:267-286 (2002)

Lee HJ and Moon SH. Enhancement of electrodialysis performances using pulsing electric fields during extended period operation. *Journal of Colloid and Interface Science* **287**:597-603 (2005)

Lee HJ, Strathmann H and Moon SH. Determination of the limiting current density in electrodialysis desalination as an empirical function of linear velocity. *Desalination* **190**:43-50 (2006)

Lee K. A media design program for lactic acid production coupled with extraction by electrodialysis. *Bioresource Technology* **96**:1505-1510 (2005)

Lee SY. High cell-density culture of *Escherichia coli*. *Tibtech* **14**:98-105 (1996)

Li H, Mustacchi R, Knowles CJ, Skibar W, Sunderland G, Dalrymple I and Jackman SA. An electrokinetic bioreactor: using direct electric current for enhanced lactic acid fermentation and product recovery. *Tetrahedron* **2004**:655-661 (2004)

Lin HY, Mathiszik B, Xu B, Enfors SO and Neubauer P. Determination of the maximum specfic uptake capacities for glucose and oxygen in glucose-limited fed-batch cultivation of *Eshcerichia coli*. *Biotechnology and bioengineering* **73**:347-357 (2001)

Linek V, Kordac M, Fujasova M and Moucha T. Gas-liquid mass transfer coefficient in stirred tanks intepreted through models of idealized eddy structure of turbulence in the bubble vicinity. *Chemical Engineering and Processing* **43**:1511-1517 (2004)

Ling LP, Leow HF and Samidi MR. Citric acid concentration by electrodialysis: ion and water transport modelling. *Journal of membrane science* **199**:59-67 (2002)

Loghavi L, Sastry SK and Yousef AE. Effect of moderate electric field on the metabolic activity and growth kinetics of *Lactobacillus acidophilus*. *Biotechnology and bioengineering* **98**:872-881 (2007)

Luli GW and Strohl WR. Comparison of growth, acetate production, and acetate inhibition of *Escherichia coli* strains in batch and fed-batch fermentations. *Applied and environmental microbiology* **56**:1004-1011 (1990)

Lye GJ and Woodley JM. Application of *in situ* product-removal techniques to biocatalytic processes. *Tibtech* **17**:395-402 (1999)

Majewski RA and Domach MM. Simple constrained-optimization view of acetate overflow in *E.coli*. *Biotechnology and bioengineering* **35**:732-738 (2009)

Meng H, Li H, Li C and Li L. Synthesis of ionic liquid using a four-compartment configuration electrodialyzer. *Journal of membrane science* **318**:1-4 (2008)

Mier MP, Ibanez R and Ortiz I. Influence of ion concentration on the kinetics of electrodialysis with bipolar membranes. *Separation and Purification Technology* **59**:197-205 (2008)

Mondor M, Masse L, Ippersiel D, Lamarche F and Masse DI. Use of electrodialysis and reverse osmosis for the recovery and concentration of ammonia from swine manure. *Bioresource Technology* **99**:7363-7368 (2007)

Moresi M and Sappino F. Electrodialytic recovery of some fermentation products from model solutions: techno-economic feasibility study. *Journal of membrane science* **164**:129-140 (2000)

Mosher RH. Using pGLO to Demonstrate the Effects of Catabolite Repression on Gene Expression in *Escherichia coli*. *Bioscene* **28**:17-23 (2002)

Mustacchi R, Knowles CJ, Li H, Dalrymple I, Sunderland G, Skibar W and Jackman SA. Enhanced biotransformation and product recovery in a membrane bioreactor through application of a direct electric current. *Biotechnology and bioengineering* **89** :18-23 (2005)

Mustacchi R, Knowles CJ, Li H, Dalrymple I, Sunderland G, Skibar W and Jackman SA. The effect of whole cell immobilisation on the biotransformation of benzonitrile and the use of direct electric current for enhanced product removal. *Biotechnology and bioengineering* **91**:436-440 (2005)

Nagarale RK, Gohil GS and Shahi VK. Recent developements on ion-exchange membranes and electro-membrane processes. *Advances in colloid and interface science* **119**:97-130 (2006)

Nakano K, Rischke M, Sato S and Markl H. Influence of acetic acid on the growth of *Escherichia coli* K12 during high-cell-density cultivation in a dialysis reactor. *Appl microbiol biotechnol* **48**:597-601 (1997)

Nikonenko V, Lebedev K, Manzanares JA and Pourcelly G. Modelling the transport of carbonic acid anions through anion-exchange membranes.

Electrochimica Acta **48**:3639-3650 (2003)

Nomura Y, Iwahara M and Hongo M. Acetic acid production by an electrodialysis fermentation method with a computerized control system. *Applied and environmental microbiology* **54**:137-142 (1988)

Oritz JM, Sotoca JA, Exposito E, Gallud F, Garcia-Garcia V, Montiel V and Aldaz A. Brackish water desalination by electrodialysis: batch recirculation operation modeling. *Journal of membrane science* **252**:65-75 (2005)

Panda AK, Khan RH, Appa Rao KBC and Totey SM. Kinetics of inclusion body production in batch and high cell density fed-batch culture of *Escherichia coli* expressing ovine growth hormone. *Journal of Biotechnology* **75**:161-172 (1999)

Panizza M and Cerisola G. Application of diamond electrodes to electrochemical processes. *Electrochimica Acta* **51**:191-199 (2005)

Park JS, Choi JH, Yeon KH and Moon SH. An approach to fouling characterization of an ion-exchange membrane using current-voltage relation and electrical impedance spectroscopy. *Journal of Colloid and Interface Science* **294**:129-138 (2006)

Pavlou A and Reichert J. Recombinant protein therapeutics-success rates, market trends and values to 2010. *Nature Biotechnology* **22**:1513-1519 (2004)

Presecki AV, Zelic B and Vasic-Racki D. Comparison of the L-malic acid production by isolated fumarase and fumarase in permeabilized baker's yeast cells. *Enzyme and microbial technology* **41**:605-612 (2007)

Raissouni I, Marraha M and Azmani A. Effect of some parameters on the improvement of the bipolar membrane electrodialysis process. *Desalination* **208**:62-72 (2007)

Reetz M and Jaeger KE. Overexpression, immobilization and biotechnological application of *Pseudomonas* lipases. *Chemistry and physics of lipids* **93**:3-14 (1998)

Reis P, Holmberg K, Watzke H, Leser ME and Miller R. Lipases at interfaces: A review. *Advances in colloid and interface science* **10**:1016-1036 (2008)

Rozkov A, Avignone-Rossa CA, Ertl PF, Jones P, O'Kennedy RD, Smith JJ, Dale JW and Bushell ME. Characterization of the metabolic burden on *Escherichia coli* DH1 cells imposed by the presence of a plasmid containing a gene therapy sequence. *Biotechnology and bioengineering* **88**:909-915 (2004)

Rozkov A, Avignone-Rossa CA, Ertl PF, Jones P, O'Kennedy RD, Smith JJ, Dale JW and Bushell ME. Fed-batch culture with declining specific growth rate for high-yielding production of a plasmid containing a gene therapy sequence in *Escherichia coli* DH1. *Enzyme and microbial technology* **39**:47-50 (2006)

Sadrzadeh M, Razmi A and Mohammadi T. Separation of different ions from wastewater at various operating conditions using electrodialysis. *Separation and Purification Technology* **54**:147-156 (2007)

Sadrzadeh M, Kaviani A and Mohammadi T. Mathematical modeling of desalination by electrodialysis. *Desalination* **206**:538-546 (2007)

Sandoval-Basurto EA, Gosset G, Bolivar F and Ramirez OT. Culture of *Escherichia coli* under dissolved oxygen gradients simulaed in a two-compartment scale-down system: Metabolic response and production of recombinant protein. *Biotechnology and bioengineering* **89**:453-463 (2005)

Shen JY, Duan JR, Yu LX and Xu P. Desalination of glutamine fermentation broth by electrodialysis. *Process Chemistry* **41**:716-720 (2006)

Shiloch J and Fass R. Growing *E.coli* to high cell density- A historical perspective on method development. *Biotechnology advances* **23**:345-357 (2005)

Smara A, Delimi R, Chainet E and Sandeaux J. Removal of heavy metals from diluted mixtures by a hybrid ion-exchange/electrodialysis process. *Separation and Purification Technology* **57**:103-110 (2007)

Stark D and von Stockar U. In situ product removal (ISPR) in whole cell biotechnology during the last twenty years. *Advances in Biochemical Engineering/Biotechnology* **80**:149-175 (2003)

Tanaka Y. Current density distribution, limiting current density and saturation current density in an ion-exchange membrane electrodialyzer. *Journal of membrane science* **210**:65-75 (2002)

Tanaka Y. Limiting current density of an ion-exchange membrane and of an electrodialyzer. *Journal of membrane science* **266**:6-17 (2005)

Turner C, Gregory ME and Turner MK. A study of the effect of specific growth

rate and acetate on recombinant protein production of *Escherichia coli* JM107. *Biotechnology Letters* **16**:891-896 (1994)

van de Walle M and Shiloach J. Proposed mechanism of acetate accumulation in two recombinant *Escherichia coli* strains during high density fermentation. *Biotechnology and bioengineering* **57**:71-78 (1998)

Varma A, Boesch BW and Palsson BO. Biochemical production capabilities of *Escherichia coli*. *Biotechnology and bioengineering* **42**:59-73 (1993)

Wang L and Song L. Flux decline in crossflow microfiltration and ultrafiltration: experimental verification of fouling dynamics. *Journal of membrane science* **160** :41-50 (1999)

Wang Z, Luo Y and Yu P. Recovery of organic acids from waste salt solutions derived from the manufacture of cyclohexanone by electrodialysis. *Journal of membrane science* **280**:134-137 (2006)

Woodley JM, Bisschops M, Staathof AJJ and Ottens M. Future directions for *in-situ* product removal (ISPR). *Journal of Chemical Technology and Biotechnology* **83**:121-123 (2008)

Xu B, Jahic M and Enfors SO. Modeling of overflow metabolism in batch and fed-batch cultures of *Escherichia coli*. *Biotechnol.Prog* **15**:81-90 (1999)

Xu B, Jahic M, Blomsten G and Enfors SO. Glucose overflow metabolism and mixed-acid fermentation in aerobic large-scale fed-batch processes with *Escherichia*

coli. *Appl microbiol biotechnol* **51**:564-571 (1999)

Xu T. Ion exchange membrane: state of their development and perspective. *Journal of membrane science* **263**:1-29 (2005)

Xu T and Huang C. Electrodialysis-based separation technologies: A critical review. *Separations* **54**:3147-3159 (2008)

Yi SS, Lu YC and Luo GS. An *in situ* coupling separation process of electro-electrodialysis with back extraction. *Journal of membrane science* **255**:57-65 (2005)

Yi SS, Lu YC and Luo GS. Separation and concentration of lactic acid by electro-electrodialysis. *Separation and Purification Technology* **60**:308-314 (2008)

Yu L, Lin T, Guo Q and Hao J. Relation between mass transfer and operation parameters in the electrodialysis recovery of acetic acid. *Desalination* **154**:147-152 (2003)

Yuan H, Yang X and Hua ZC. Optimization of expression of an Annexin V-Hirudin chimeric protein in *Escherichia coli*. *Microbiology research* **159**:147-156 (2004)

Appendices

Appendix A Publications

Wong M, Wright M, Woodley JM, Lye GJ. Enhanced recombinant protein expression in batch and fed-batch *Escherichia coli* fermentation based on removal of inhibitory acetate by electrodialysis. *Journal of Chemical Technology and Biotechnology* **84**: 1284-1291 (2009)

Wong M, Woodley JM, Lye GJ. Application of bipolar electrodialysis to *E.coli* fermentation for simultaneous acetate removal and pH control. *Biotechnology Letter* **32** :1053-1057 (2010)

Appendix B- Experimental data

Appendix B.1 Assay kits calibration curves (Chapter 2)

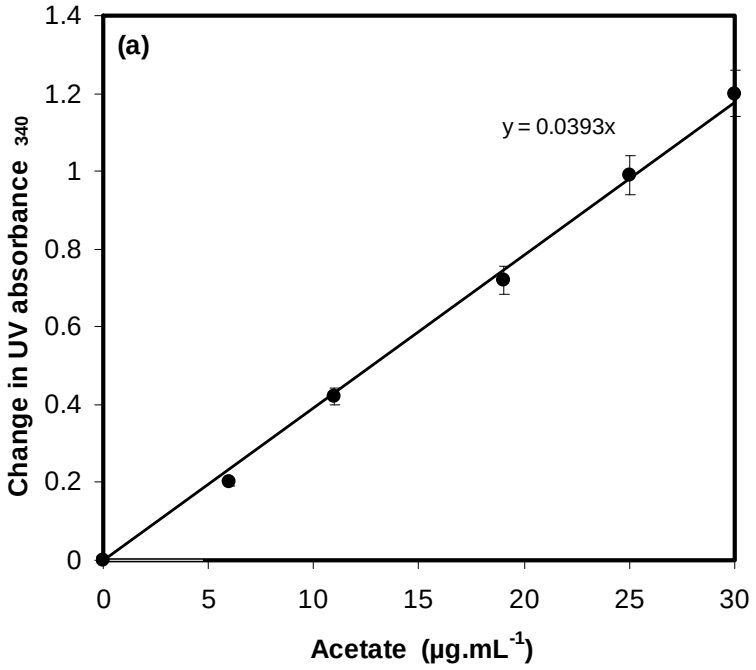

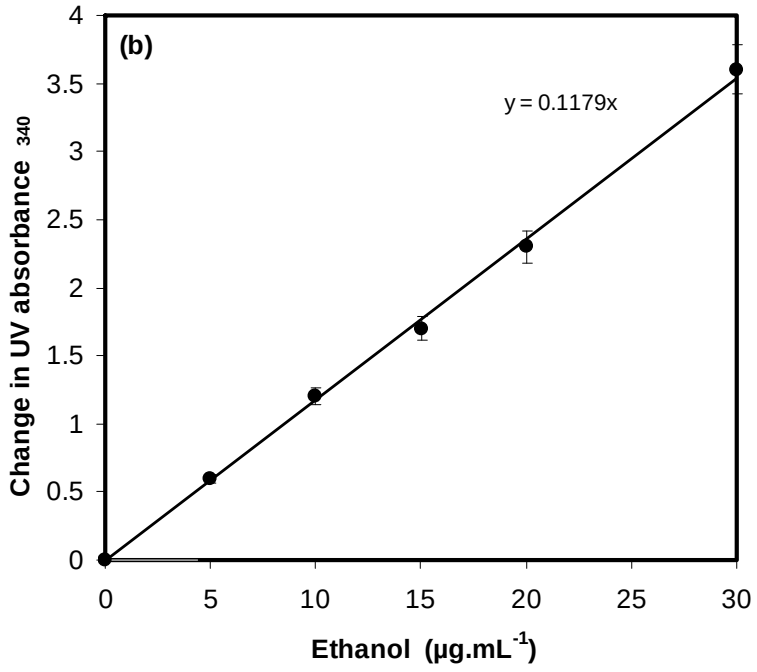

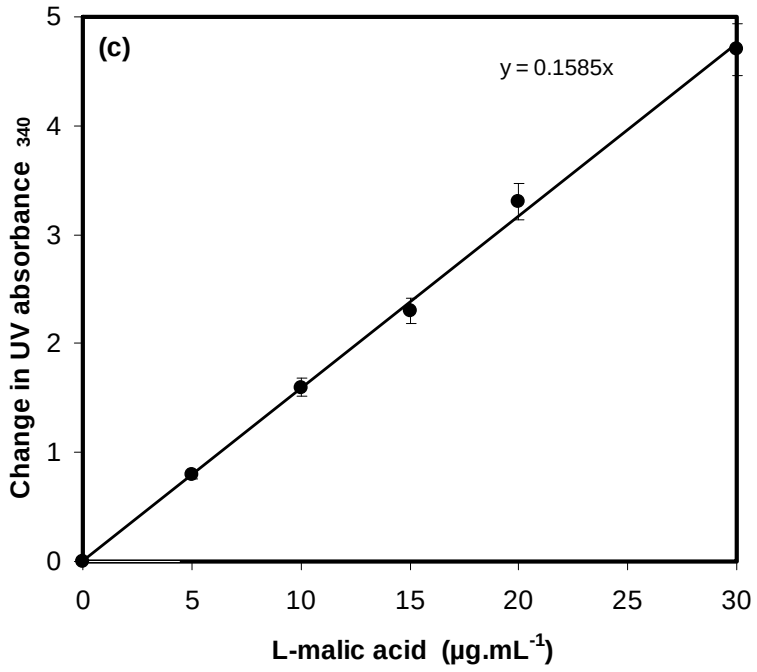

Figure B.1. Calibration curves of assay kits for the quantification of **(a)** acetate, **(b)** ethanol and **(c)** L-malate (Section 2.2.6.5).

Appendix B.2 ED control experiment (Chapter 4)

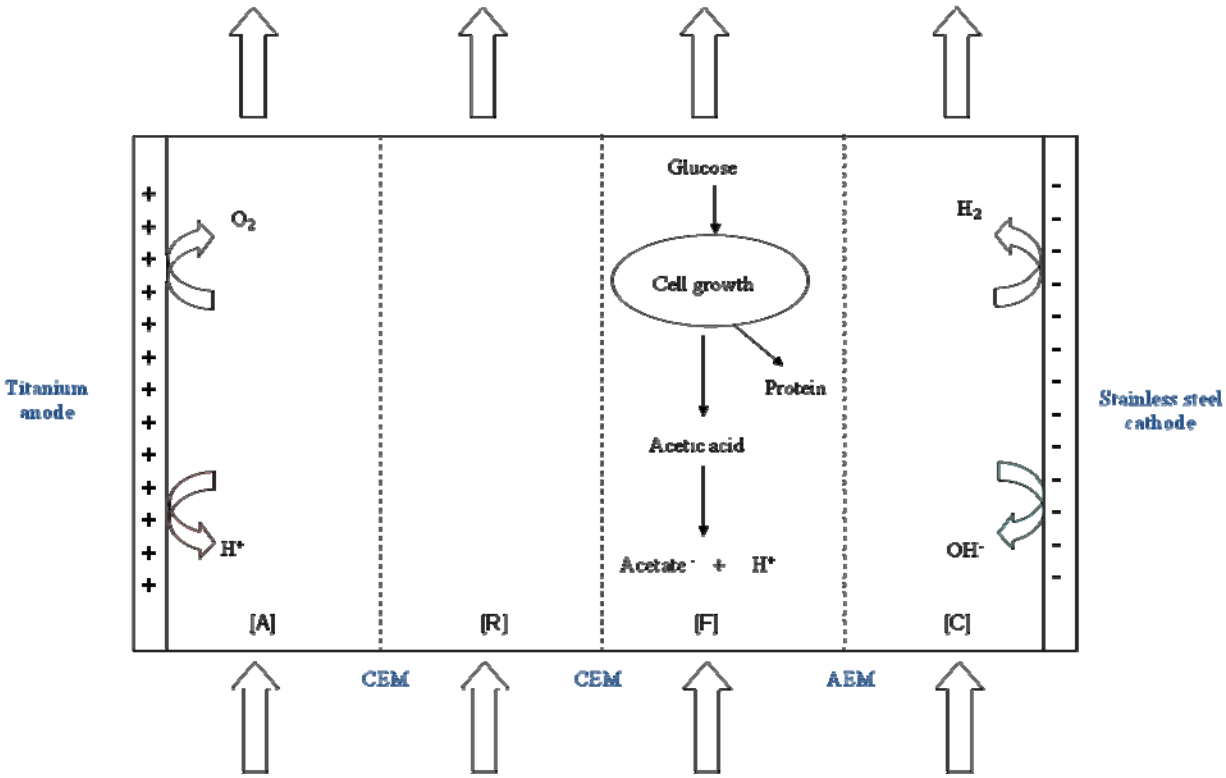

Figure B.2. Principle of electrodialysis module set-up and operation for ED batch **control** experiment (Section 2.2.3). The membrane configuration of C-C-A do not allow any movements of ion from compartment F.

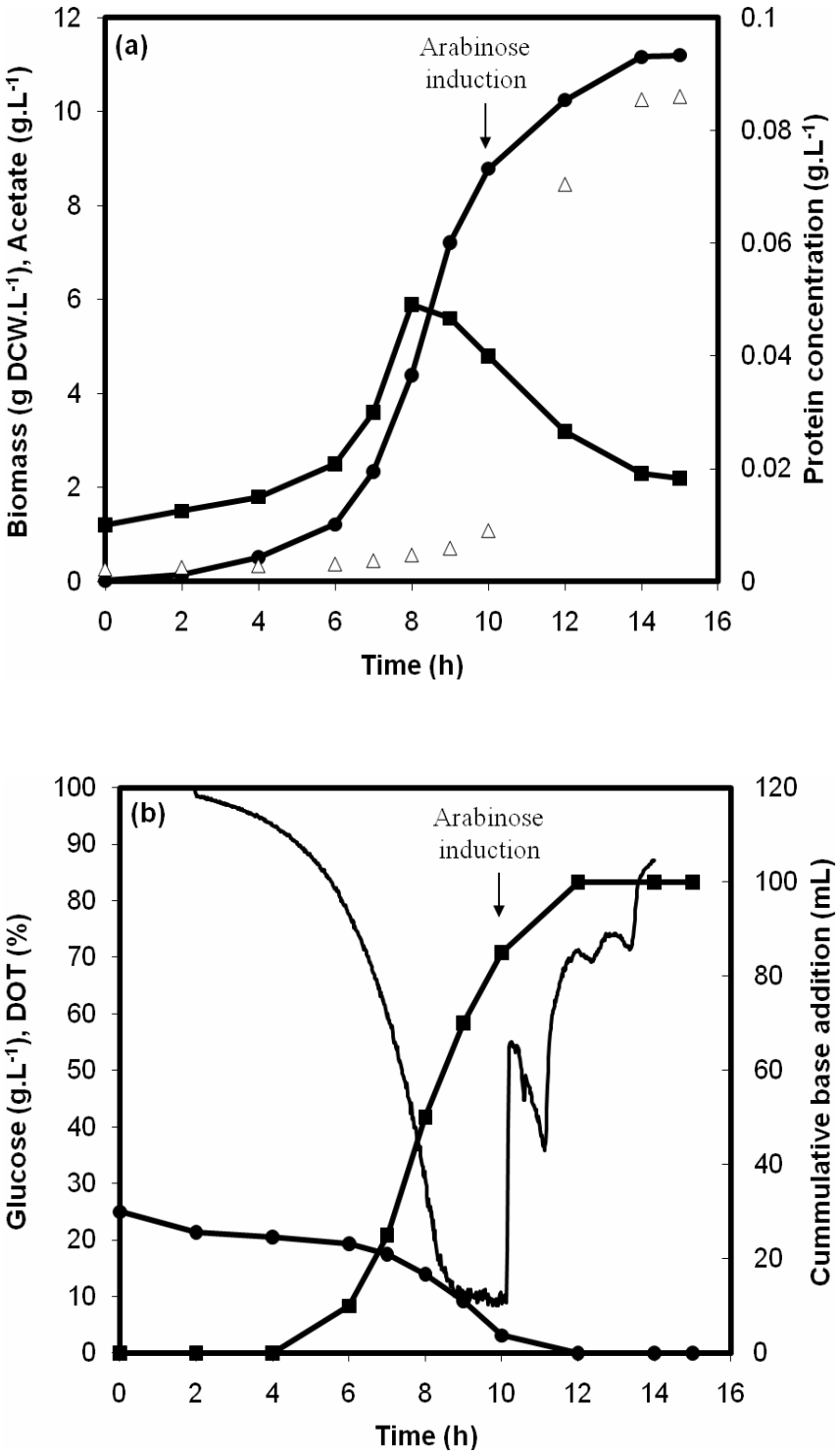

Figure B.3. Electrodialysis batch **control** fermentation kinetics of *E.coli* TG1 pGLO with late GFP induction. **(a)** Offline data for biomass (●), acetate (■) and recombinant protein, GFP, (Δ) concentration. **(b)** On-line measurements of glucose (●), dissolved oxygen tension (-) and base addition (■) (Section 4.2.3).

Appendix B.3 Fermentations off-gas analysis (Chapters 4, 5 and 6)

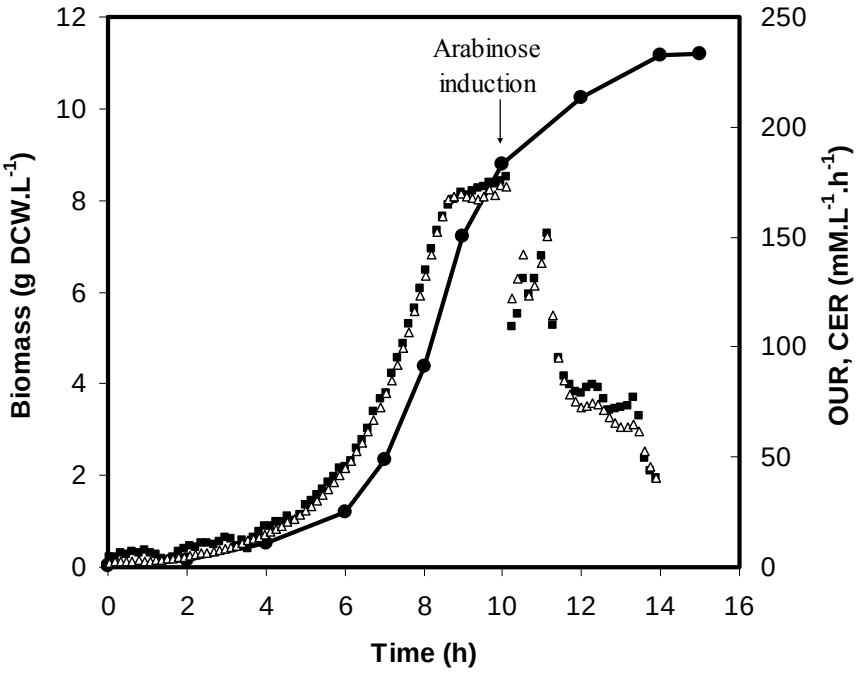

Figure B.4. Batch fermentation kinetics of *E.coli* TG1 pGLO with late exponential phase GFP induction (Section 4.2). **(a)** Offline data for biomass (●), CER (■) and OUR (Δ). The arrow indicates the time of induction. Results show a typical profile from triplicate fermentations. Experiments performed as described in Section 2.2.2.3. Similar profiles were seen with early exponential phase GFP induction (Section 5.2).

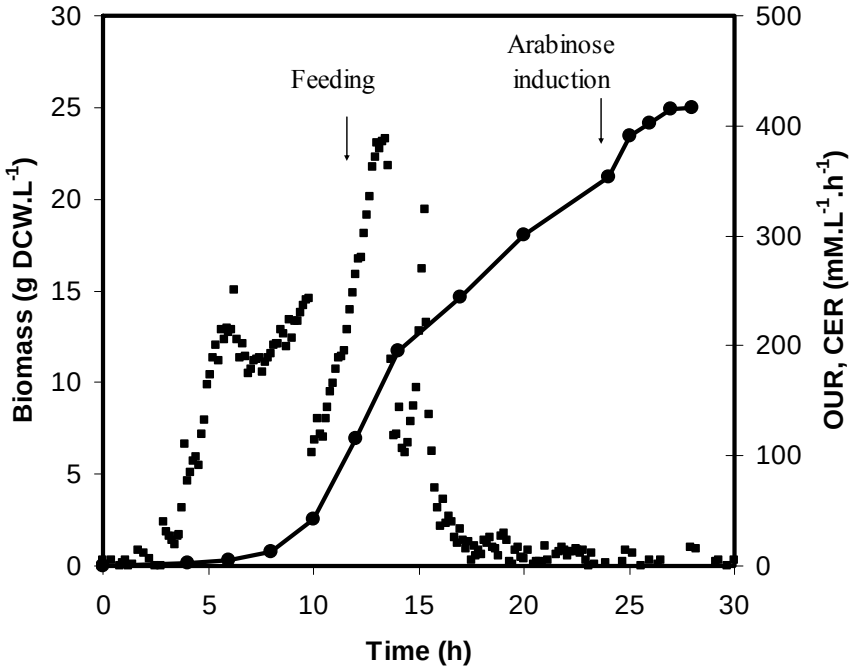

Figure B.5. Fed-batch fermentation kinetics of *E.coli* TG1 pGLO with late exponential phase GFP induction (Section 4.2). **(a)** Offline data for biomass (●), CER (■) and OUR (Δ). The arrow indicates the time of induction. Results show a typical profile from triplicate fermentations. Experiments performed as described in Section 2.2.2.4. Similar profiles were seen with early exponential phase GFP induction (Section 5.2).

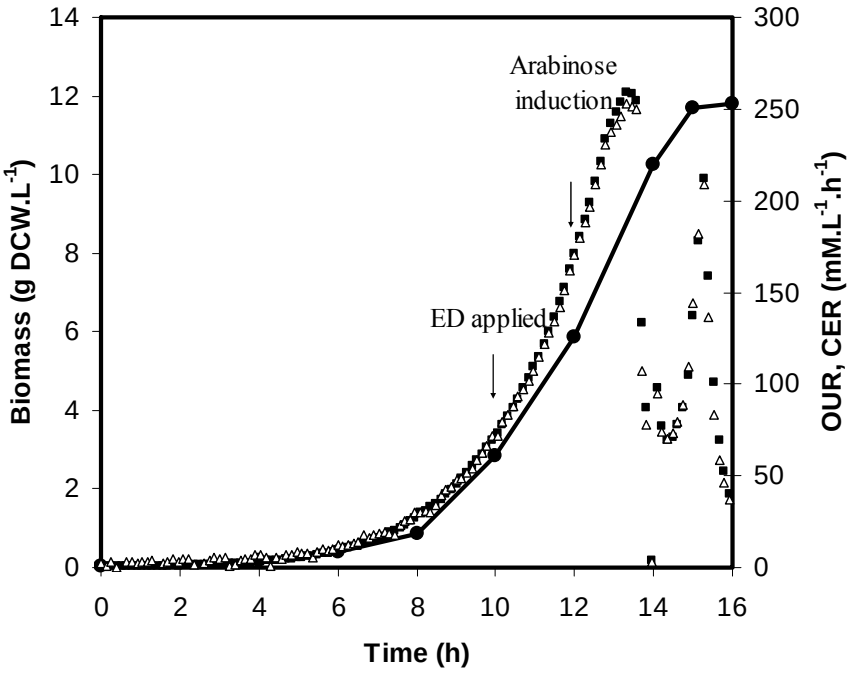

Figure B.6. ED batch fermentation kinetics of *E.coli* TG1 pGLO with late exponential phase GFP induction (Section 4.2). **(a)** Offline data for biomass (●), CER (■) and OUR (Δ). The arrow indicates the time of induction. Results show a typical profile from triplicate fermentations. Experiments performed as described in Section 2.2.3. Similar profiles were seen with early exponential phase GFP induction (Section 5.2) and BPED batch fermentation (Section 6.2).

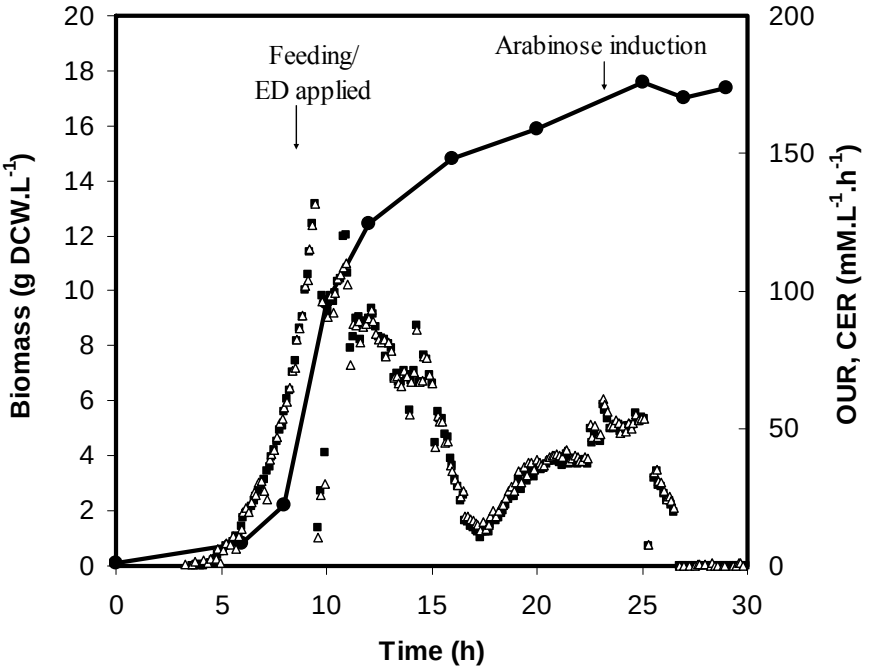

Figure B.7. ED fed-batch fermentation kinetics of *E.coli* TG1 pGLO with late exponential phase GFP induction (Section 4.2). **(a)** Offline data for biomass (●), CER (■) and OUR (Δ). The arrow indicates the time of induction. Results show a typical profile from triplicate fermentations. Experiments performed as described in Section 2.2.3. Similar profiles were seen with early exponential phase GFP induction (Section 5.2) and BPED fed-batch fermentation (Section 6.2).

Appendix B.4 Application of ED to form free malic acid (Chapter 7)

Following experiments in Section 7.2.2.2, fumaric acid was converted to malic acid. However, sodium hydroxide was unavoidably added to both initially dissolve the substrate and then during the course of the bioconversion for pH control. In this case the product of the bioconversion would be sodium malate rather than the preferred free malic acid. The resulting supernatants from previous bioconversions (Figure 7.7a and 7.7b) were consequently processed using the electrodialysis module (Figure 2.5a) in order to explore salt separation and production of the free acid. This membrane configuration only allows the movement of negatively charged malate ions from compartment F to R. As shown in Figure B.8 at 210min, there were 7.5 and 8.1 $g.L^{-1}$ of free malic acid recovered for both sets of experiments, so the use of BPED was not significant. The positively charged sodium ions would remain in compartment F, so the concentrations of sodium in compartment F and R were constant throughout the experiments.

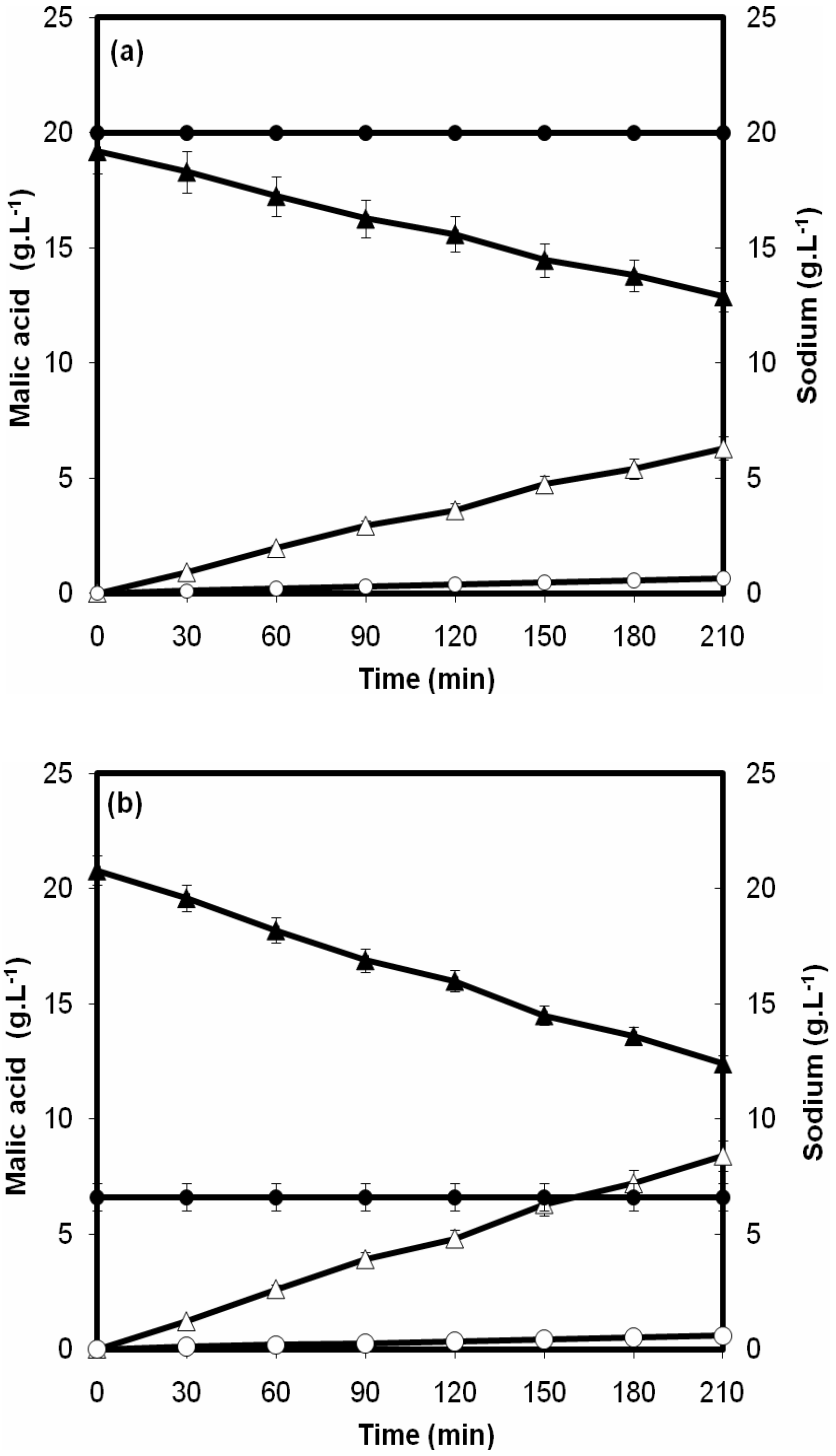

Figure B.8. Dissociation of sodium (●) malate (▲) in compartment F and the formation of free malic acid (△) and sodium (○) presents in compartment R. **(a)** supernatant from Figure 7.7(a) **(b)** supernatnat from Figure 7.7(b). Error bars represent one standard deviation about the mean (n=3). Experiments performed as described in Section 2.2.5.2.